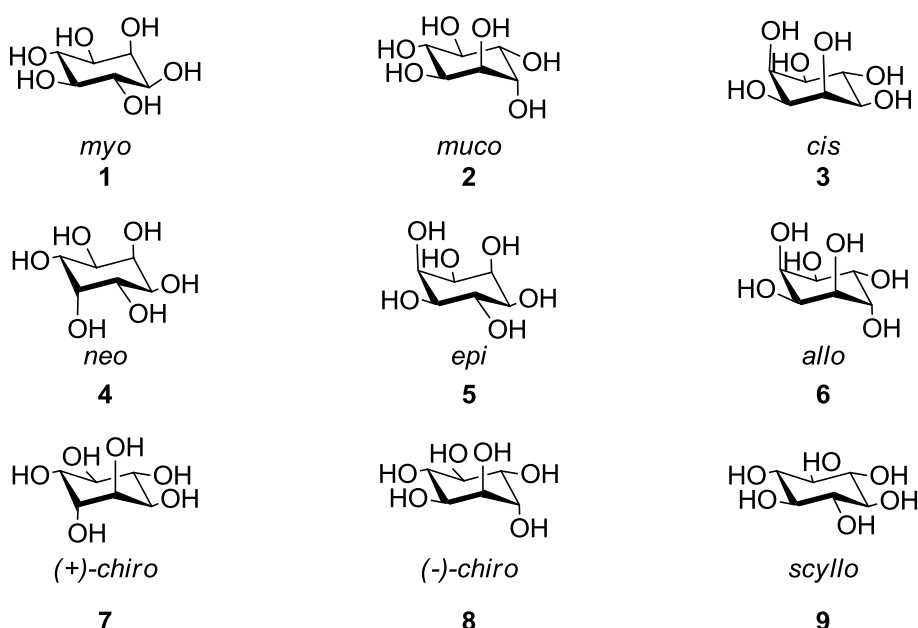


# CHAPTER 1: NHC-CATALYSED CARBOCYCLISATION REACTIONS OF ALDITOL-DERIVED DIALDEHYDES

## INTRODUCTION

### Inositols in Their Natural Reservoirs

Inositols (cyclohexane-1,2,3,4,5,6-hexol) are ubiquitous in nature and are found in both plants and mammals. There are nine possible isomers of inositol **1-9**: *myo*-, *scyllo*-, *muco*-, (+)-*chiro*-, *neo*-, (-)-*chiro*-, *allo*-, *epi*- and *cis*-inositol, shown in Figure 1. The prevalent form of inositol found in nature is the *myo*-isomer however the *chiro*- and *scyllo*- isomers also occur in small amounts.<sup>1</sup>



**Figure 1: Stereoisomers of inositol**

In plants, inositol is present as phytic acid (inositol hexakisphosphate) and is the principle method of phosphate storage. In mammals, inositol phospholipids serve a structural function in cell membranes and membrane receptors and also mediate cell responses to external stimuli, acting in the regulation of cellular concentrations of calcium.<sup>1</sup> Figure 2 shows glycosylphosphatidylinositol **10**, a lipid anchor that links a variety of proteins to the external leaflet of the plasma in a cell membrane.

Inositol is also a key intermediate in the phosphatidylinositol secondary messenger pathway activated by numerous serotonergic, cholinergic, and noradrenergic receptors.<sup>2</sup> It is this function which has seen it as a focus in studies on the treatment of various disorders including depression, obsessive-compulsive disorder, anxiety, panic, bulimia and binge-eating.<sup>2-8</sup> These studies suggest

a certain parallelism between the therapeutic profiles of inositol and serotonin reuptake inhibitors (SSRIs) commonly used to treat these types of psychiatric disorders, with inositol providing an attractive alternative in terms of side effects to common SSRIs such as fluvoxamine. *D-chiro*-inositol has also been shown to be a putative mediator of intracellular insulin action, with a study revealing that Type 2 diabetics have a defect *in vivo* with their ability to epimerise *myo*-inositol to *chiro*-inositol, and that administration of *chiro*-inositol aids in increasing insulin sensitivity and glucose disposal.<sup>9</sup>

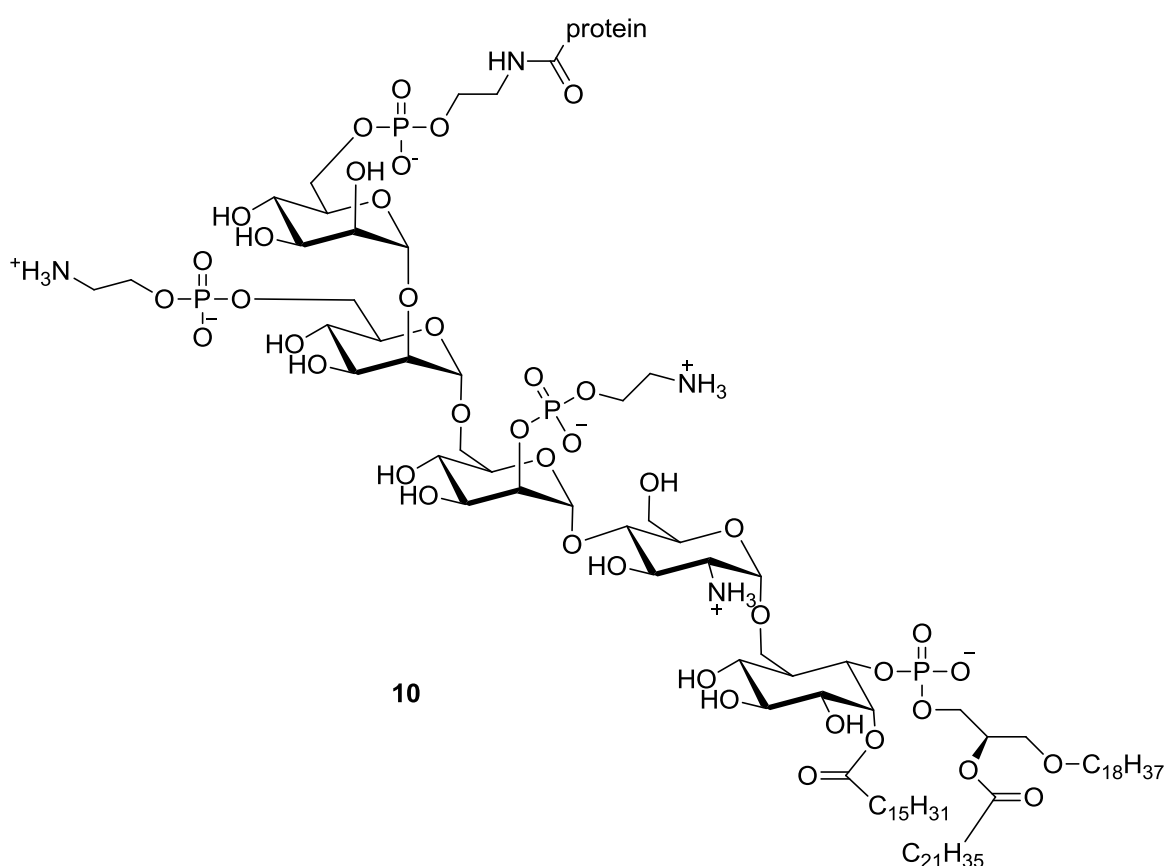


**Figure 2 Glycosylphosphatidyl inositol**

Carbocyclic sugars and their derivatives are also a ubiquitous structural element in a wide variety of natural products with biological activity such as compounds **11-19** shown in Figure 3. Perhaps one of the most significant classes is the aminocyclitol antibiotics. The first such compound, streptomycin **11**, was first isolated by Selman Waksman in 1942 from *Streptomyces griseus* bacterium and was the first effective antibiotic against tuberculosis.<sup>10</sup> The discovery led to Waksman being awarded the Nobel Prize in 1952. Related to streptomycin are the important aminocyclitol antibiotics hygromycin A **16** and B **17**, obtained from *Streptomyces hygroscopicus*

around the same time.<sup>11</sup> Hygromycin B **17** is currently used as an anthelmintic agent in chicken and swine feedstock.

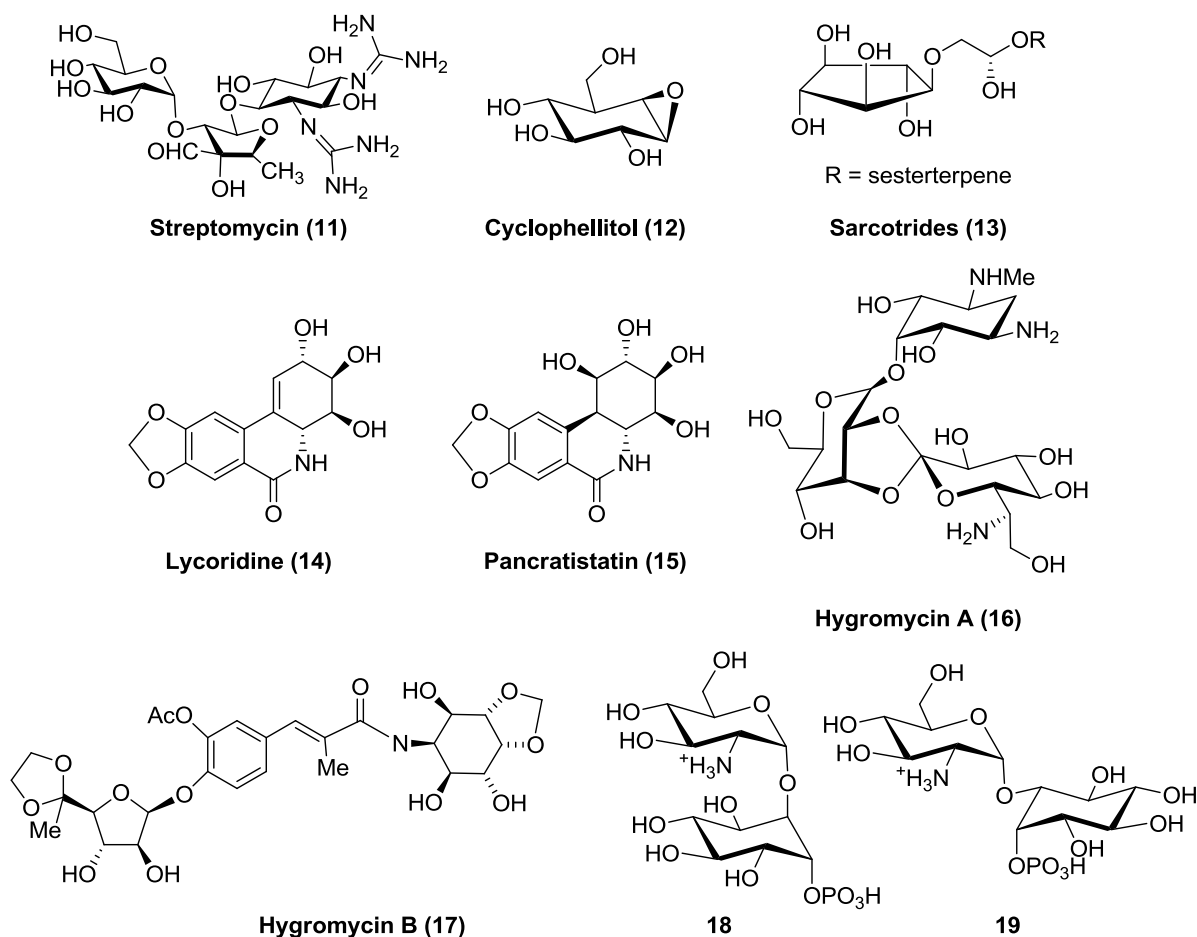
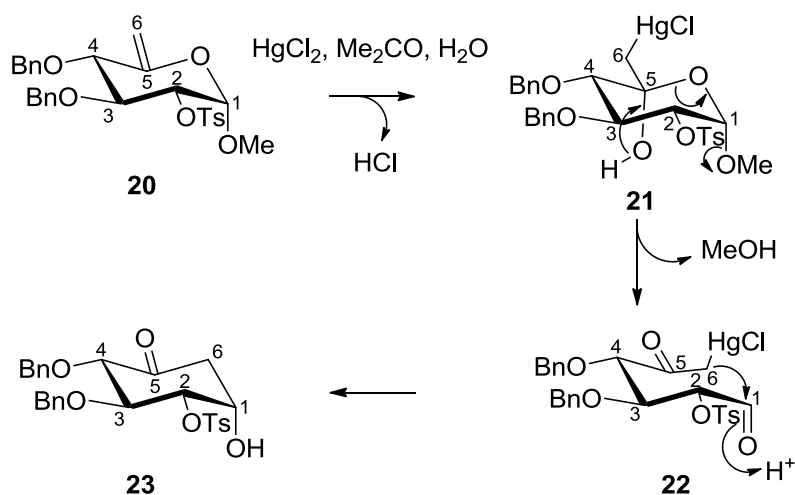


**Figure 3 Subset of biologically active compounds containing carbocyclic sugars**

Other examples of carbocyclic sugar-containing natural products include cyclophellitol **12**, which is a potent and selective  $\beta$ -glucosidase inhibitor isolated from *Phellinus sp.* mushrooms.<sup>12</sup> The sarcotride series **13** are potent cytotoxic compounds isolated from *Sarcotragus* marine sponge species and are less common examples of five-membered cyclitol-containing natural products. Lycoricidine **14**<sup>13</sup> and the related pancratistatin **15**<sup>14</sup> are amaryllidaceae alkaloids with anti-cancer properties. While not naturally occurring, 6-*O*-(2-amino-2-deoxy- $\alpha$ -D-glucopyranosyl)-D-*chiro* and D-*myo*-inositol 1-Phosphate (**18** and **19** respectively), are biologically-inspired scaffolds that are putative insulin mimetics.<sup>15</sup>

## Synthesis of Carbocyclic Sugars from Carbohydrates

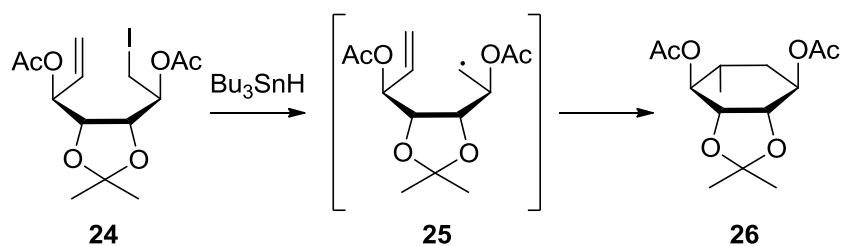
With the fundamental importance of inositol in eukaryotic biology and their presence in a wide variety of biologically active compounds, their synthesis has been widely studied. Total syntheses of natural products generally require orthogonally protected derivatives which is challenging in the case of inositols due to the numerous secondary alcohols of similar reactivity. An attractive route to protected inositols is from the corresponding carbohydrates. Carbohydrates are generally inexpensive and their numerous stereoisomers are readily available in an enantiopure form. This makes them ideal chiral pool starting materials and a host of protocols exist for their conversion into carbocycles.<sup>16-18</sup> A powerful tool that has emerged in the past few decades is the Ferrier II reaction in which cyclitols and deoxycyclitols may be formed from the appropriate glycals and 6-deoxyglycals respectively, mediated by mercury (II) chloride or palladium (II) chloride. The mechanism for this reaction is shown in Scheme 1.



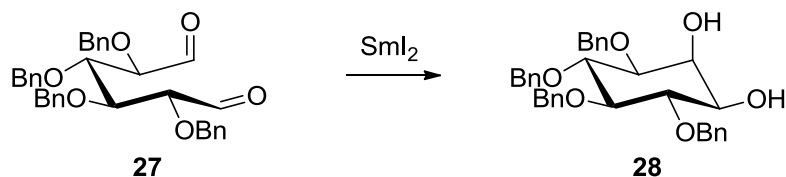
Scheme 1

The carbocyclisation has been shown to be highly diastereoselective, with the predominant epimer formed having a *trans*-relationship between the hydroxyl group at the newly formed chiral centre and the substituent on C3.<sup>16,19</sup> Highly tolerant of various functional groups and stereochemistry, the Ferrier reaction has found widespread use in total synthesis, notably the synthesis of (+)-galanthamine,<sup>20</sup> fumagillin analogue FR65814,<sup>21</sup> (+)-lycoridine<sup>22</sup> and (-)-hygromycin A.<sup>23</sup>

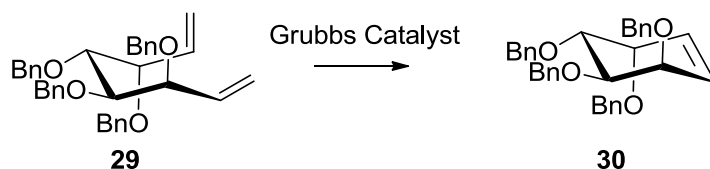
The demonstrated utility of the Ferrier II reaction has been a motivating factor in the development of new alternative syntheses of inositols from carbohydrates. Scheme 2 shows selected examples of the synthesis of carbocyclic compounds using carbohydrate starting materials. Methods include radical cyclisations,<sup>28,29</sup> samarium diiodide reductive couplings of carbonyls,<sup>24,25</sup> ring-closing olefin metathesis,<sup>26</sup> as well as anionic ring-closures.<sup>27</sup>



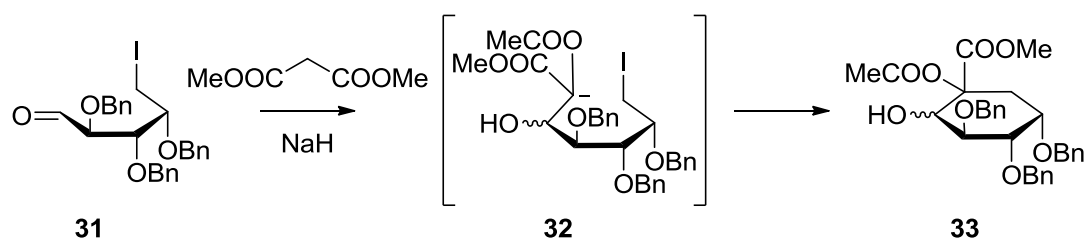
Redlich et al., *Carb. Res.*, 1992, 57 (Ref. 29)



Guidot et al., *Tetrahedron*, 1994, 6671 (Ref. 25)



Gallos et al., *J. Chem. Soc. Perkin Trans. 1*, 1999, 3075 (Ref. 26)



Suami et al., *Chem. Lett.*, 1989, 1919 (Ref. 27)

## Scheme 2

### **N-Heterocyclic Carbenes as Organocatalysts and the Benzoin Condensation**

N-heterocyclic carbenes (NHCs, Figure 4) are a widely studied class of nucleophilic carbenes that have well established utility in organic synthesis.<sup>30-33</sup> Historically, carbenes have always been of great interest to the synthetic chemist as reactive intermediates that exhibit a broad range of reactivity. NHCs are unique in that the carbene formed from the deprotonation of the ammonium salt is highly stable, yet retains a reactivity profile that is characteristic of carbenoid species. Typical of any carbene, the main feature is a divalent carbon with two non-bonding electrons, which may be spin-paired (singlet) or unpaired (triplet state) (Figure 5). The singlet state is much lower in energy due to the formation of a quasi-aromatic system in which the empty p-orbital on the carbene carbon is available for the donation of electrons by the flanking heteroatoms.<sup>34,35</sup> The

carbene is also stabilised by electron withdrawing effects by the heteroatoms in the  $\sigma$ -framework as well as through steric effects of substituents on these heteroatoms. Taken together there is a net attenuation of the nucleophilic character of the carbene.

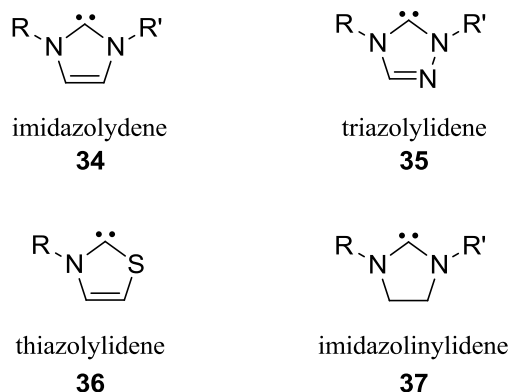


**Figure 4** Classes of carbenes used in organocatalysis

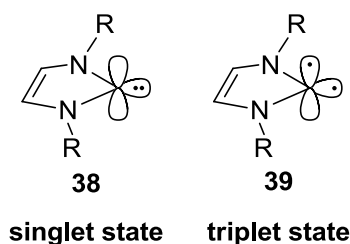
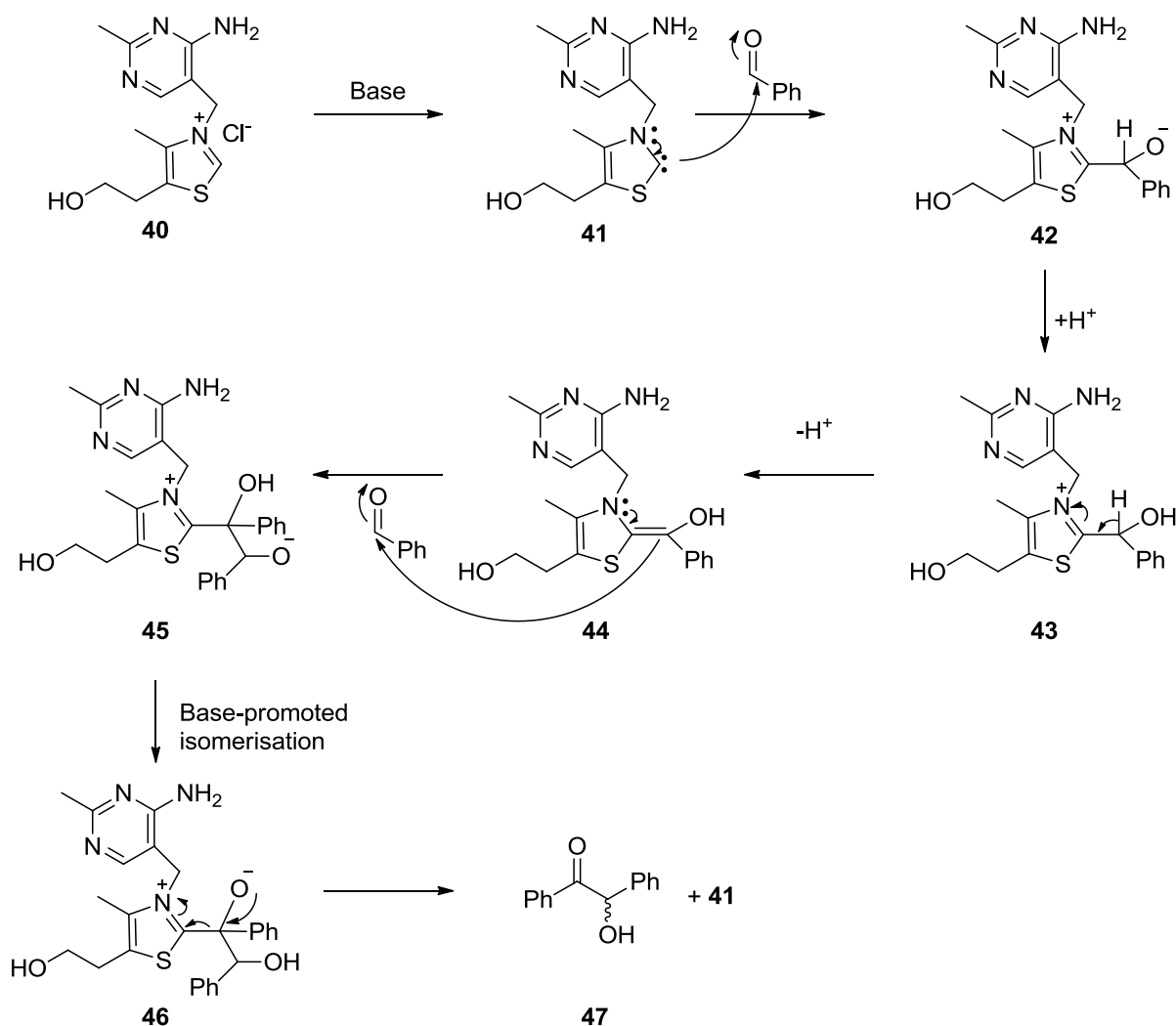


**Figure 5** Singlet and triplet state of an NHC represented for an imidazolydine ring

The advent in the use of NHCs in organic synthesis stems from one of the general tenets of organocatalysis, in which simple systems are sought after that mimic the reactivity of enzymes capable of rapid and highly selective chemical transformations, without the need for their proteinaceous bulk.<sup>31</sup> Transketolase enzymes affect many nucleophilic acylation reactions in the presence of the coenzyme thiamine (vitamin B<sub>1</sub>), a naturally occurring thiazolium NHC.<sup>36,37</sup> In 1943, Ugai showed that thiamine on its own also catalyses the self-condensation of benzaldehyde in the presence of base to give benzoin.<sup>38</sup> A decade later, Breslow proposed a carbene intermediate formed via deprotonation of the thiazolium ring as the active catalytic species in both the enzymatic processes and in Ugai's experiments, and this is the generally accepted mechanism in reactions catalysed by NHCs involving acyl anion equivalents.<sup>39</sup> Breslow's mechanism for the benzoin condensation, which is analogous to Lapworth's classic mechanism for benzoin formation catalysed by cyanide,<sup>40</sup> is presented in Scheme 3. The thiazolydene carbene catalyst **41** undergoes nucleophilic addition to benzaldehyde affording the intermediate **42**. Tetrahedral intermediate **42** undergoes proton transfer to give enamine **44** via **43**, with **44** being widely

referred to as the Breslow intermediate. Intermediate **44** then acts as an acyl anion equivalent and becomes the Umpolung partner that couples with another molecule of benzaldehyde to form **45**. Proton transfer and elimination of the catalyst yields the dimeric product **47** and regenerated carbene. As a carbon-carbon bond forming tool that generates a new stereocentre, the NHC-catalysed benzoin condensation has received much attention in synthetic chemistry.



**Scheme 3**

Attempts to render the benzoin condensation asymmetric were undertaken as early as 1966 by Sheehan et al. with the use of a chiral thiazolylidene NHC (**48**, Figure 6), which gave a relatively low *ee* of 22% in the self-condensation of benzaldehyde.<sup>41</sup> Although many efforts have been made with variations of chiral thiazolium precatalysts, including bicyclic scaffolds synthesised by Leeper et al. (**49** and **50**, Figure 6),<sup>42</sup> only modest chiral induction and relatively low yields of product were observed.<sup>43,44</sup>

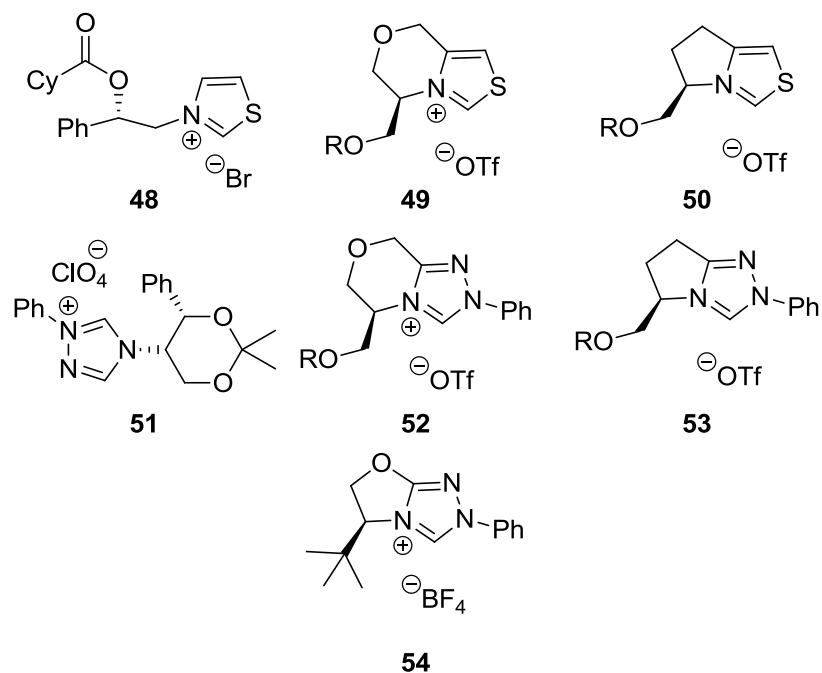
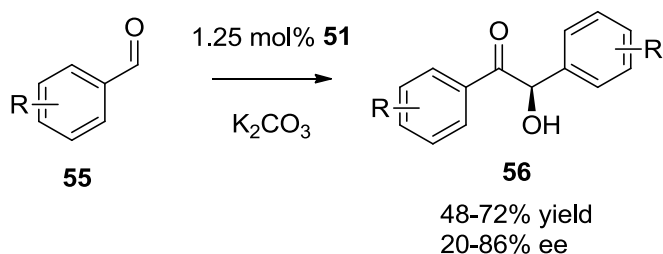


**Figure 6 Chiral thiazolium and triazolium precatalysts developed for the benzoin condensation**

It wasn't until the advent of triazolium NHCs, the development and application of which was pioneered by Enders and co-workers in the mid-90s,<sup>45</sup> that high enantioselectivities for benzoin condensations were achieved. In early work, Enders achieved self-condensation of a variety of aldehydes in moderate to high yields and low to excellent enantiomeric excess at an unprecedented low catalyst loading of 1.25 mol % using triazolium precatalyst **51** (Scheme 4).<sup>46</sup> Later work by Enders in 2002 further increased the enantioselectivity by introducing a rigid chiral bicyclic scaffold to the triazolium catalyst in **52**, albeit at the expense of requiring a higher catalyst loading of 10 mol%.<sup>47</sup>

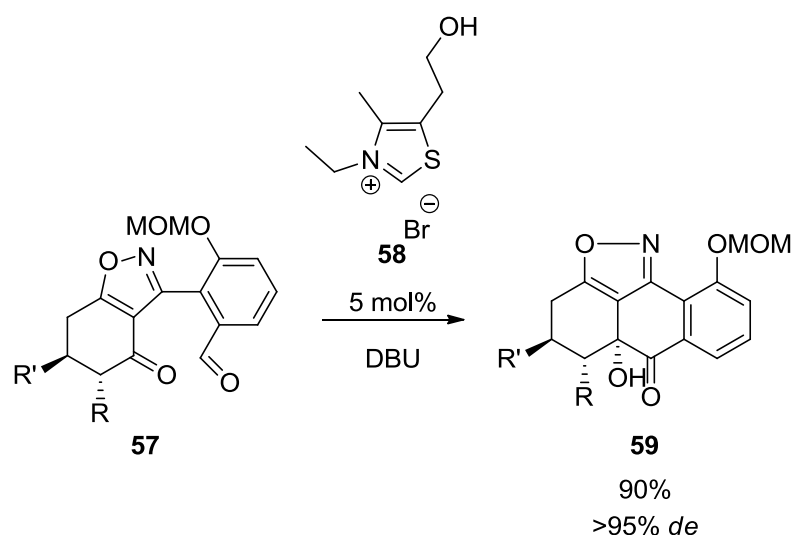


**Scheme 4**

Leeper's direct comparison of chiral thiazolium NHCs versus analogous chiral triazolium catalysts (**49**, **52**, **50**, **53**) also clearly demonstrated the superiority of the latter in achieving asymmetric induction.<sup>48</sup> Leeper reasoned that the *N*-phenyl substituent, which lies almost

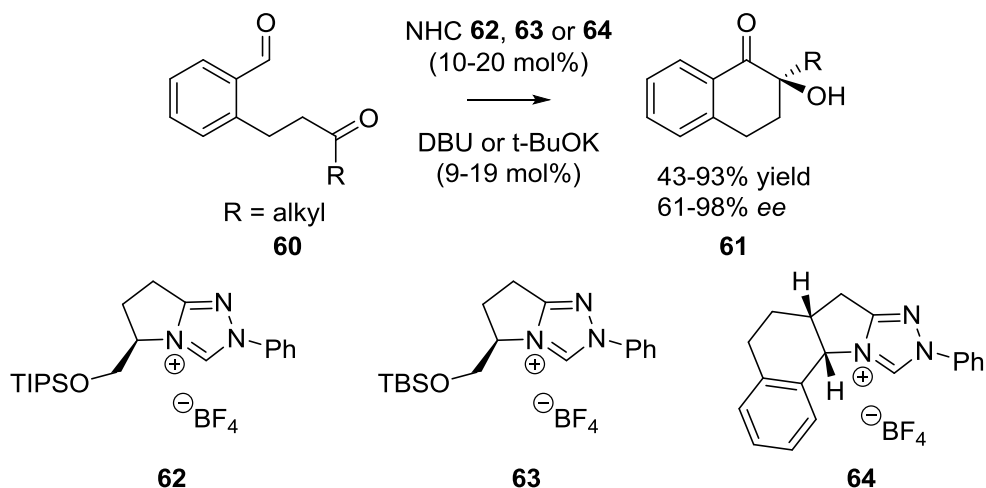
perpendicular to the heterocyclic ring, played an important role in promoting selective reaction at one face of the enamine Breslow intermediate. Enders did not explicitly state the importance of the *N*-phenyl substituent in directing attack, however it is conceivable that it indeed plays a role as free rotation about the *N*-bound chiral auxiliary in **51** would make facial selectivity difficult to predict on steric arguments involving the chiral auxiliary alone. Indeed, development of novel NHC precatalysts for use in acyl anion-type chemistry in recent years has focused on the triazolium scaffold, due to greater control of the steric and electronic nature of the ring when divalent sulphur is replaced by trivalent nitrogen at the crucial position that flanks the carbene centre.<sup>49</sup>

The first crossed acyloin condensation in which the coupling partners are an aldehyde and a ketone was reported by Suzuki et al. in their efforts to prepare substituted preanthroquinones (Scheme 5).<sup>50</sup>



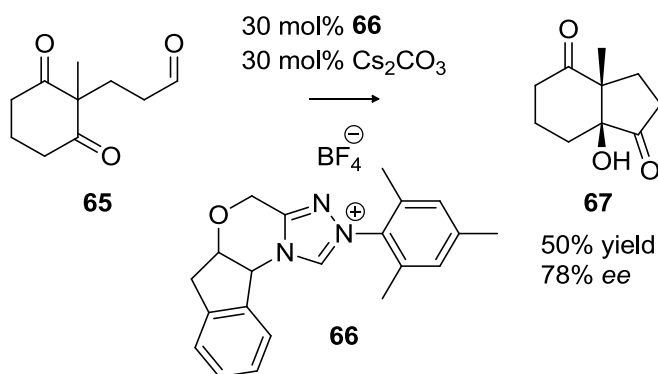
**Scheme 5**

As a crossed benzoin-type reaction, challenges can be faced in suppressing homocoupling of the aldehyde as well as undesired aldol reactions. In some cases these products are not observed and the cross-coupling dominates (as in the above example), but in other cases may be controlled by high dilution or preforming of the carbene catalyst with a substoichiometric amount of base compared to precatalyst.<sup>51</sup> These controls were successfully employed by Enders et al. with asymmetric intramolecular cross benzoin-type condensations between aldehyde and ketone functional groups in dicarbonyl compound **60** with good to high yield and good to excellent enantioselectivity (Scheme 6).<sup>52</sup>



**Scheme 6**

Ema et al. have synthesised a wide range of bicyclic tertiary alcohols from cyclic 1,3-diketones.<sup>53</sup> The use of chiral catalysts gave moderate to good enantioselectivities (Scheme 7). Apart from this report there is relatively little exploration of the potential of aliphatic aldehydes and ketones as coupling partners in an NHC-catalysed acyloin condensation.

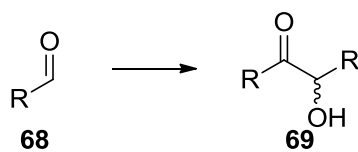


**Scheme 7**

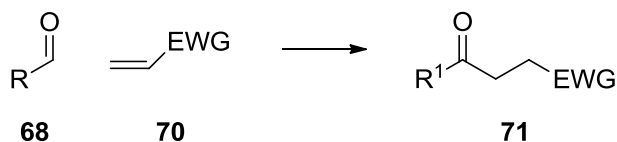
A 1995 patent claims the synthesis of *D-chiro* inositol directly from glucodialdose using a thiazolium catalyst, however no information on yield, stereoselectivity, characterisation data or even the specific catalyst used was given.<sup>54</sup>

In addition to self-condensations, NHCs have also been demonstrated to efficiently catalyse a diverse range of chemical transformations. These are shown in Scheme 8 as examples of possible chemistry and include Stetter reactions,<sup>55,56</sup> transesterifications,<sup>57</sup> and Diels-Alder chemistry via homoenolate formation.<sup>58</sup>

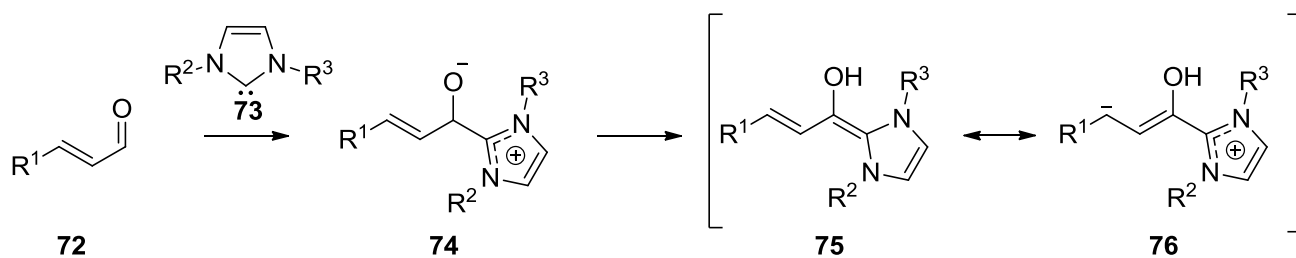
### Benzoin Condensation



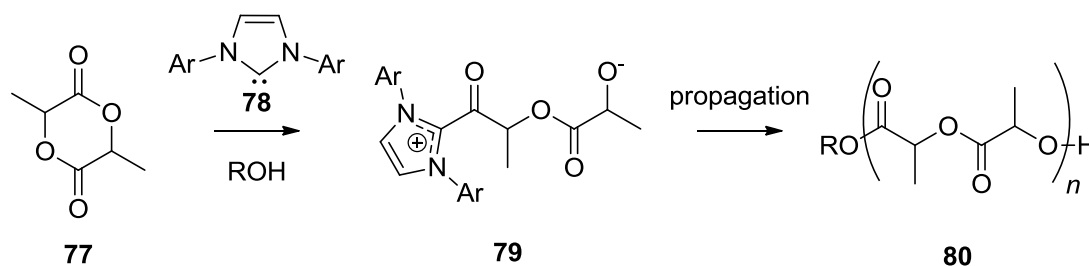
### Stetter Reaction



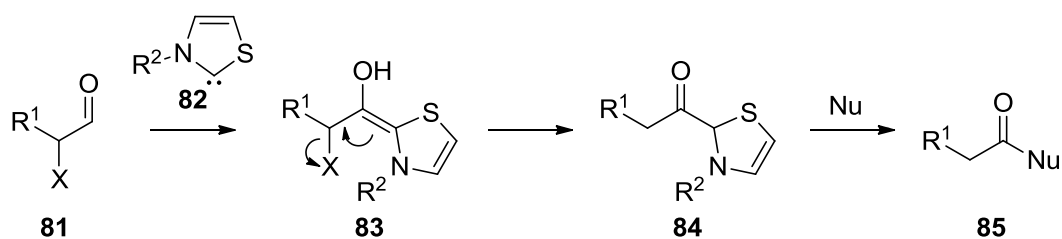
### Homoenolate formation



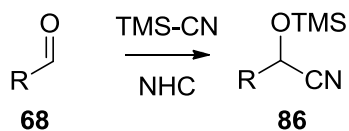
### Ring-opening polymerisation



### Redox Esterification/Amidation



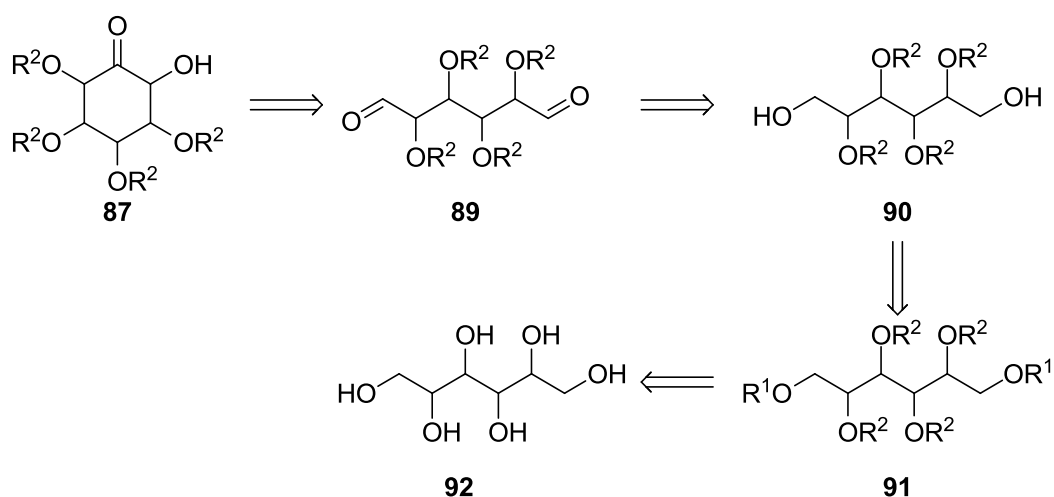
### 1,2-Addition



Scheme 8

There has been some recent applications of NHC organocatalysis in carbohydrate chemistry, notably the deoxygenation of hexose and pentose sugars to give 2-deoxylactones<sup>59</sup> and C-glycosylations of nitroglycals.<sup>60</sup>

Due to the importance of the inositol ring-system and the difficulty in accessing protected derivatives, the application of NHC catalysis was investigated. It was envisaged that a benzoin-type condensation mediated by NHCs may furnish cyclic acylolins **87** from protected carbohydrate-derived dialdehydes **89** (Scheme 9). The dialdehydes **89** could be prepared simply from a suitable alditol **90** and the protocol could be theoretically extended to both hexitols and pentitols. This would potentially be of use as an alternative to existing protocols for synthesising carbocyclic sugars, and serve as a platform for the synthesis of more complex molecules.

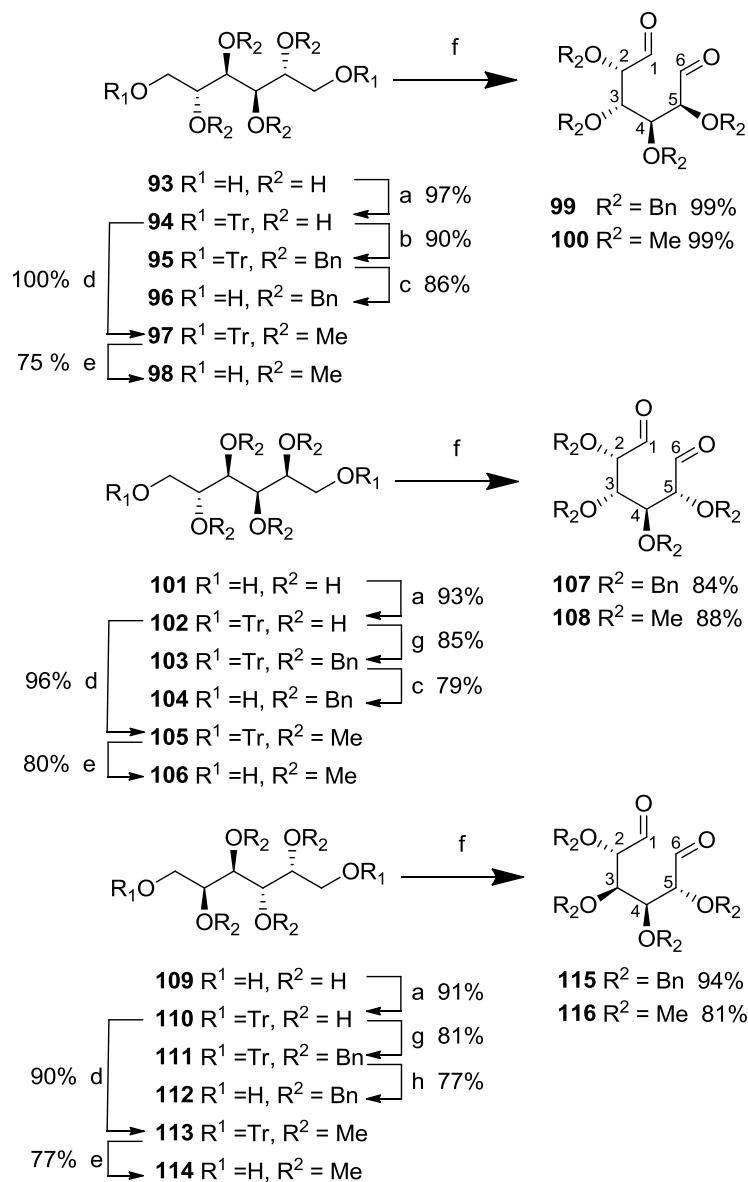


**Scheme 9**

## RESULTS AND DISCUSSION

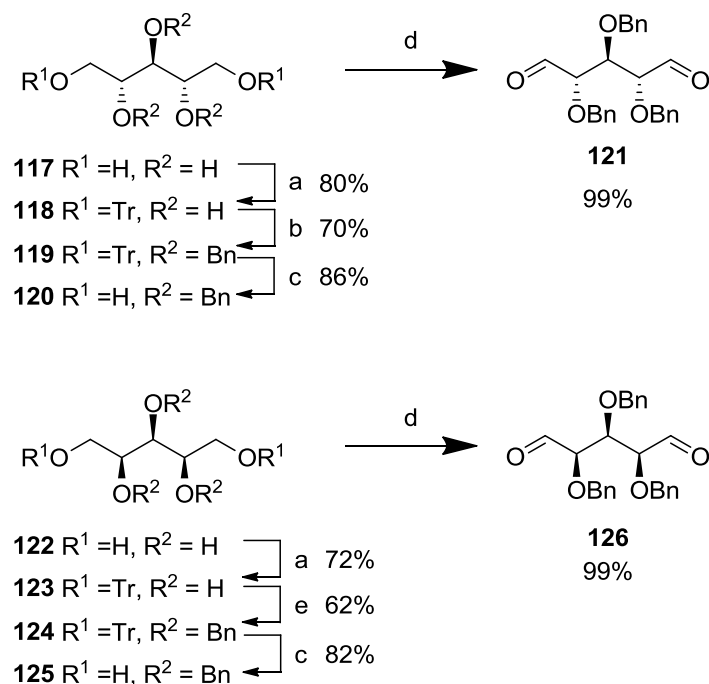
### Synthesis of dialdehydes

Simple protocols for protection of the primary alcohols of alditols as their trityl ethers followed by *O*-benzylation or *O*-methylation of the remaining secondary alcohols and subsequent acid hydrolysis of the trityl groups and oxidation have been established in the literature.<sup>25,61-65</sup> These protocols were successfully applied to both hexitols (*manno*-, *gluco*- and *galacto*-, Scheme 10) and pentitols (*xylo*- and *ribo*-, Scheme 11) to yield the appropriate dialdehyde substrates **100**, **108**, **116**, **120** and **125**.



a) TrCl, pyr., reflux, 1.5 h; b) BnBr, NaH, Bu<sub>4</sub>NI, THF 25 °C, 6 h, reflux, 19 h; c) 2:1 DCM/MeOH, TFA, 18 h; d) MeI, NaH, THF, 25 °C, 18 h; e) 1:1 DCM:MeOH, *p*-TSA, 18 h; f) i) (COCl)<sub>2</sub>, DMSO, DCM, -78 °C, 25 min. ii) Et<sub>3</sub>N, -78 °C - rt., 1.5 h; g) BnBr, NaH, THF, 25 °C; h) 3:1 Toluene/MeOH, TFA, 65 °C, 16 h.

**Scheme 10**



a) TrCl, pyr., reflux, 1.5 h; b) BnBr, NaH, Bu<sub>4</sub>Ni, THF rt. 18 h, reflux 4.5 h; c) 2:1 DCM/MeOH, TFA, 18 h; d) i) (COCl)<sub>2</sub>, DMSO, DCM, -78 °C, 25 min. ii) Et<sub>3</sub>N, -78 °C - rt., 1.5 h; e) BnBr, NaH, Bu<sub>4</sub>Ni, THF rt. 18 h, reflux 24 h.

### Scheme 11

The general approach involved bis-*O*-tritylation of the alditol at the 1,6 or 1,5 positions for hexitols or pentitols respectively. The steric bulk of the trityl group makes it highly selective for primary alcohols and suited for this purpose. Refluxing the alditol in pyridine with trityl chloride over the course of 1.5 hours afforded the partially-protected sugars **93**, **101**, **109**, **117** or **122** in good to excellent yield (72-97%). Spectroscopic data was consistent with the literature for compounds **94**<sup>61</sup>, **102**<sup>65</sup>, **110**<sup>62</sup> and **118**.<sup>66</sup>

Assignment of the structure of **123** was made on the basis of <sup>1</sup>H and <sup>13</sup>C NMR spectroscopy. Although 1,5-di-*O*-trityl-D-xylitol **123** is reported in the literature by Gallos et al.,<sup>64</sup> they do not report spectral data. The symmetrical structure of **123** gave rise to six unique resonances in the aliphatic region of the <sup>1</sup>H NMR spectrum, however the three hydroxyl protons had similar chemical shifts appearing as a broad singlet at 3.80 ppm. The two sets of equivalent diastereotopic methylene protons appeared as overlapping *dd* signals at 3.38 ppm and 3.30 ppm. Although a *ddd* signal was expected for the two equivalent protons at C2 and C4, coupling to adjacent protons was weak and only a broadened singlet was observed for these protons at 3.05 ppm. Lack of coupling between the protons at C2/C4 and C3 was further evidenced by the multiplicity of the C3 proton which appeared as a doublet at 2.94 ppm due to coupling with the hydroxyl proton. As

expected, five unique  $^{13}\text{C}$  NMR signals were observed for the benzylic, *ipso*-, *ortho*-, *meta*- and *para*-carbons of the trityl groups as well as three unique signals in the aliphatic region for the remaining carbons.

The remaining secondary alcohols in **94**, **102**, **110**, **118** and **123** were benzylated or methylated under standard conditions using NaH and BnBr or MeI in THF.<sup>67</sup> Minor modifications to these procedures were made to adapt them to the various sugars. Benzylations in particular appeared to occur ideally differently for each sugar. Some substrates required reflux or addition of a catalytic amount of  $\text{Bu}_4\text{NI}$  to reach completion.<sup>68</sup> Benzyl ether-protected hexitols and pentitols were obtained in good yield by this method (70-85%) except for **124** which was only obtained in moderate yield (62%). Methyl ether-protected hexitols were obtained in high to excellent yield (82-100%). Spectroscopic data for **95**,<sup>69</sup> **97**,<sup>61</sup> **103**,<sup>69</sup> **105**,<sup>65</sup> **113**<sup>62</sup> and **119**<sup>66</sup> was consistent with the literature.

The structural assignment of 1,6-di-*O*-trityl-2,3,4,5-tetra-*O*-benzyl-D-galactitol **111** was made on the basis of  $^1\text{H}$  and  $^{13}\text{C}$  NMR spectroscopy. The diastereotopic benzylic protons appeared as a series of overlapping doublets between 4.32-4.56 ppm. The two sets of equivalent diastereotopic methylene protons of the back bone appeared as broadened multiplets between 3.95-4.04 and 3.83-3.93 ppm. The remaining four protons signals overlap to give a multiplet between  $\delta$  3.25-3.41 ppm. Six unique  $^{13}\text{C}$  NMR resonances were observed as expected for the symmetrical protected sugar.

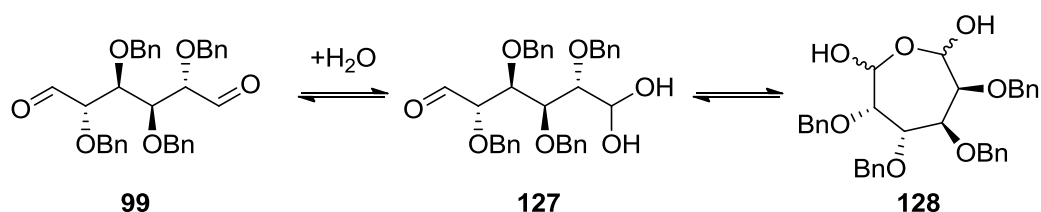
The structural assignment of 1,5-Di-*O*-trityl-2,3,4-tri-*O*-benzyl-D-xylitol **124** was made on the basis of  $^1\text{H}$  and  $^{13}\text{C}$  NMR spectroscopy. Gallos et al.<sup>64</sup> also report the synthesis of **124**, however no spectral data was provided. The  $^1\text{H}$  NMR spectrum of **124** is consistent with a symmetrical structure. The diastereotopic methylene protons at C1/C5 appear as *dd* signals at 3.30 and 3.59 ppm. A *ddd* signal is expected for the equivalent protons at C2 and C4 however they are observed as a broadened multiplet at 3.94 ppm. The proton at C3 is observed as a triplet due to coupling with the equivalent protons at C2 and C4. The six benzylic protons are identified as two doublets and a broadened singlet at 4.32, 4.57 and 4.90 ppm respectively. As expected, the  $^{13}\text{C}$  NMR spectrum displayed six unique resonances in the aliphatic region. Overlapping of  $^{13}\text{C}$  NMR signals of the aromatic carbons was observed.

Removal of the trityl group from the fully-protected alditols has been achieved by hydrolysis by strong acid such as sulphuric acid, *p*-TSA or TFA in an alcoholic solvent.<sup>64,66,70</sup> Addition of a co-solvent is generally necessary to solvate the starting material. In the current work, detritylations of

the benzyl-ether-protected alditols in all but one case were achieved by stirring overnight in 2:1 MeOH/DCM with TFA. Ether **111** was poorly soluble in a wide variety of solvents, and the detritylation of **111** to give **112** had to be performed in refluxing 1:3 MeOH/toluene, again with TFA. The benzyl ether-protected diols were obtained by these methods in good to high yield (70-83%). Efficient detritylation of the methyl ether-protected alditols was affected in 1:1 DCM/MeOH with *p*-TSA.H<sub>2</sub>O in good yield (75-80%). Spectroscopic and mass data for **96**,<sup>71</sup> **98**,<sup>61</sup> **104**,<sup>71</sup> **106**,<sup>65</sup> **112**,<sup>70</sup> **114**<sup>62</sup> and **120**<sup>66</sup> was consistent with the literature.

The structural assignment of 2,3,4-tri-*O*-benzyl-D-xylitol **125** was made on the basis of <sup>1</sup>H and <sup>13</sup>C NMR spectroscopy. Gallos et al.<sup>64</sup> also reported the synthesis of **125** however no spectral data was given. The protons of the pentitol backbone were poorly resolved at 300 MHz and appeared as two multiplet signals in the region 3.57–3.85 ppm. Similar to **124**, in the <sup>1</sup>H NMR spectrum of **125**, the benzylic protons appear as two doublets and a broadened singlet at 4.64, 4.66 and 4.72 ppm respectively. The hydroxyl protons appeared as a broadened singlet at 2.37 ppm. Five unique <sup>13</sup>C NMR resonances were observed in the aliphatic region as expected for the symmetrical diol.

Standard Swern oxidation<sup>72</sup> of diols **96**, **98**, **104**, **106**, **112**, **114**, **120**, **125** gave excellent yields of the corresponding dialdehydes (82-100%). Spectroscopic data for **100**,<sup>61</sup> **108**<sup>65</sup> and **116**<sup>62</sup> was consistent with the literature. Although dialdehydes **99**,<sup>70</sup> **107**,<sup>70</sup> **115**,<sup>70</sup> and **126**<sup>64,73</sup> are reported in the literature, their spectroscopic data has not been reported until now. Over the course of 24 hours it was noticed that the resonances assigned to dialdehyde **99** were replaced with a complex mixture of resonances that have been tentatively assigned to products of hydration **127** and subsequent hemiacetal formation to give isomers of **128** based on a series of peaks in the <sup>13</sup>C NMR spectrum from 99.9 – 97.3 ppm.



**Scheme 12**

It was determined that the new mixture was in equilibrium with the dialdehyde **99** as treatment with ethyl (triphenylphosphoranylidene) acetate afforded diethyl (2*E*,8*E*)-4,5,6,7-tetra(benzyloxy)decan-2,8-diendioate as the sole product by NMR. The diols were not stable to column chromatography and were stored at -15 °C before use. It was found that dialdehydes **121**

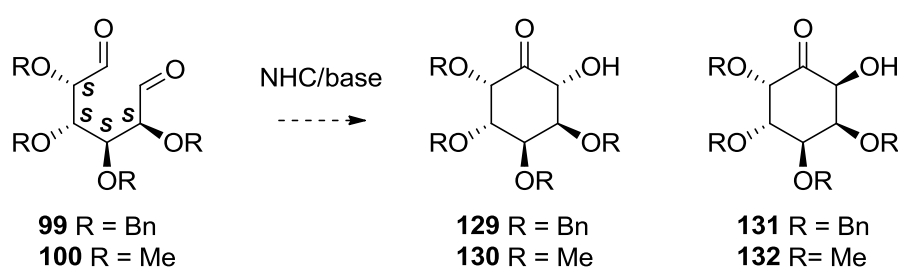
and **126** underwent much more rapid hydration and hemiacetal formation on exposure to moisture. It is reasoned that this is due to the fact that **121** and **126** would be expected to form more favourable six-membered hemiacetals compared to the hexitol dials which form seven-membered hemiacetals following hydration.

$^1\text{H}$  and  $^{13}\text{C}$  NMR data for dials **99**, **100**,<sup>61</sup> **107**, **108**,<sup>65</sup>, **115**, **116**,<sup>62</sup> **121**, and **126** appear in the Experimental section. Although individual spectra will not be discussed, general features of the spectroscopic data will be noted here. As expected for the symmetrical dials **99**, **100**, **115**, **116**, **121** and **126** a single aldehyde proton resonance was observed at  $\sim 10$  ppm. This corresponded through a HSQC correlation to a  $^{13}\text{C}$  NMR carbonyl resonance at  $\sim 205$  ppm. The aldehyde protons for these compounds coupled weakly or not at all with vicinal protons. For non-symmetrical dials **107** and **108**, two separate aldehyde resonances were observed in both the  $^1\text{H}$  and  $^{13}\text{C}$  NMR spectra.

## Carbocyclisation Reactions

### Carbocyclisation reactions of *manno*-dialdehydes

With the appropriate dialdehyde substrates in hand, the NHC-catalysed intramolecular benzoin condensations of these substrates were investigated. The carbocyclisations of *manno*-dialdehydes **99** and **100** were investigated first as their symmetry simplifies the reaction outcome with only two diastereomers being possible (Scheme 13).



**Scheme 13**

The three NHCs that were screened are shown in Figure 7 and the results are represented in Table 1.

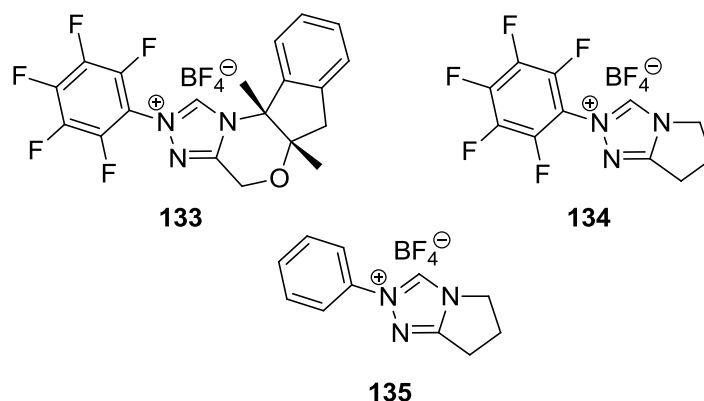
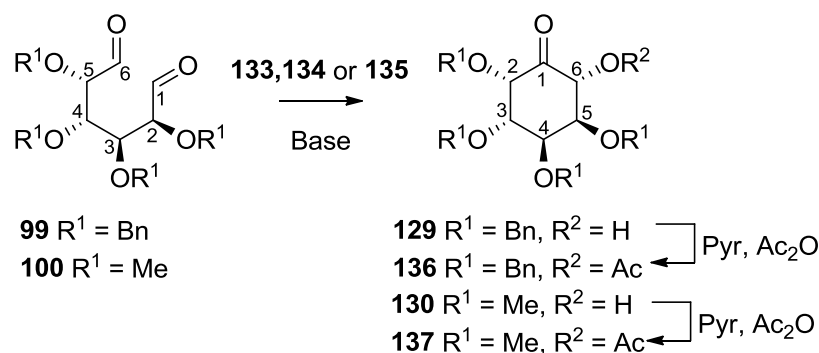


Figure 7 NHC pre-catalysts used in this study



Entry <sup>a</sup>	Aldehyde	Base (mol%)	Precatalyst (mol%)	Solvent	Temp	Time (hr)	Product	Yield <sup>b</sup>
1	<b>99</b>	DBU (15)	<b>133</b> (20)	Dioxane	100	24	<b>129</b>	22
2	<b>99</b>	DBU (15)	<b>134</b> (20)	Dioxane	100	24	<b>129</b>	40-50
3	<b>99</b>	Et <sub>3</sub> N (15)	<b>134</b> (20)	DCE	40	16	<b>129</b>	50
4	<b>99</b>	Et <sub>3</sub> N (100)	<b>134</b> (20)	DCE	40	16	<b>129</b>	70 <sup>c</sup>
5	<b>99</b>	DBU (15)	<b>135</b> (20)	Dioxane	25	24	-	-
6	<b>99</b>	Et <sub>3</sub> N (10)	<b>134</b> (15)	DCE	40	16	<b>129</b>	55
7 <sup>d</sup>	<b>99</b>	Et <sub>3</sub> N (15)	<b>134</b> (20)	DCE	40	16	<b>129</b>	75
8	<b>100</b>	Et <sub>3</sub> N (15)	<b>134</b> (20)	DCE	40	16	<b>130</b>	62
9	<b>100</b>	Et <sub>3</sub> N (100)	<b>134</b> (20)	DCE	40	16	<b>130</b>	59

<sup>a</sup> Reactions were performed on 100 mg of dialdehyde in 5 mL of solvent. <sup>b</sup> Isolated yield by flash chromatography. <sup>c</sup> Crude yield after filtration through silica and elution with 1:1 EtOAc/hexanes. <sup>d</sup> The crude mixture was peracetylated prior to chromatography.

Table 1 NHC-promoted cyclisations of **99** and **100**

The dialdehyde **99** was completely consumed in 24 hours when stirred with **133**, **134** or **135** with DBU or NEt<sub>3</sub>. A single diastereomer was isolated from the reactions with **133** and **134** and assigned as inosose **129**. Reactions performed starting with the relatively electron-rich pre-catalyst **135** yielded complex mixtures and it was subsequently excluded from further experiments.

Similar yields were obtained using methyl ether protected dial **100** and the stereochemistry of the major product **130** was found to be the same. The choice of base played an important role in the reaction outcome for which there is ample literature precedence.<sup>52,53</sup> Triethylamine gave superior yields to DBU while early attempts using potassium *tert*-butoxide gave complex mixtures. Crude NMR spectra from the reactions suggested that yields should have been higher and some material was decomposing during silica gel chromatography. Acetylation of the crude reaction mixture from the carbocyclisation of **99** afforded an increased yield of cyclised product **136** which had greater stability during isolation (entry 7).

### Structural assignments

Structural assignment of inosose **129** was made on the basis of <sup>1</sup>H and <sup>13</sup>C NMR experiments as well as 2D NMR experiments. Observation of the coupling constants in the <sup>1</sup>H NMR spectra gave strong evidence for a chair conformation, with large couplings observed consistent with *trans*-diaxial <sup>3</sup>J<sub>H,H</sub> interactions.<sup>74</sup> Acetate ester **136**, prepared on small scale using acetic anhydride in pyridine, had improved resolution in the <sup>1</sup>H NMR spectrum and so was used to assign the structure. It is noted that the eight diastereotopic benzylic protons appeared as a series of doublets at ~4.25-4.80 ppm however attempts were not made to specifically assign their position in the ring. The assigned <sup>1</sup>H and <sup>13</sup>C NMR spectra of both **129** and **136** are presented for reference in Figure 8 and Figure 9 respectively.

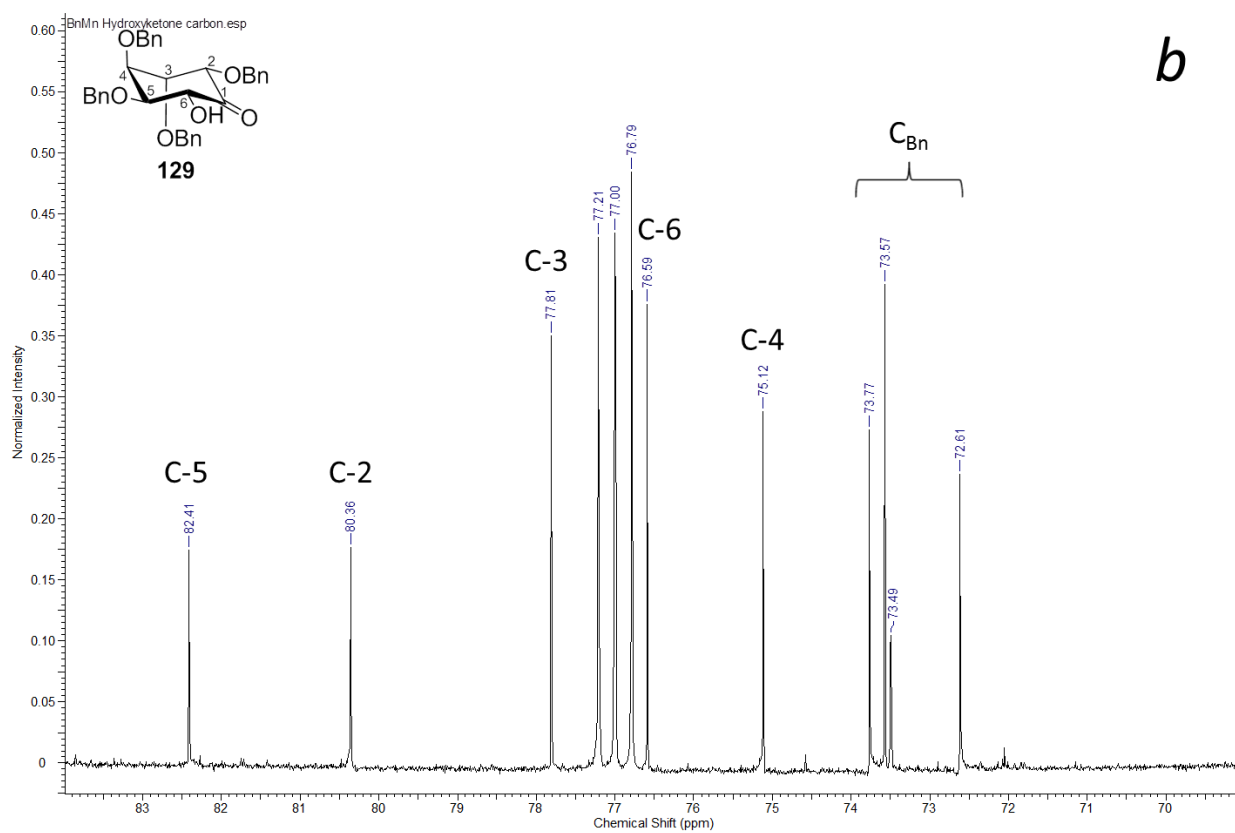
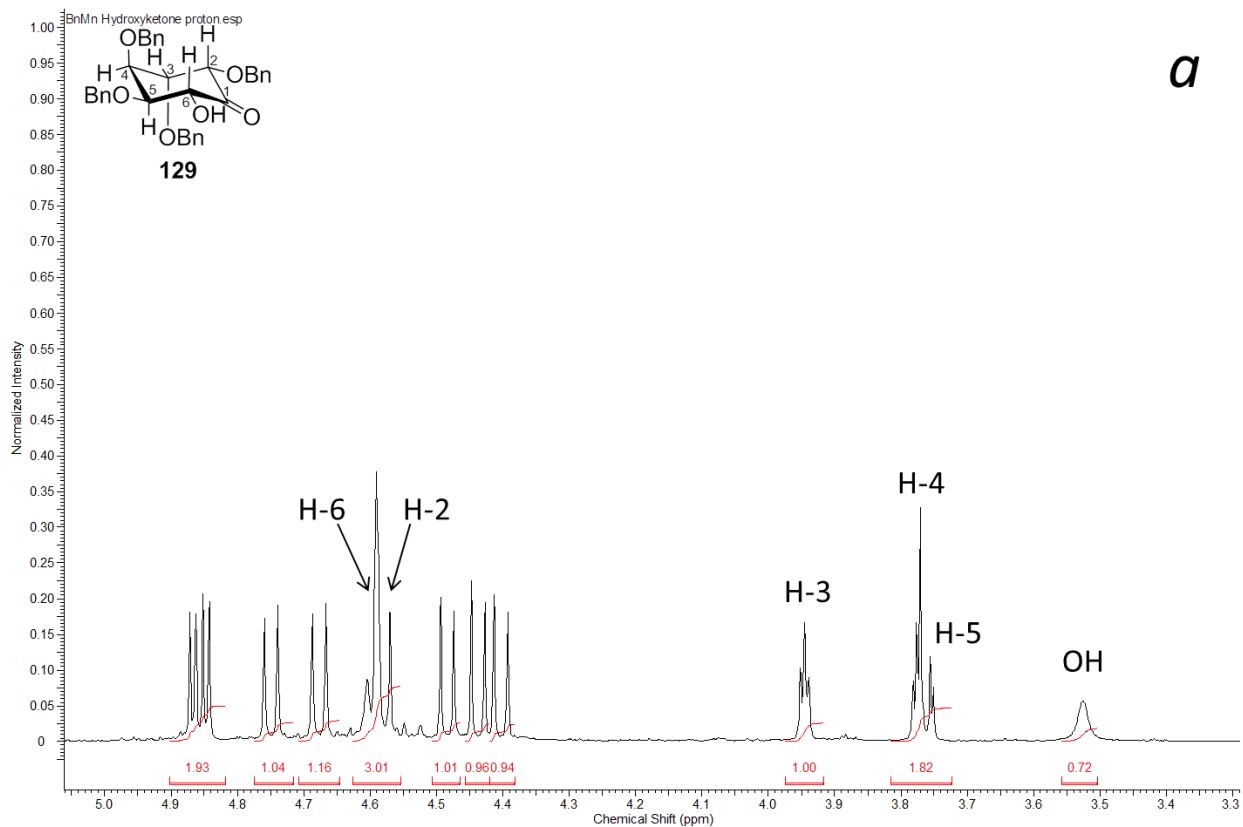
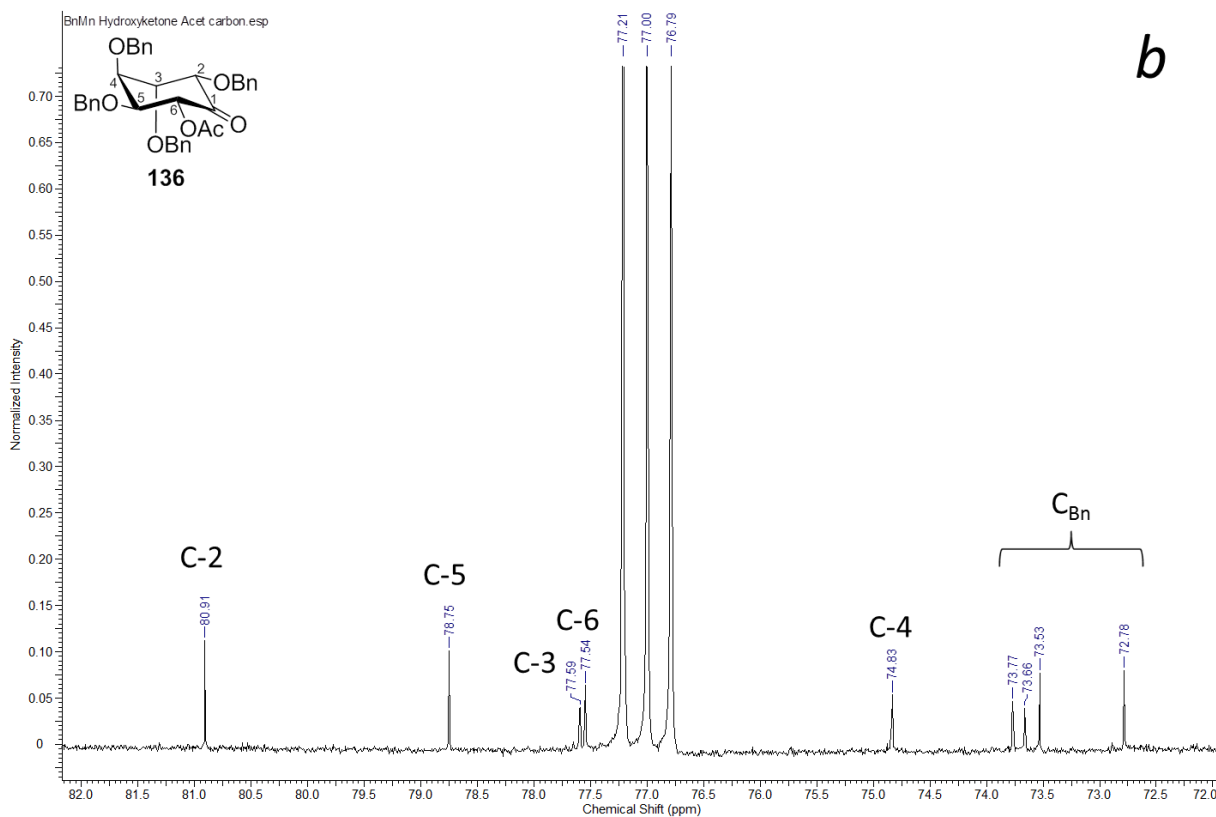
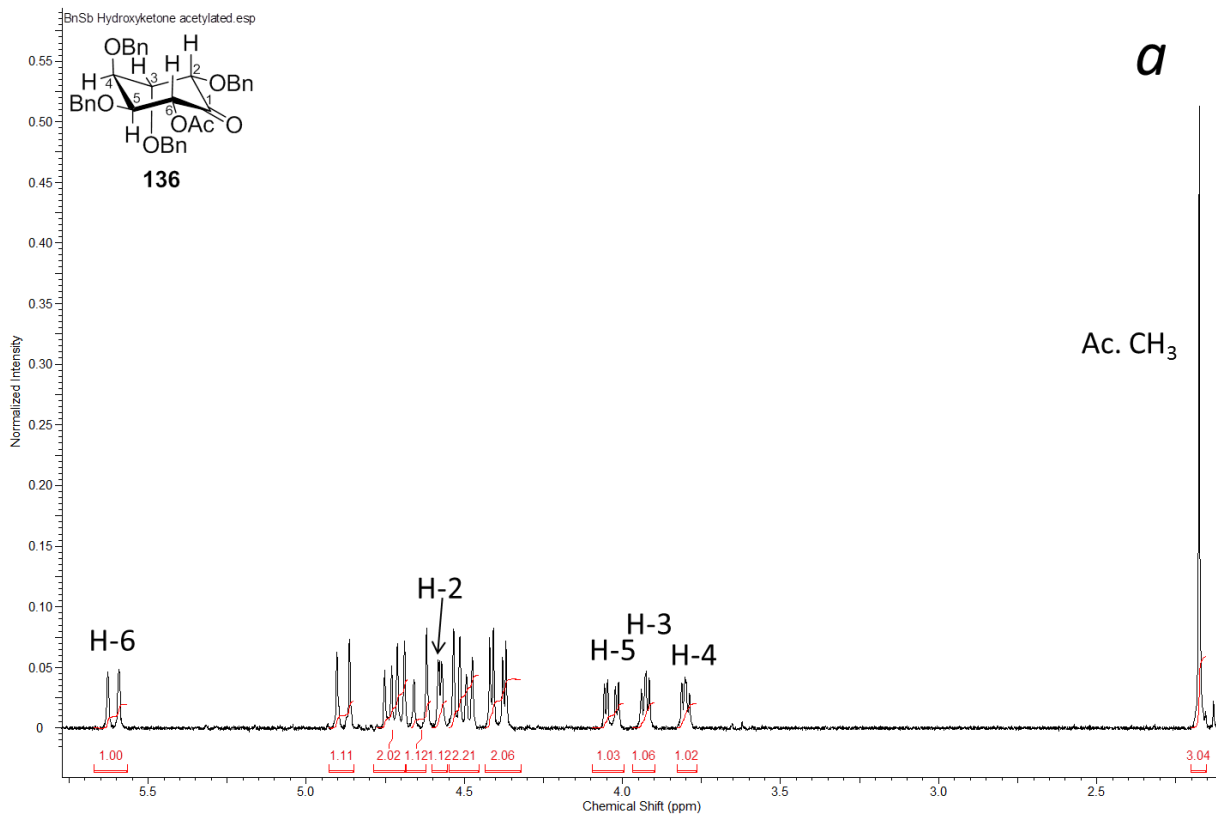


Figure 8a) 300 MHz  $^1\text{H}$  and b) 75 MHz  $^{13}\text{C}$  NMR spectra of 129 in  $\text{CDCl}_3$



**Figure 9 a) 300 MHz <sup>1</sup>H and b) 75 MHz <sup>13</sup>C NMR spectra of 136 in CDCl<sub>3</sub>**

Protons H6 and H2 of **129** were assigned on the basis of an expected downfield shift in relation to the other ring protons due to proximity to the carbonyl. The multiplicity of the two resonances could not be distinguished at 300 or 600 MHz as both protons had similar chemical shifts in the region 4.56–4.64 ppm and also overlapped with one of the doublet signals of a benzylic proton. The chemical shift of proton H6 was determined to be slightly downfield compared to H2 based on coupling information from a 2D COSY experiment once protons H5 and H3 had been assigned. Proton H3 was assigned as the *dd* signal at 3.95 ppm with two *gauche* couplings to protons H4 and H2 both of 3.8 Hz. The assignment was validated by a crosspeak in the 2D COSY spectrum indicating a coupling between this proton and H2. This would not be expected for proton H4 (although the multiplicity for this proton and coupling magnitude would be expected to be similar), nor is the multiplicity consistent with an assignment of proton H5, which would be expected to have a large *trans*-diaxial coupling with proton H6. Although the chemical shifts of protons H4 and H5 were similar, overlapping signals made the multiplicity difficult to distinguish and so their relative chemical shifts were assigned on the basis of coupling to the previously assigned signal for proton H3. Carbon resonances were assigned on the basis of a 2D HSQC experiment. The carbonyl is not shown in Figure 8b but appeared at 205 ppm.

Referring to Figure 9a, the signal for H6 in the acetate derivative **136** was shifted downfield compared to the  $\alpha$ -hydroxyketone **129** due to deshielding by the acetate group. Identification of H6 allowed unambiguous assignment of the other ring proton resonances with a 2D COSY NMR experiment. Coupling constant data for the ring protons was extracted and used to assign the stereochemistry of the product.

In the acetate derivative **136**, a single large coupling of 10.4 Hz between H6 and H5 was observed, indicative of a *trans*-diaxial relationship. The smaller 3.2 Hz coupling of H5 and H4 indicated a *cis*-configuration. H3 could not be assigned as axial or equatorial on coupling information alone as coupling constants would be expected to be small for either configuration. A crosspeak in the 2D ROESY spectrum (Figure 10) shows a through-space interaction between H6 and H2 which would only be expected if they were on the same face of the ring, indicating a 1,3-diaxial relation. The small 3.2 Hz coupling between H2 and H3 confirmed a *cis*-configuration and a through-space interaction was also observed between these protons (as well as between H5 and H4). A  $^4J$  coupling between H2 and H6 across the carbonyl group was also observed in the COSY NMR spectrum. This coupling manifested as line broadening at H2 and H6 in the 1D  $^1\text{H}$  NMR spectrum at 600 MHz, although a clear *dd* signal was observed for H2 at 300 MHz. Normally  $^4J$

couplings are observed with protons which are bonded along an “M” or “W” path in a  $H_1XYZH_2$  system where all elements are completely coplanar. The strength of the coupling is observed to fall off rapidly with loss of coplanarity in these systems, however exception is found if Y is  $sp^2$  hybridised, and  $^4J$  couplings may still be observed even if  $H_1$  and  $H_2$  are perpendicular.<sup>75</sup> On this basis,  $^4J$  couplings could not be used to reliably assign stereochemistry. With all proton resonances assigned for the acetylated derivative,  $^{13}C$  NMR resonances were assigned by a 2D HSQC experiment. The carbonyl carbon resonances are not shown but appear at 198 ppm (ketone) and 170 ppm (ester). The methyl carbon of the acetyl group appeared at 20.6 ppm.

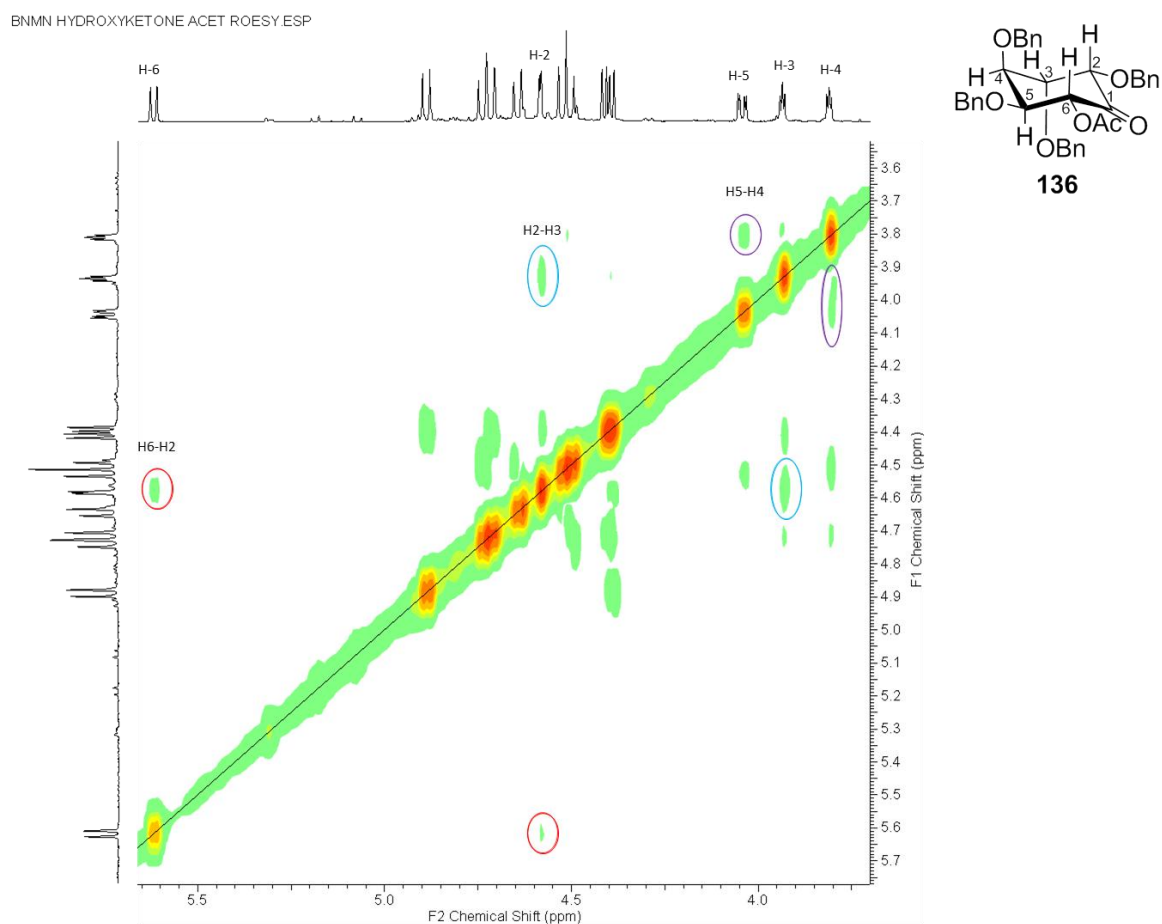


**Figure 10** 600 MHz 2D ROESY spectrum of **136** in  $CDCl_3$

The assigned  $^1H$  NMR and  $^{13}C$  NMR spectra for methyl ether-protected inosose **130** and its acetate derivative **137** based on 2D COSY and HSQC experiments are presented in Figure 11 and Figure 12 respectively.

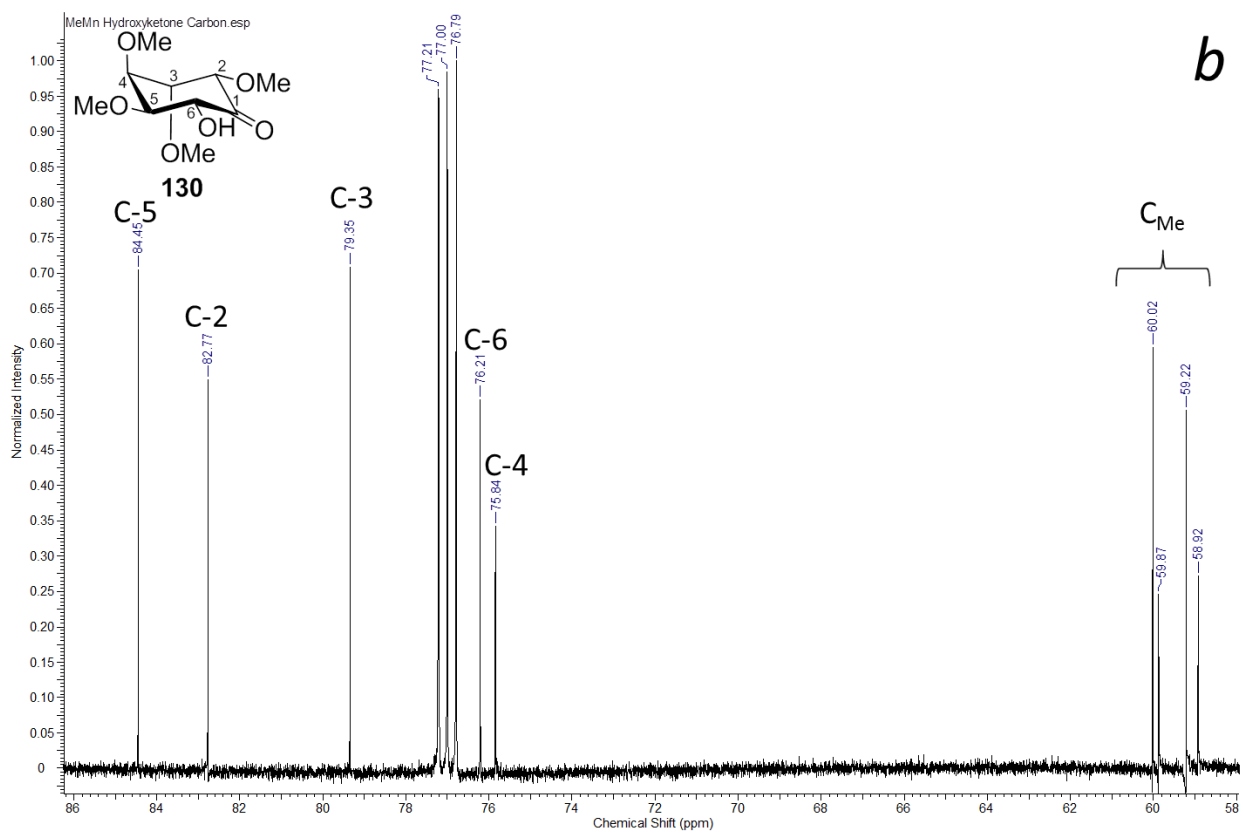
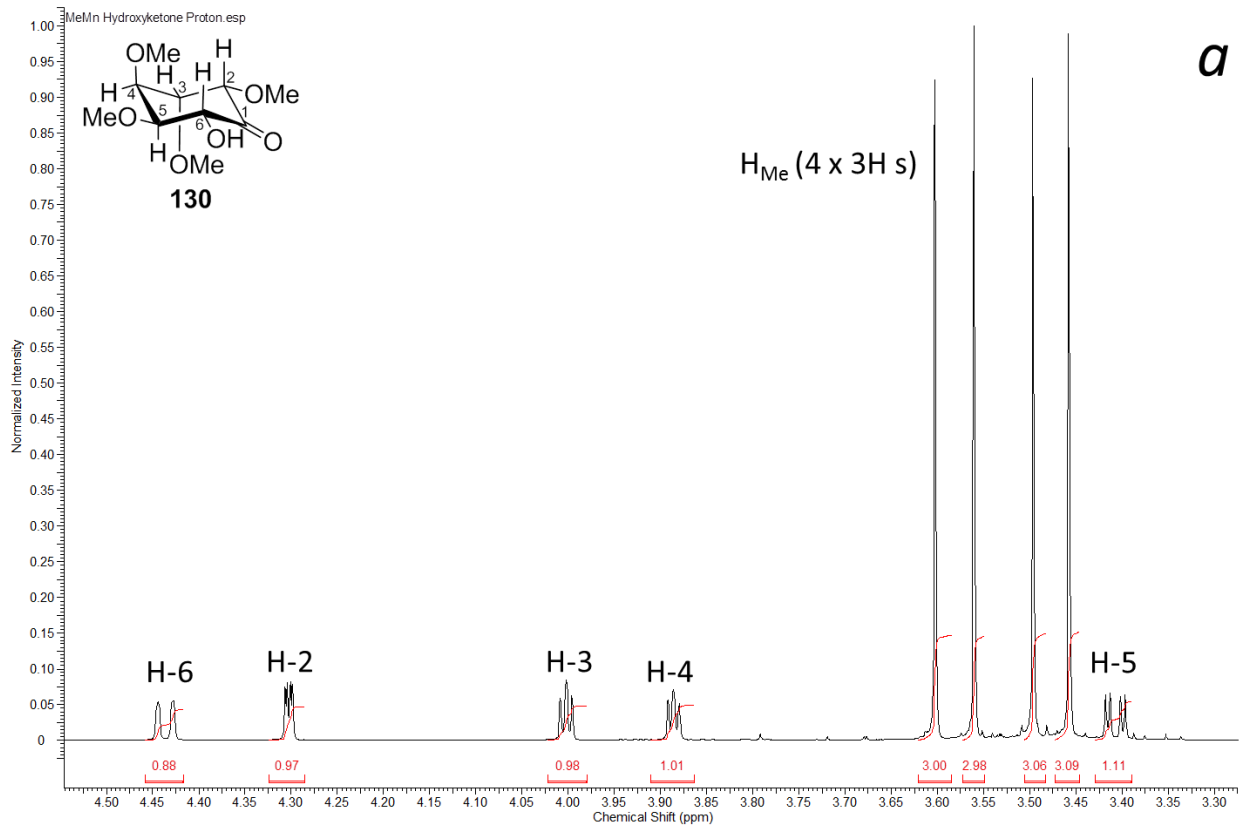


Figure 11 a) 600 MHz  $^1H$  NMR and b) 150 MHz  $^{13}C$  NMR spectra of 130 in  $CDCl_3$

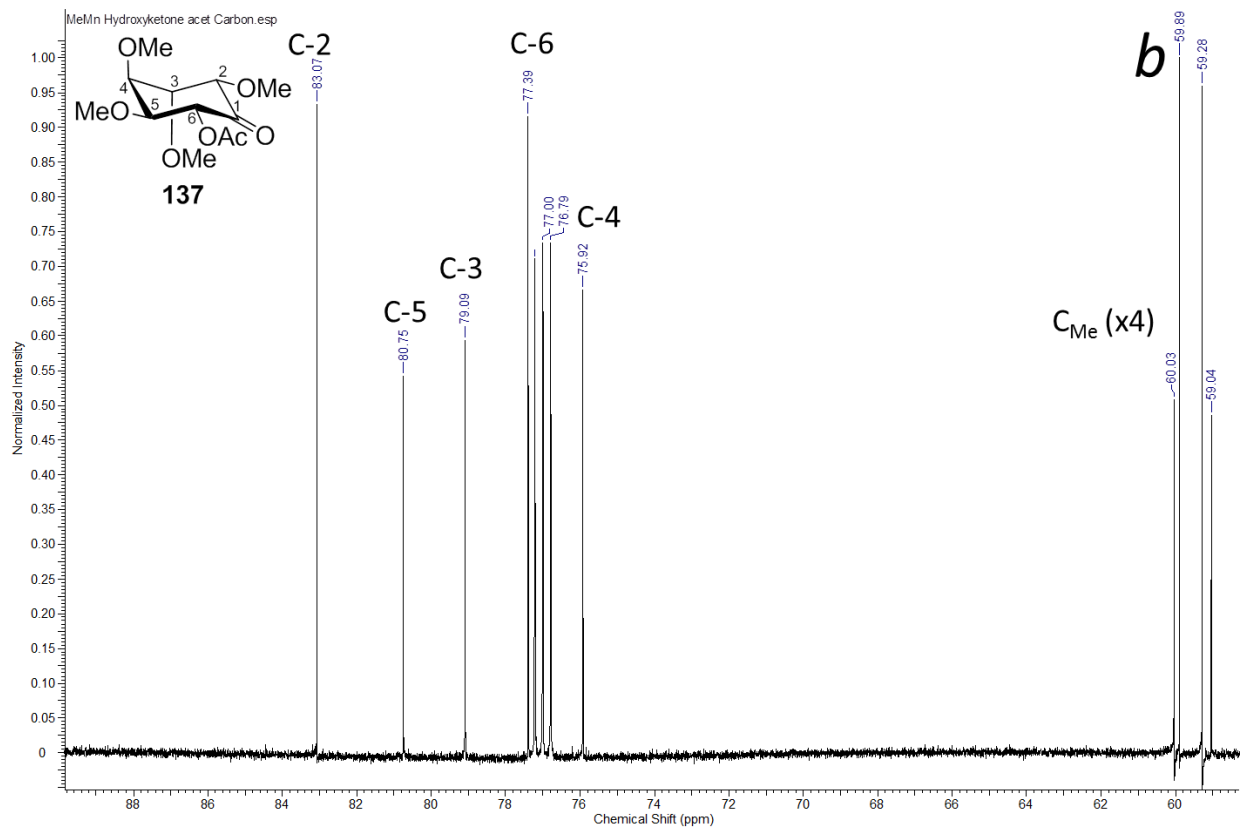
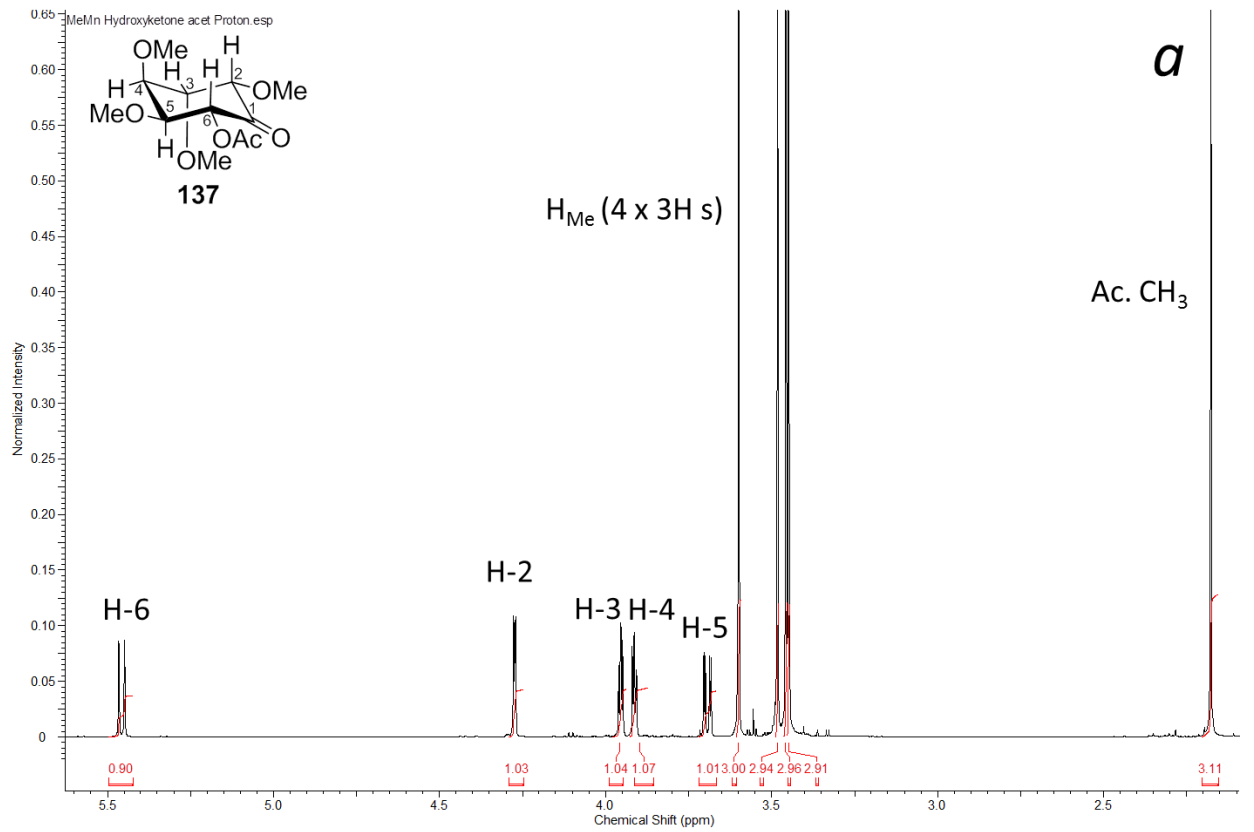
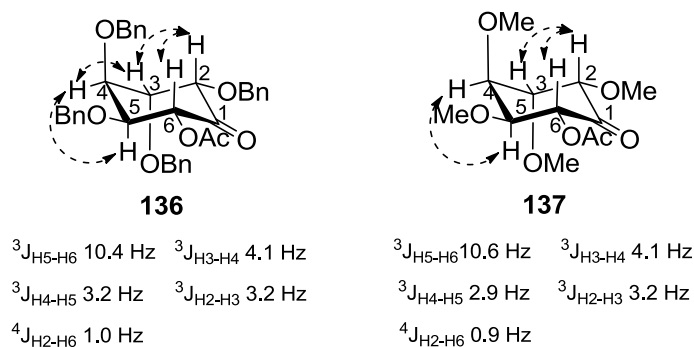


Figure 12a) 600 MHz <sup>1</sup>H NMR and b) 150 MHz <sup>13</sup>C NMR of 137

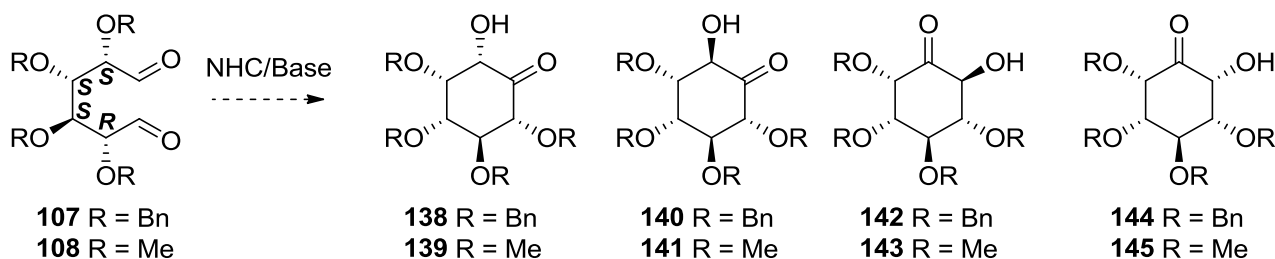
Coupling around the ring for the methyl ether analogue **130** and its acetate derivative **137** showed identical coupling patterns and similar ROESY interactions to those observed for **129** and **136**. A summary of coupling constants and ROESY interactions for acetate derivatives **136** and **137** is provided in Figure 13.



**Figure 13** Conformation, assignment, ROESY interactions (dashed arrows) and coupling constants of **136** and **137**.

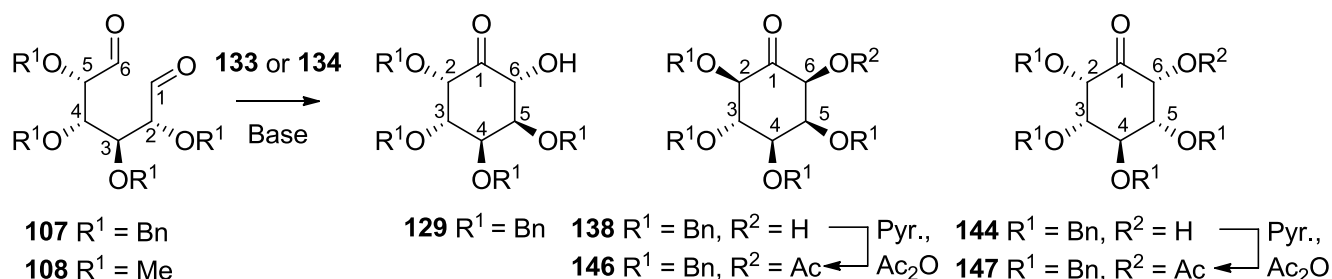
### Carbocyclisation reactions of sorbitol-derived *gluco*-dialdehydes

Sorbitol-derived dials **107** and **108** have no plane of symmetry and so four possible stereoisomers could arise from the cyclisations assuming all other stereocentres remained unchanged (Scheme 14).



**Scheme 14**

Table 2 shows the results of the carbocyclisations of **107** and **108** using the NHC precatalysts **133** and **134**.



Entry <sup>a</sup>	Aldehyde	Base (mol%)	Precatalyst (mol%)	Solvent	Temp (°C)	Products	Ratio <sup>b</sup>	Yield
1 <sup>c</sup>	<b>107</b>	Et <sub>3</sub> N (15)	<b>134</b> (20)	DCE	40	<b>129:138:144</b>	32:23:45	61
2	<b>107</b>	DBU (15)	<b>134</b> (20)	CH <sub>3</sub> CN	40	<b>129:138:144</b>	ND <sup>d</sup>	25
3	<b>107</b>	DBU (15)	<b>134</b> (20)	Diox.	40	-	-	0
4 <sup>e</sup>	<b>107</b>	DBU (15)	<b>134</b> (20)	DCE	25	<b>129:138:144</b>	42:19:39	35
5	<b>107</b>	Et <sub>3</sub> N (15)	<b>134</b> (20)	DCE	25	<b>129:138:144</b>	36:22:46	38
6	<b>107</b>	<i>i</i> -Pr <sub>2</sub> EtN (100)	<b>134</b> (20)	DCE	40	<b>129:138:144</b>	ND <sup>d</sup>	33
7	<b>107</b>	imidazole	<b>134</b> (20)	DCE	40	<b>129:138:144</b>	ND <sup>d</sup>	38
8	<b>108</b>	Et <sub>3</sub> N (15)	<b>133</b> (20)	DCE	25	-	- <sup>f</sup>	0

<sup>a</sup> Reactions were performed on 100-127 mg of dialdehyde in 50 mL/g solvent and left for 16 hours and products isolated by flash chromatography. <sup>b</sup> Ratios determined from isolated products. <sup>c</sup> Scale was 1.7 g of **107**. <sup>d</sup> The mixture of isomers isolated from the first column was not further purified and the ratio could not be accurately determined. <sup>e</sup> Reaction took 40 hours to reach completion. <sup>f</sup> Decomposition occurred on silica gel.

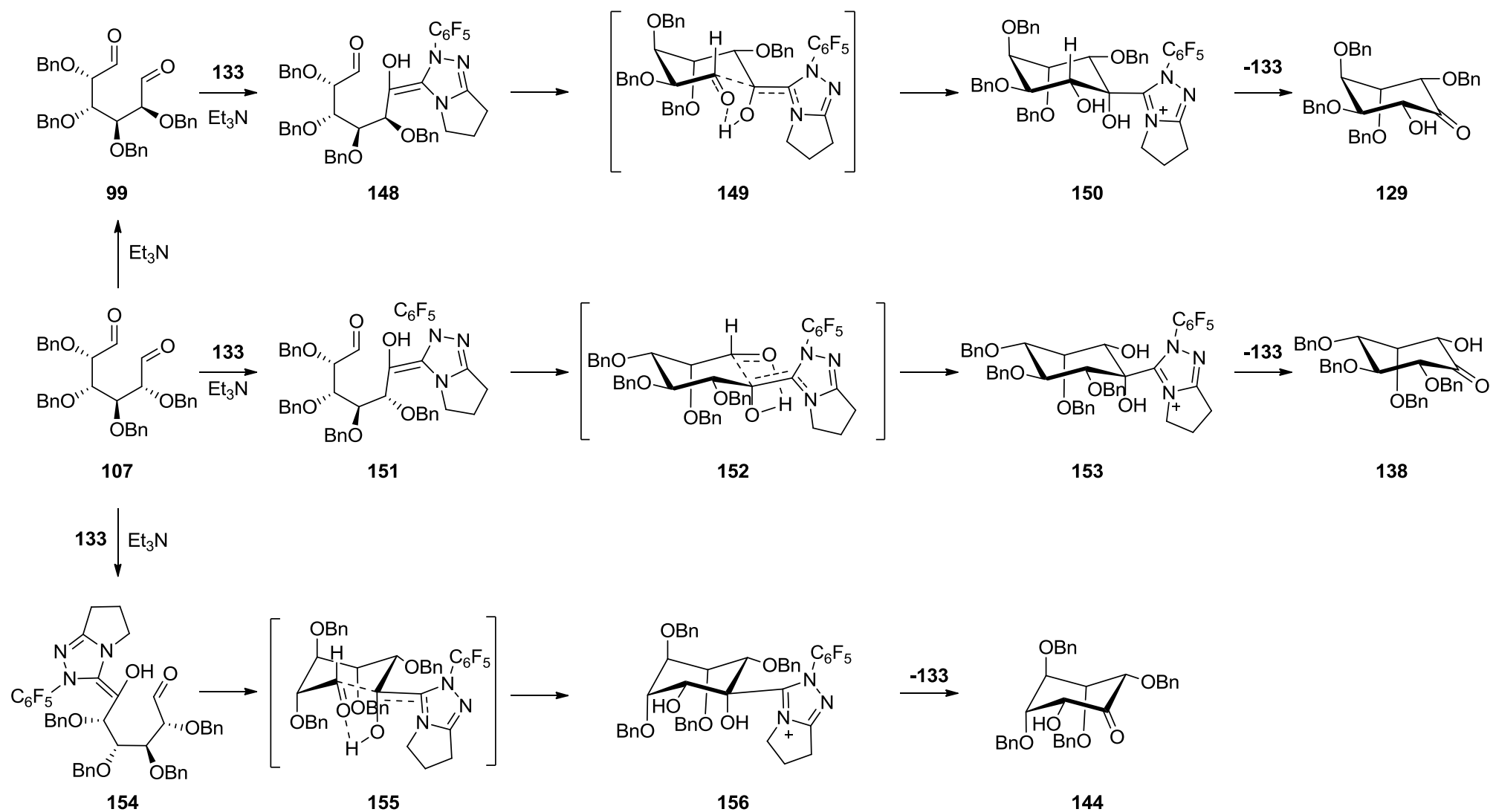
**Table 2 Carbocyclisations of *gluco*-dials **107** and **108****

In the best case (entry 1), a 61% yield of cyclisation products was isolated from the benzyl ether protected dialdehyde **107** using triethylamine, with extensive chromatography required to separate all stereoisomers. Initial purification with 7:13 EtOAc/hexanes in hexanes as eluent was sufficient in separating **129** ( $R_f = 0.43$ ) from **138** and **144** ( $R_f = 0.40$ ). Separation of **138** and **144** was achieved by switching eluent to 1:19 MeOH/toluene. Surprisingly, one of the isomers **129** isolated from the reaction mixtures of **107** was spectroscopically identical to that isolated from the

cyclisation of *manno*-dialdehyde **99**. The stereochemistry of the starting materials differ at C2 and epimerisation must occur prior to or during the cyclisation as the C5 centre is remote from the ketone moiety in the product. Cyclisation was observed for the methyl ether analogue **108**, however, decomposition occurred on silica and so the diastereomers were not separated or characterised.

The reaction manifold for dialdehyde **107** is shown in Scheme 15. Isomer **129** results from epimerisation at C2 in the starting material **107** generating *manno*-dialdehyde **99** and then formation of the Breslow intermediate **148** at C1 or C6. Cyclisation occurs through a possible transition state **149** which necessarily has two axial and two equatorial benzyl ethers and presumably an equatorial catalyst as this also allows for hydrogen bonding in the transition state. The cyclisation leads, after proton transfer, to the intermediate **150** which eliminates the catalyst affording observed **129**. This sequence, minus the initial epimerisation, is presumably in operation when starting with mannitol derived alditol **99**. The stereoisomer **138** can be derived directly from **107** by formation of the Breslow intermediate at C1 to give **151** followed by cyclisation of C1 onto C6 generating a new equatorial stereocentre via the possible transition state **152**. The cyclised intermediate **153** then eliminates the catalyst giving **138**. The pathway to isomer **144** involves formation of the regioisomeric Breslow intermediate **154** at C6 and then cyclisation of C6 onto C1 through a possible transition state **155** with three axial benzyl ethers and an equatorial catalyst (or its ring-flipped conformer) to afford **156** which eliminates the catalyst to give **144**. The observed conformation of **144** also has these three axial benzyl ethers so it is reasonable to propose a transition state such as **154**. Isomer **144** was difficult to isolate analytically pure as the compound was prone to decomposition on silica gel and several columns were required to remove other isomers.

When **129**, **138** and **144** were separately resubmitted to the reaction conditions, they were recovered unchanged indicating that the pathways to **129**, **138** and **144** are under kinetic control. Higher temperatures improved the yield of products but did not greatly affect isomeric ratios (compare entries 1 and 5 in Table 2).



**Scheme 15**

## Structural Assignments

Overlapping of signals in the  $^1\text{H}$  NMR spectrum of hydroxyketone **138** made assignment of stereochemistry difficult. Greater dispersion was observed in the spectrum of its acetate derivative **146** and stereochemistry was assigned with reference to this compound using 1D and 2D NMR experiments. The assigned  $^1\text{H}$  (Figure 14a) and  $^{13}\text{C}$  NMR (Figure 14b) spectra, as well as the ROESY NMR spectrum for **146** (Figure 15) are provided as reference. The chemical shift of H6 was assigned as the furthest downfield in comparison to **138** as expected due to increased deshielding of this proton by the acetate group. Proton H6 was observed as a *dd* signal with a 2.3 Hz coupling to proton H5 and as with **138** it exhibited a small 1.5 Hz  $^4J_{\text{H6-H2}}$  coupling. Resolution of the signals for H5 and H2 was poor at 300 and 600 MHz, however H2 could be assigned as the resonance slightly upfield in comparison to H5 on the basis of COSY crosspeaks between these protons and H3 and H6 respectively. Proton H3 was identified as the *dd* signal at 4.20 ppm with two large 9.1 Hz couplings due to *trans*-diaxial interactions with H4 and H2. H4 was observed as a *dd* signal with a large 9.1 Hz *trans*-diaxial coupling to H3 and smaller 2.3 Hz *cis* coupling with H5. The 2D ROESY NMR spectrum showed crosspeaks between H2, H4 and H6 making H6 axial and *cis* to the other axial hydrogens.  $^{13}\text{C}$  NMR resonances were assigned on the basis of a 2D HSQC experiment. The carbonyl resonances are not shown in Figure 14b but appeared at 198 ppm (ketone) and 170 ppm (ester). The methyl carbon of the acetyl group appeared at 20.6 ppm.

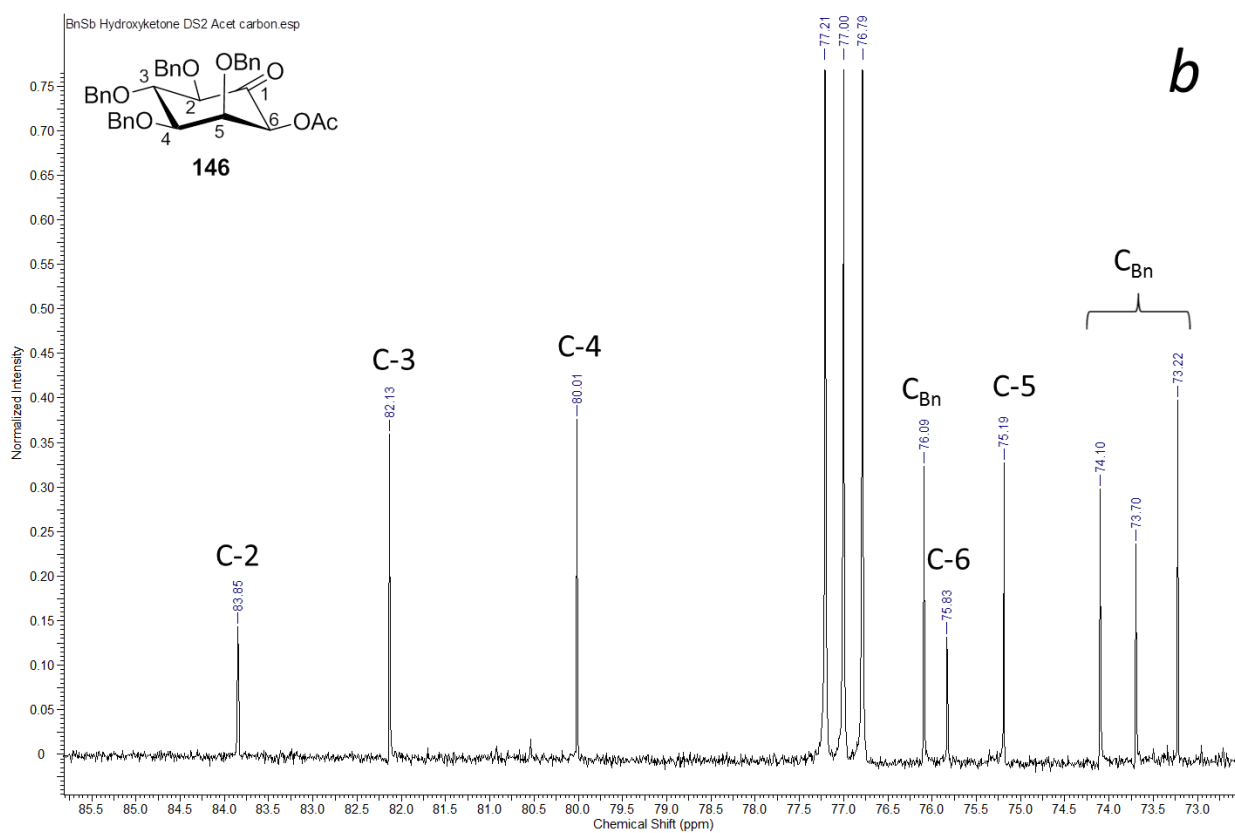
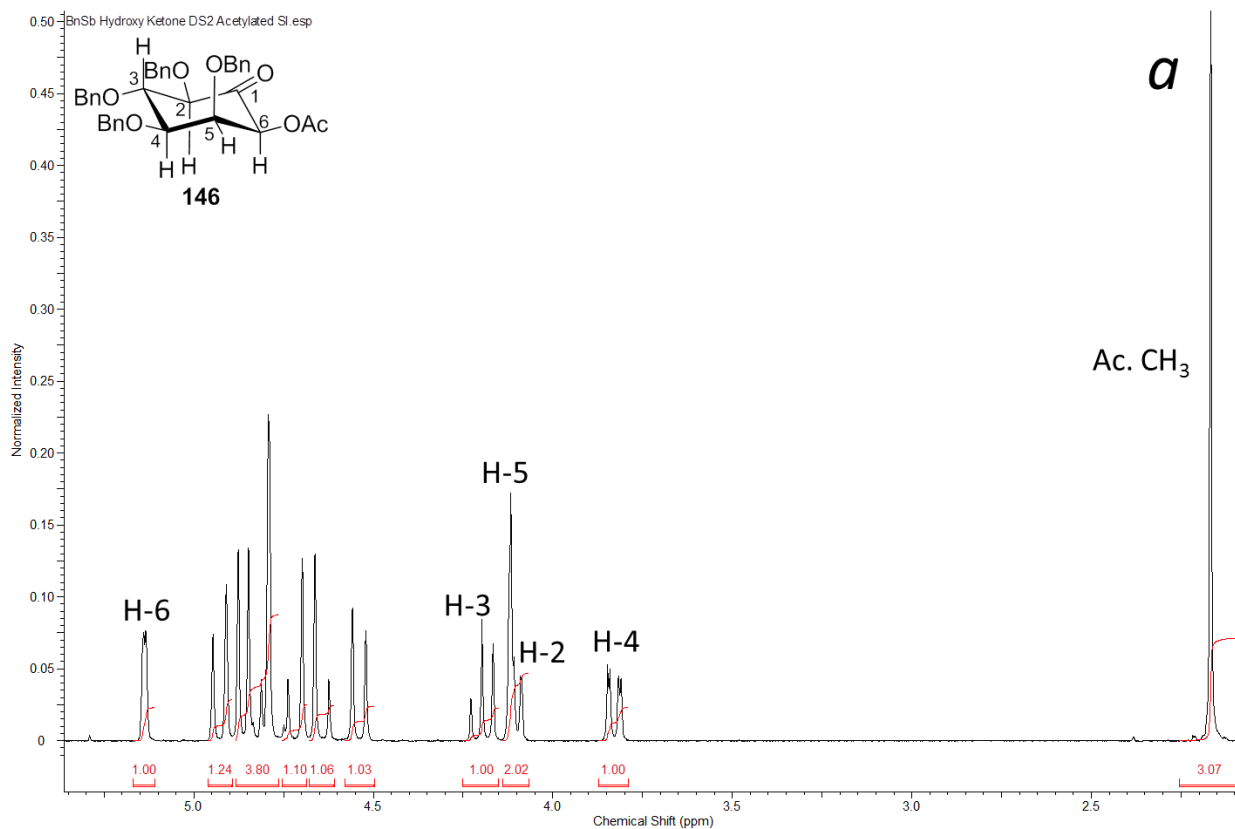
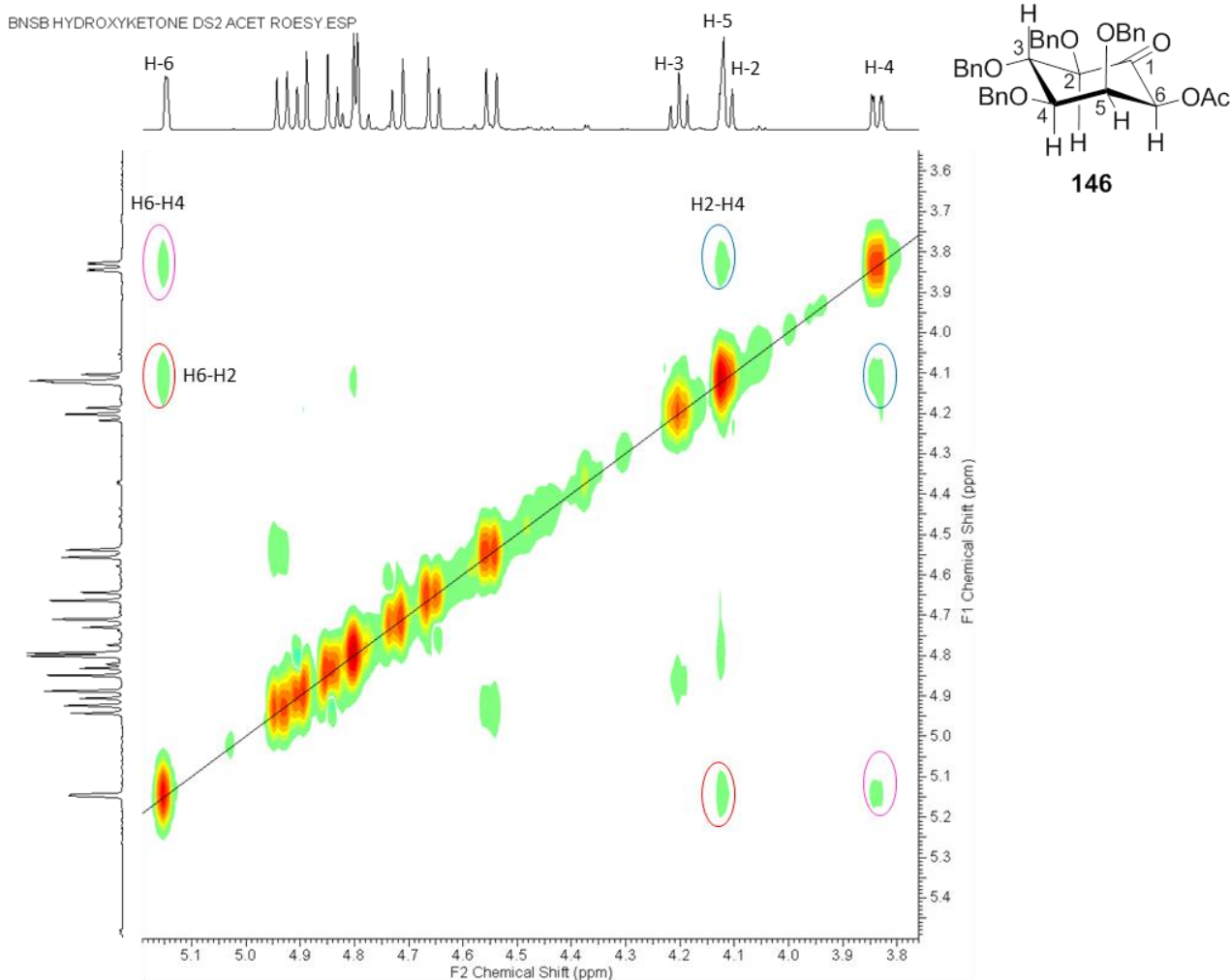
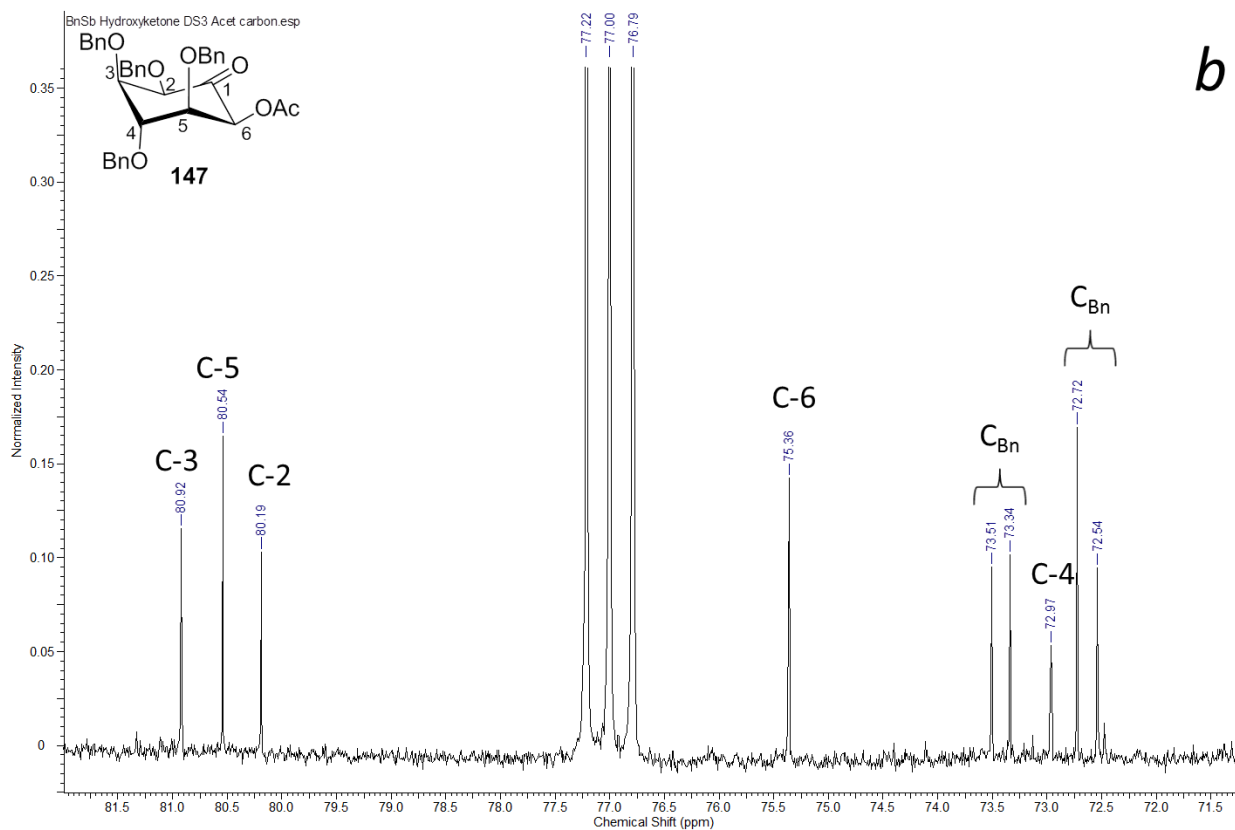
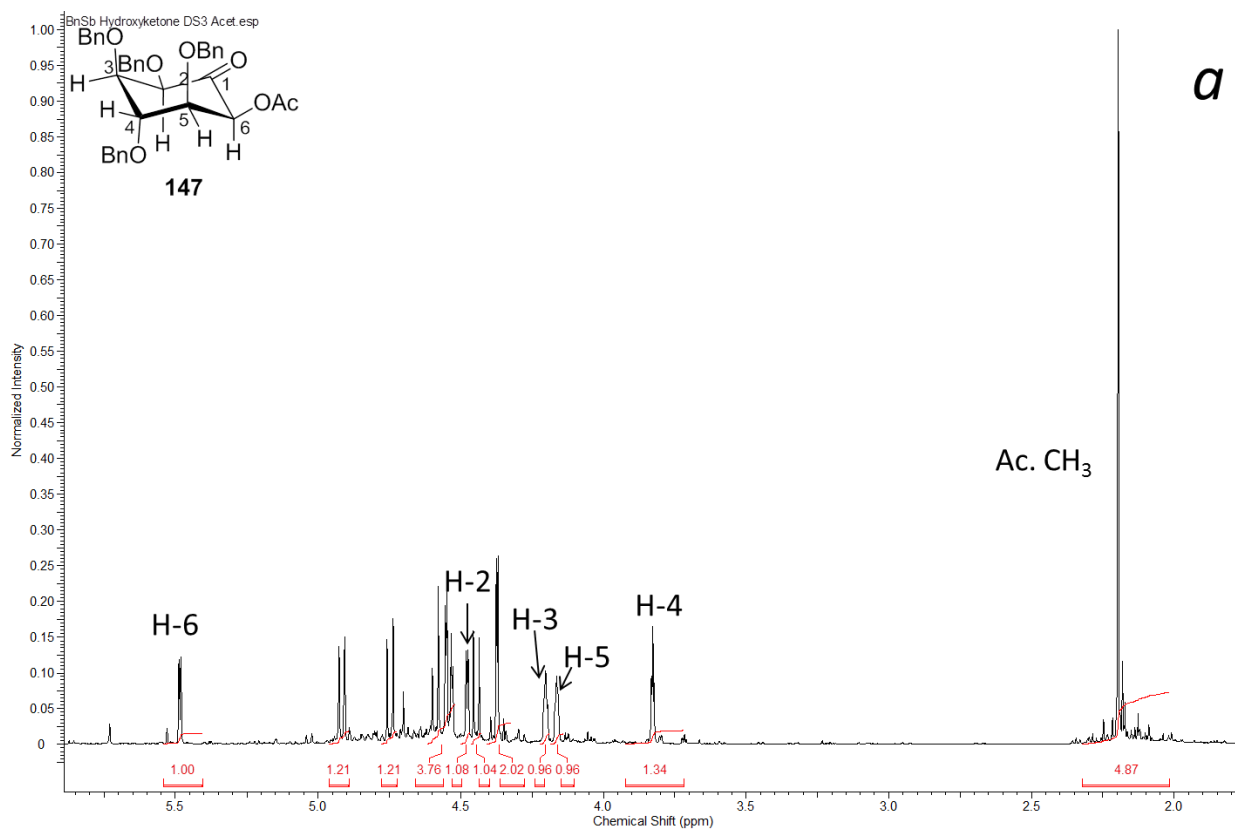


Figure 14 a) 300 MHz <sup>1</sup>H and b) 75 MHz <sup>13</sup>C NMR spectra of 146 in CDCl<sub>3</sub>



**Figure 15 600 MHz 2D ROESY spectrum of 146**

It was difficult to isolate hydroxyketone **144** or its acetate derivative **147** in an analytically pure state as it underwent some decomposition on silica. The assigned  $^1\text{H}$  and  $^{13}\text{C}$  NMR spectra for the acetate derivative **147** are presented in Figure 16. For ease of viewing the  $^{13}\text{C}$  NMR resonances of the carbonyl and methyl resonances are not shown but these appear at 199 ppm (ketone), 170 ppm (ester) and 30 ppm (methyl). At 600 MHz all resonances for ring protons were resolved and specific  $^1\text{H}$  and  $^{13}\text{C}$  NMR resonances were assigned on the basis of 2D COSY and HSQC experiments respectively. Both **138** and its acetate derivative **147** lacked characteristic *trans*-diaxial couplings in their  $^1\text{H}$  NMR spectra. The ROESY spectrum of the acetate ester **147** (Figure 17) showed a through-space interaction between H2 and H6 indicating that these atoms were *cis* and axial. Coupling constants around the ring indicated all gauche couplings (2.9-4.7 Hz) assuming a chair structure, and H3 and H5 were therefore equatorial while the remaining centre at H4 was assigned on the basis of the stereochemistry of the starting material.



**Figure 16 a) 300 MHz <sup>1</sup>H and b) 75 MHz <sup>13</sup>C NMR spectra of 147 in CDCl<sub>3</sub>**

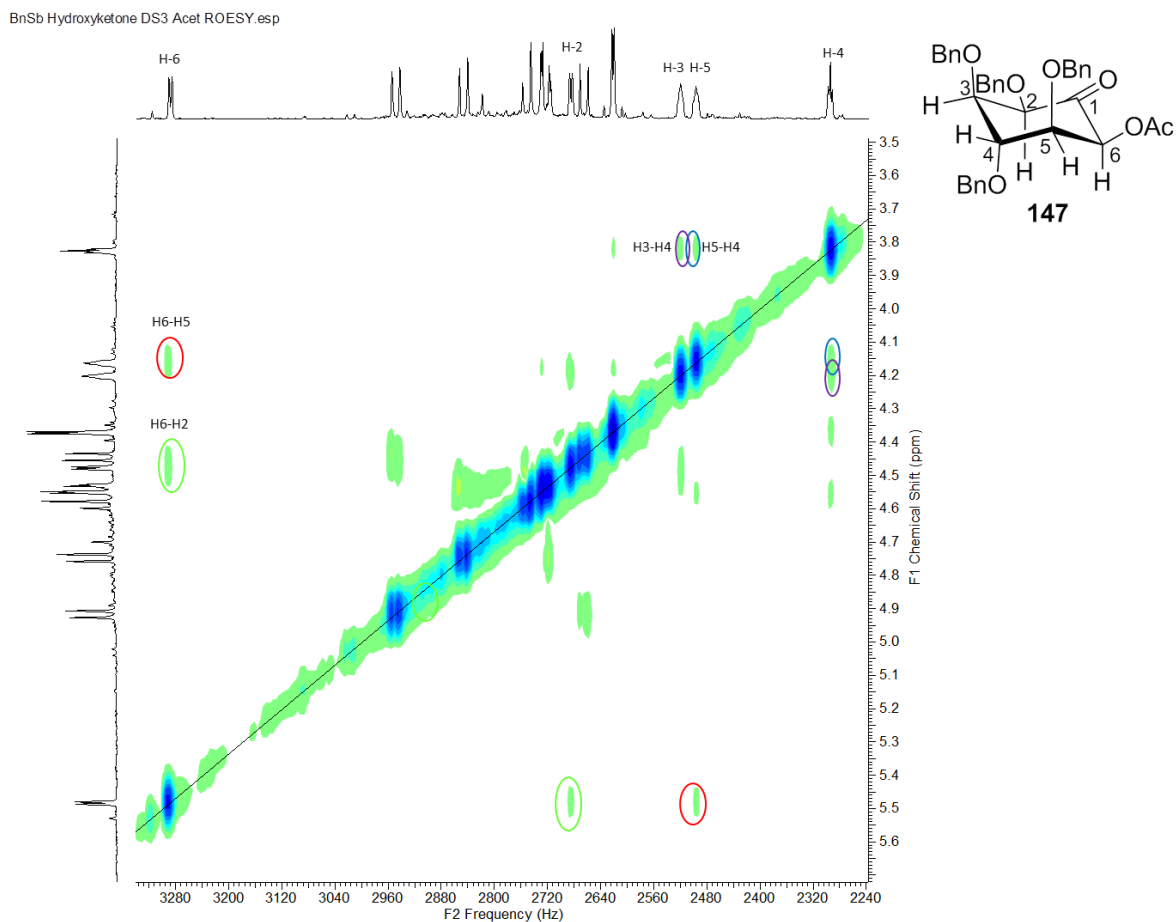


**Figure 17 600 MHz 2D ROESY spectrum of 147 in  $\text{CDCl}_3$**

A summary of the structural assignments with observed couplings and ROESY interactions for the acetate derivatives of the products of the carbocyclisation reaction of *gluco*-dial **107** is presented in Figure 18 below:

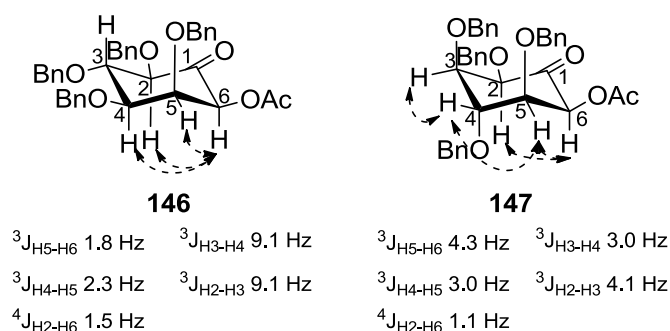
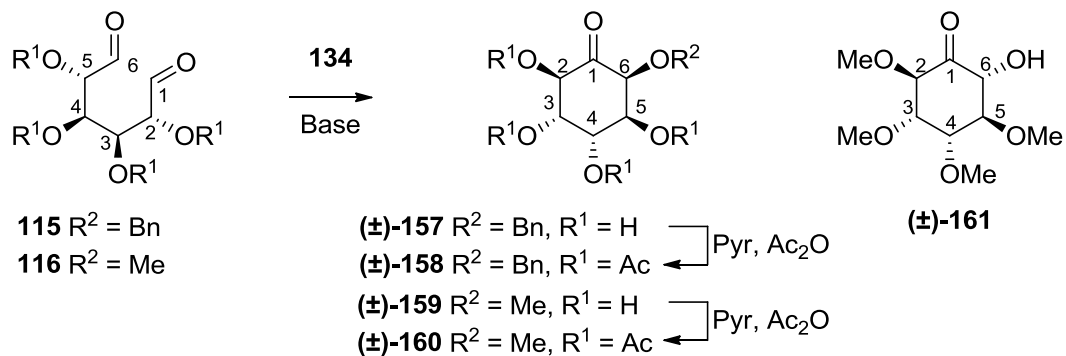


**Figure 18 Conformation, selected ROESY interactions (dashed arrows) and coupling constants of 146 and 147**

## Carbocyclisation products of the *galacto*-dials

The carbocyclisations of the *meso*-substituted dialdehydes **115** and **116** could be expected to yield two racemic diastereomers, the results of which are presented in Table 3.



Entry <sup>a</sup>	Aldehyde	Base (mol%)	Precatalyst (mol%)	Solvent	Temp (°C)	Products	Ratio <sup>b</sup>	Yield
1	<b>115</b>	$\text{Et}_3\text{N}$ (15)	<b>1</b> (20)	DCE	40	<b>157</b>	-	12
2	<b>115</b>	$\text{Et}_3\text{N}$ (100)	<b>1</b> (20)	DCE	40	<b>157</b>	-	12
3 <sup>c</sup>	<b>115</b>	DBU (15)	<b>1</b> (20)	DCE	60	<b>157</b>	-	18
4	<b>116</b>	$\text{Et}_3\text{N}$ (15)	<b>1</b> (20)	DCE	60	<b>159:161</b>	92:8	65
5	<b>116</b>	$\text{Et}_3\text{N}$ (15)	<b>1</b> (20)	DCE	40	<b>159:161</b>	87:13	54

<sup>a</sup> Reactions were performed on 100-127 mg of dialdehyde in 50 mL/g solvent and left for 16 hours and products isolated by flash chromatography. <sup>b</sup> Ratios determined from isolated products. <sup>c</sup> Scale was 1.07 g of **115**.

**Table 3 Carbocyclisations of *galacto*-dials **115** and **116****

The cyclisation of benzyl ether-protected *galacto*-dial **115** afforded a single diastereomer **157** in low yield. Attempts to isolate the benzyl-protected **157** free from impurities were unsuccessful due to a close running unidentified byproduct which lacked ketone resonances in its <sup>13</sup>C NMR spectrum and so the product was converted to the acetate derivative **158**. Due to the low yield of products it was not clear if small amounts of other stereoisomers were produced in the reactions of **115**. Switching protecting groups to methyl ethers gave good yields for the cyclisation reactions and two isomers **159** and **161** were isolated from the reaction although the major isomer **159** was again isolated containing an impurity which was removed upon acetylation. Based upon the stereochemistry of the products, it is clear that no epimerisation occurs in the reactions of **115** and the stereoisomers are generated in the ring-closure step.

## Structural assignments

The assigned  $^1\text{H}$  and  $^{13}\text{C}$  NMR spectra for **158** are provided in Figure 19.

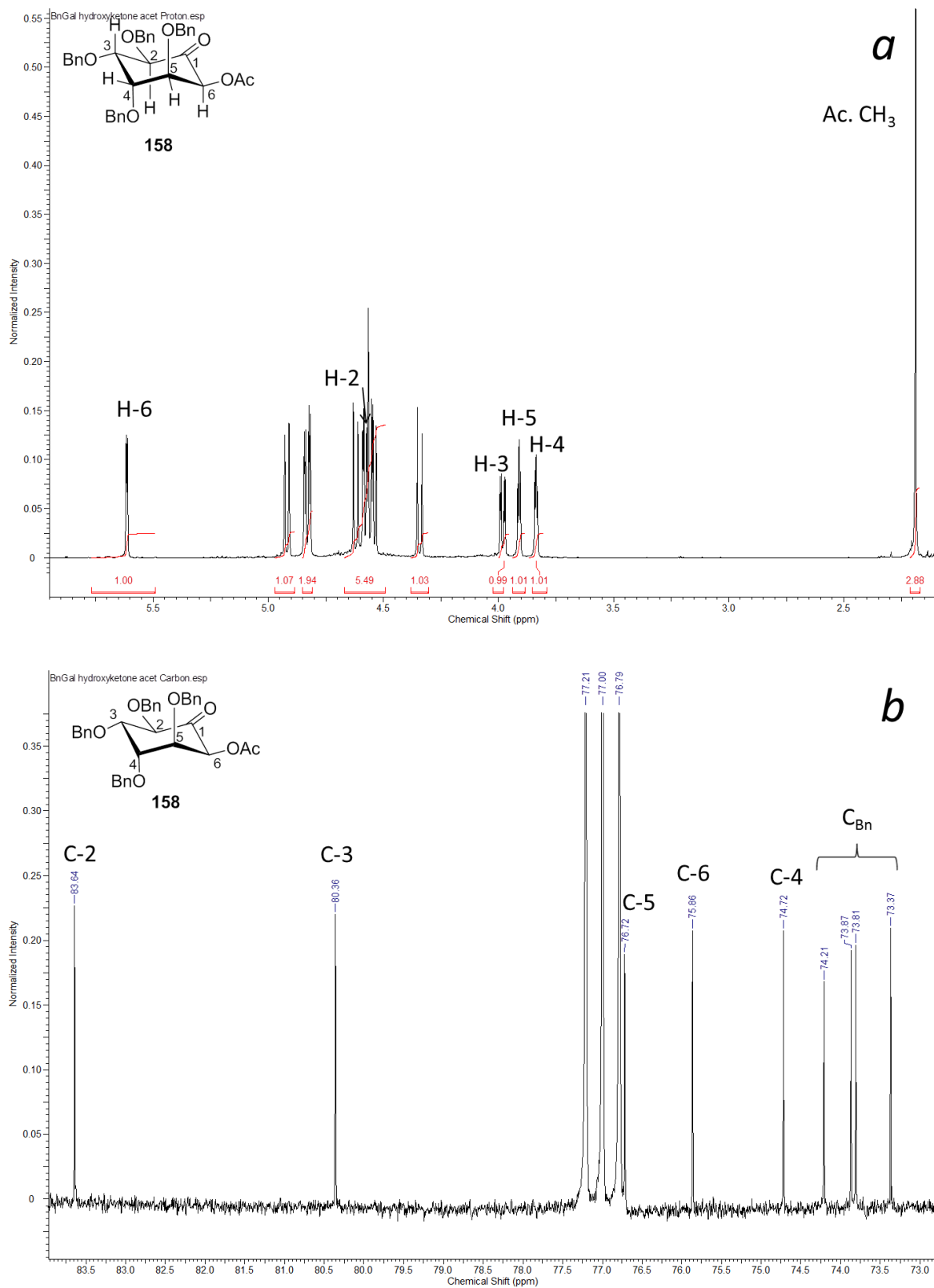
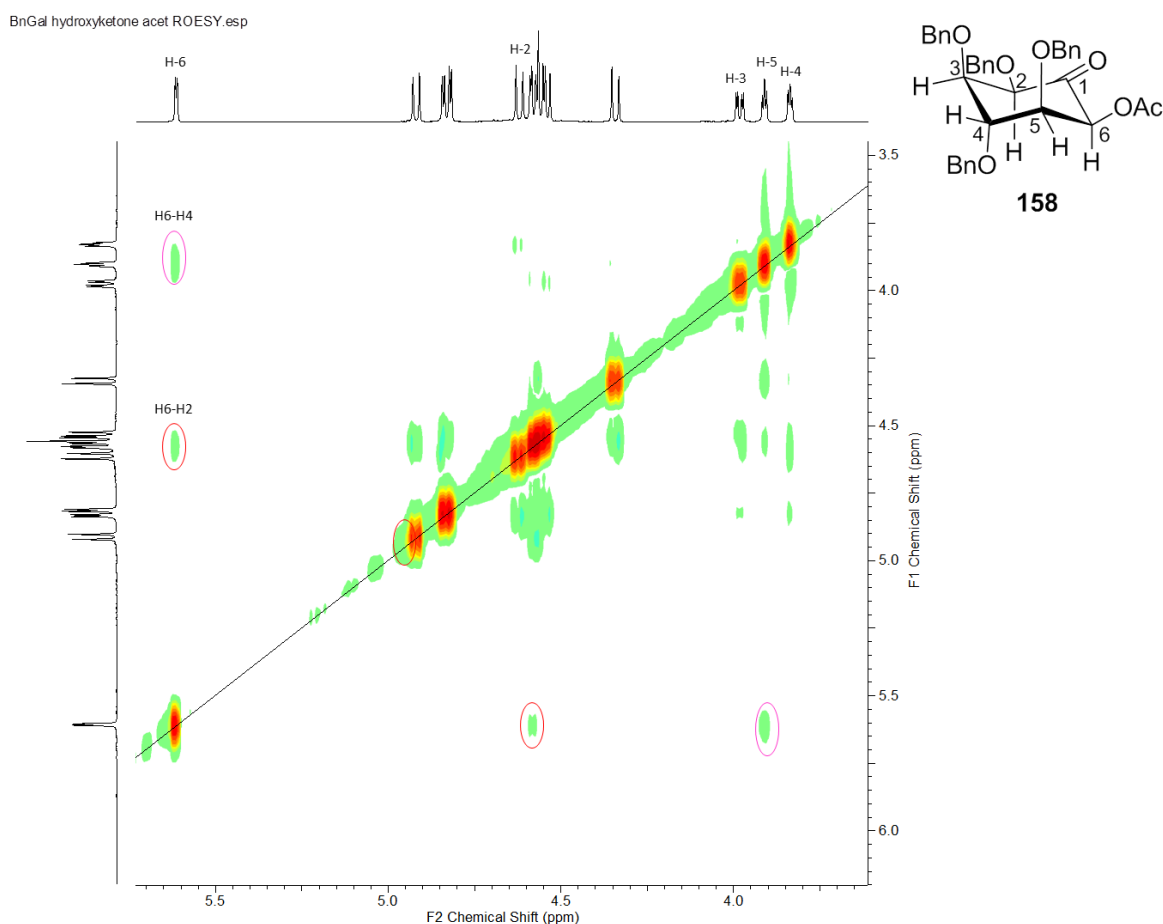


Figure 19 a) 600 MHz  $^1\text{H}$  and b) 150 MHz  $^{13}\text{C}$  NMR spectra of **158** in  $\text{CDCl}_3$

H6 of **158** was assigned first on the basis of chemical shift being the furthest downfield due to deshielding by the acetate group. The other proton resonances were then assigned on the basis of a 2D COSY experiment. Only one *trans*-diaxial coupling was observed between protons H2 and H3 (10 Hz) with the smaller 2.9 Hz coupling of protons H3 and H4 indicating that proton H4 was *cis* and equatorial. Assignment of proton H6 as axial was made on the basis of a 2D ROESY experiment (Figure 20) in which a 1,3-diaxial through-space interaction is observed between protons H6 and H2. The small 2.6 Hz coupling between H6 and H5 indicates that H5 must be *cis*-equatorial in relation to H6 and this is further evidenced by the appearance of a cross peak in the 2D ROESY spectrum between these two protons. The stereochemistry of the major product from the carbocyclisation of the methyl ether-protected dialdehyde **116**, **159**, was found to be the same with similar coupling patterns and ROESY interactions observed.



**Figure 20 600 MHz 2D ROESY spectrum of 158**

The minor alcohol **161** was epimeric at the newly created hydroxyl centre and ring-flipped relative to the major isomer **159** (and its acetate derivative **160**). Assignment of the stereochemistry in **161** was made on the basis of coupling constants and supported by ROESY

interactions between H4 and H6. The  $^3J_{\text{H5-H6}}$  8.5 Hz and  $^3J_{\text{H4-H5}}$  9.1 Hz couplings indicate that H5 was axial and had two axial neighbours and the small H3 to H4 coupling made H3 equatorial and *cis* to the axial H4. The equatorial assignment of H2 was supported by the lack of ROESY interactions seen with other axial protons and the stereochemistry of the starting material.

A summary of the structural assignments with observed couplings and ROESY interactions for **158**, **160** and **161** are presented in Figure 21 below:

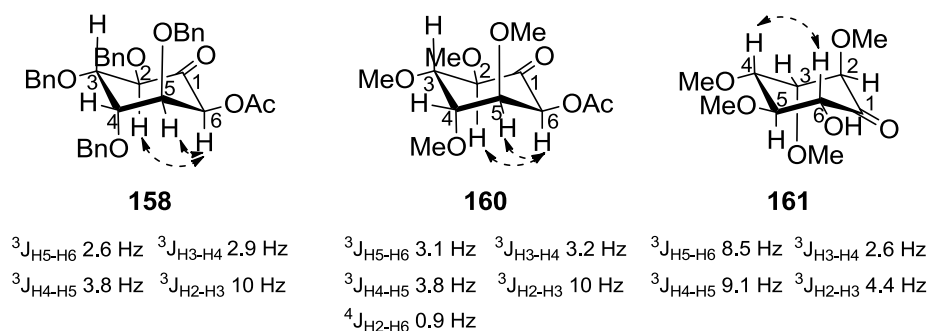
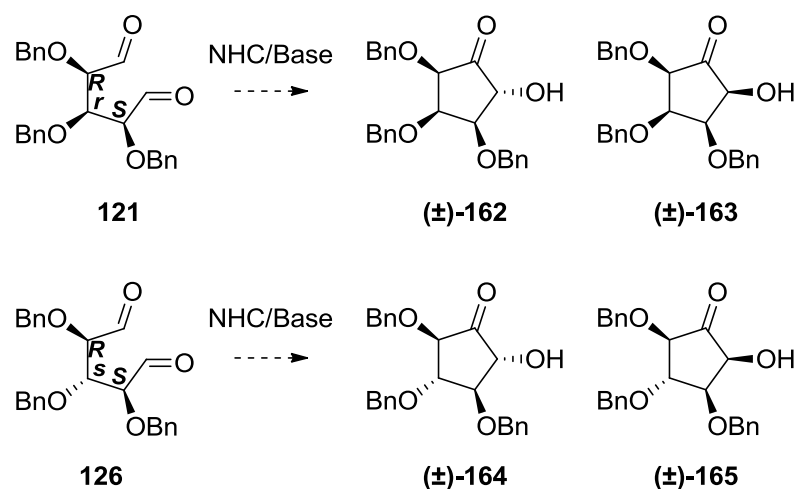


**Figure 21 Conformation, selected ROESY interactions (dashed arrows) and coupling constants of 158, 160 and 161**

### Carbocyclisation reactions of pentitol-derived dialdehydes

It was envisaged that protected dialdehydes **121** and **126** derived from xylitol and ribitol respectively might give access to five-membered carbocyclic sugars. The *meso*-substitution of these stereoisomers would give rise to two possible racemic diastereomers, Scheme 16.



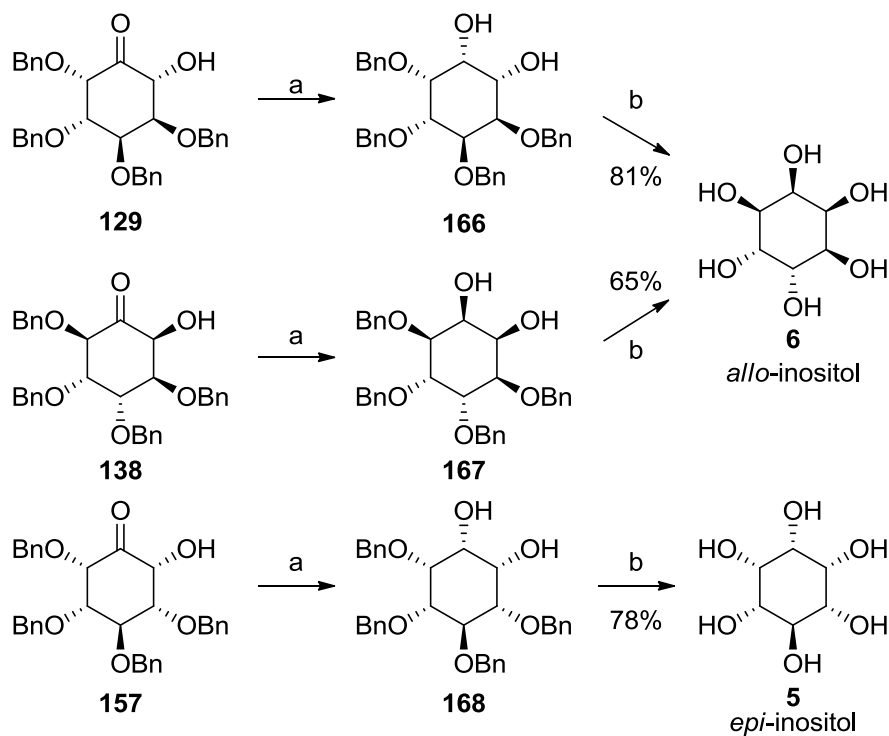
**Scheme 16**

Unfortunately, under all conditions tested, including conditions that had previously proved successful for the hexitol-derived diols, no cyclisation of **121** or **126** was observed. Compounds either underwent decomposition or were returned unchanged.

### **Stereospecific reduction of inososes and synthesis of inositols**

In order to demonstrate the utility of the cyclisation process and to confirm the structure and stereochemistry assigned to these products, sodium borohydride reductions of inososes **129**, **138** and **157** were performed to generate protected inositols and ultimately inositols upon deprotection (Scheme 17). The reduction of hydroxyketone **129** gave a single product **166** in good yield, however, the diol **166** exhibited a broadened  $^1\text{H}$  NMR spectrum from which it was difficult to assign resonances (Figure 22a). Conformations were slowly exchanging at room temperature and the spectrum at  $-100\text{ }^\circ\text{C}$  gave only partially resolved signals (Figure 22b). Removal of the benzyl groups using  $\text{PdCl}_2/\text{H}_2$  gave an 81% yield of *allo*-inositol **6** for the two steps from which the stereochemistry of the reduction **129** was deduced. There is literature precedent for the slow conformational exchange of *allo*-inositol derivatives,<sup>76</sup> and this may explain the observed broadening in the  $^1\text{H}$  NMR spectrum of diol **166**. The reduction of the hydroxyketone **138** also yielded *allo*-inositol **6** as the final product in 65% overall yield after removal of the benzyl groups.

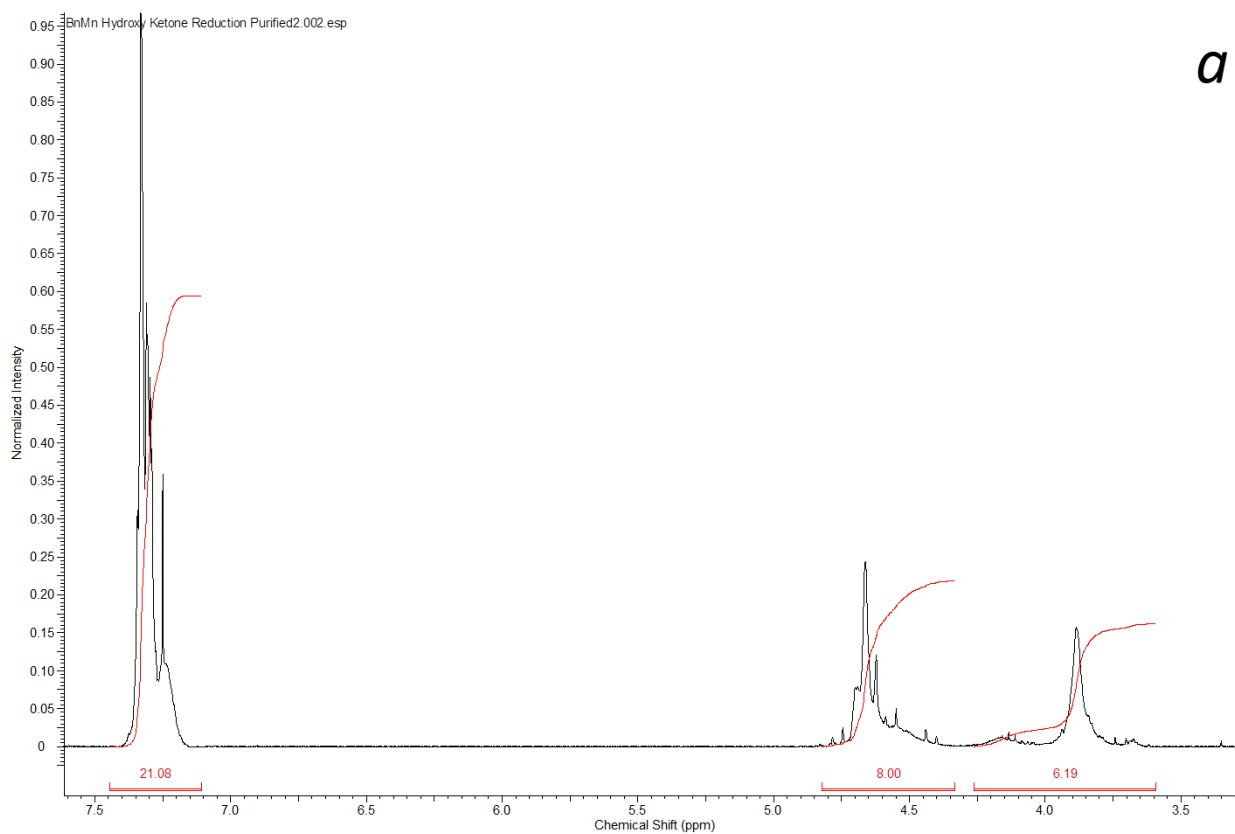
The intermediate diol **167** differed to diol **166** obtained from **129** in the position on the ring of the two hydroxyl groups, however, interpreting the  $^1\text{H}$  and  $^{13}\text{C}$  NMR spectra of the diol was again difficult due to coalescence near ambient temperature. The sodium borohydride reduction of the inosose **157** also afforded a single diol **168**. Hydrogenolysis of the benzyl groups yielded *epi*-inositol **5** from which the stereochemistry of the reduction could once more be deduced.



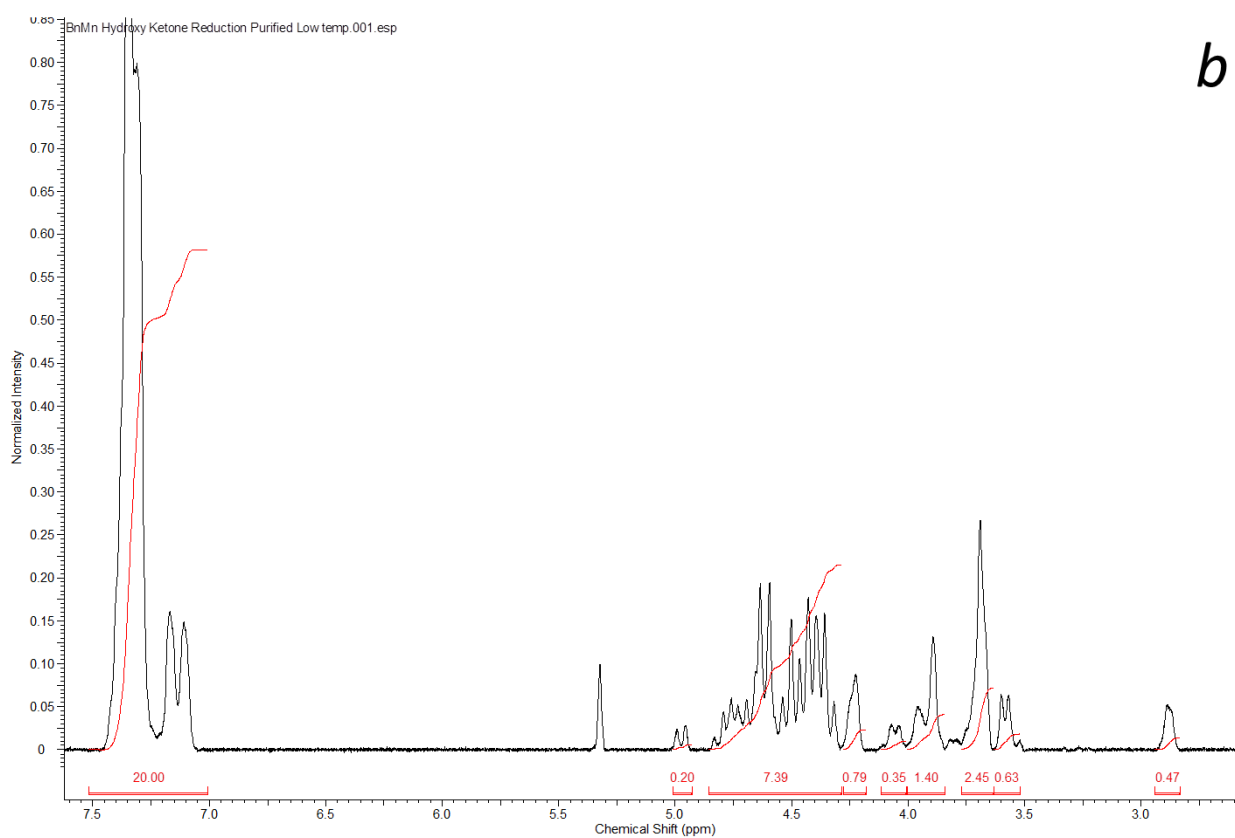
a)  $\text{NaBH}_4$ , EtOH 60°C; b)  $\text{PdCl}_2$ ,  $\text{H}_2$ , EtOH, rt

### Scheme 17

In all three reductions using sodium borohydride, the substrates have an axial 3-benzyloxy substituent hindering one face of the carbonyl which has been shown to control inosose reduction.<sup>77</sup> It is likely that the reactive conformations match the conformations determined by NMR spectroscopy as the alternative conformers have either 3 or 4 unfavourable axial benzyloxy groups. Furthermore, the alternative conformers would still have one axial 3-benzyloxy substituent and an axial 2-hydroxy substituent which would direct hydride to the opposite face to that observed.<sup>78</sup> Stereoelectronic factors must also be considered as they play a deciding role in the stereochemical outcomes. In Cieplak's model, stabilisation of the LUMO in the transition state during nucleophilic attack in cyclohexanones is a key factor.<sup>79</sup> In this model, the antibonding orbital ( $\sigma_{\ddagger}^*$ ) of the incipient nucleophile is more stabilised by the C2-H axial bond than the C2-C3 bond and so axial hydride approach is preferred (Figure 23). It is apparent from the products that the approach of the hydride is from the equatorial face giving **166**, **167** and **168**. It is clear that in the reduction of **129**, **138** and **157** the stereoelectronic stabilisation of axial hydride approach cannot overcome the steric hindrance encountered on this face.



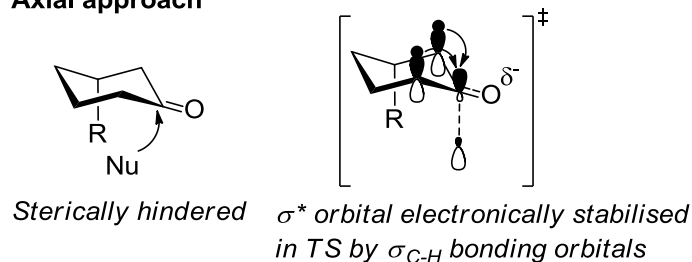
*a*



*b*

**Figure 22** 300 MHz <sup>1</sup>H NMR spectrum of 166 at a) 30 °C and b) -100 °C in CD<sub>2</sub>Cl<sub>2</sub>

### Axial approach



### Equatorial approach

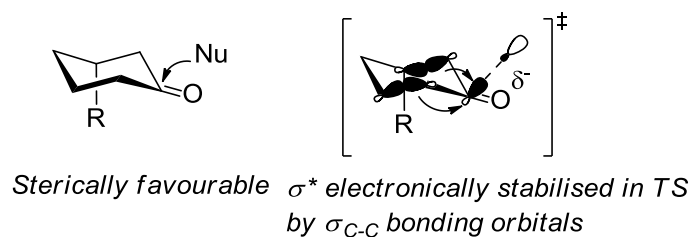
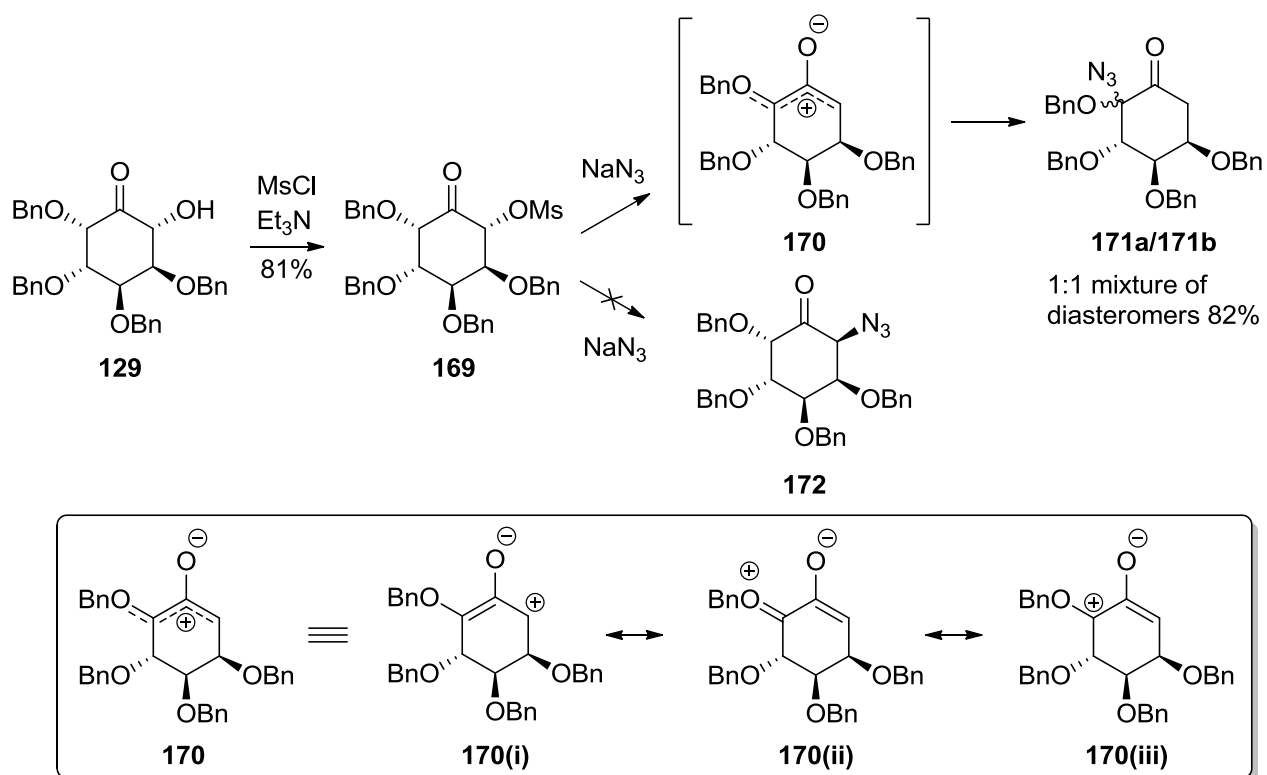


**Figure 23** Steric and stereoelectronic factors in axial vs equatorial approach of nucleophiles on cyclohexanones

### Attempted synthesis of aminocyclitol via inosose-2-O-mesylates

In an attempt to generate an aminocyclitol from **129**, the inosose **129** was converted to its methanesulfonate ester **169** and nucleophilic substitution with sodium azide performed. Products of  $S_N2$  displacement of the mesylate were not observed, rather azidoacetal **171a** and **171b** were formed in a 1:1 ratio in excellent yield. To explain the outcome it was reasoned that the reaction was taking place via an oxyallyl intermediate **170** (Scheme 18). Chapter 2 of this thesis examines the validity of such a mechanism and explores the scope of both the substrate and nucleophile in the rearrangement.



Scheme 18

## CONCLUSION

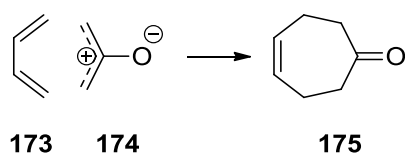
In conclusion, NHC catalysis provides a novel method for the synthesis of inosose derivatives in moderate to good yield from readily synthesised mannitol-, sorbitol- and galactitol-derived 1,6-dialdehydes. While the reactions of *manno*- and *galacto*-dials yielded mainly single isomers from the cyclisation, the reaction of *gluco*-dials yielded mixtures of hydroxyketone stereoisomers. Substitution of benzyl ethers by methyl groups dramatically improved the yield for the *galacto*-substituted dialdehyde indicating the sensitivity of the cyclisation to stereochemistry and to steric effects. The inosose products of cyclisation were converted to inositols by a stereoselective reduction using  $\text{NaBH}_4$  and protecting group removal. The inositols were consistent with the assigned stereochemistry in the inosose products of cyclisation. The synthesis of *allo*-inositol was achieved in an overall yield of 33% over 6-steps, however, *epi*-inositol was produced in low yield due to an unsatisfactory cyclisation step. It was discovered serendipitously that the 2-*O*-mesylate derivative of the inosose **129** underwent an unexpected rearrangement in the presence of azide to give a 1:1 mixture of  $\alpha$ -azidoacetals **171a** and **171b** and it was proposed that the reaction outcome could be rationalised on the basis of a transient oxyallylic intermediate. This rearrangement is investigated further in the proceeding chapter.

## CHAPTER 2: REARRANGMENTS OF INOBOSE-2-*O*-MESYLATES

### INTRODUCTION

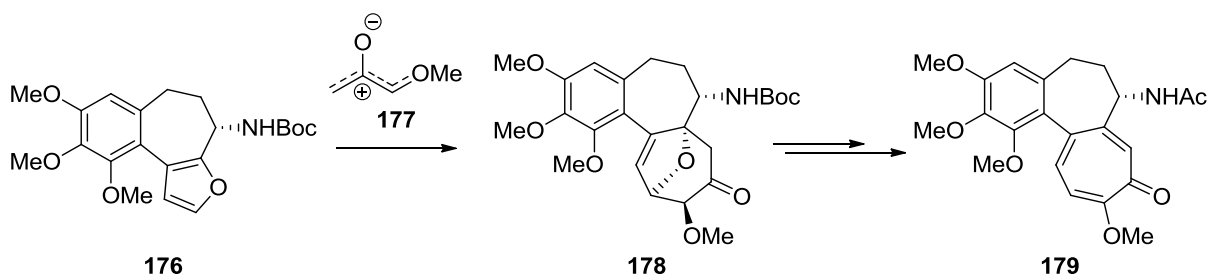
#### The oxyallyl system

In the previous chapter of this thesis, a rearrangement of the 2-*O*-mesylate derivative of protected inosose **129** in the presence of azide to give  $\alpha$ -azidoacetals **171a** and **171b** was described (Scheme 18). The observed preference for  $\alpha'$ -addition over an  $S_N2$  reaction was rationalised on the basis of an oxyallylic intermediate. The oxyallyl system is a well-known transient reactive group often used in (4+3) cycloaddition reactions to form seven-membered rings and bicyclic structures.<sup>80-82</sup> The cycloaddition is homologous to the Diels-Alder reaction in which the dienophile is a 3 atom/ $2\pi$  electron system (Scheme 19).



Scheme 19

The (4+3) cycloaddition was a key step in the total synthesis of colchicine **179**, an antimetabolic alkaloid.<sup>83</sup> In this total synthesis, one of the seven-membered rings was constructed via a regio- and stereoselective cycloaddition of furan **176** with  $\alpha$ -methoxyoxyallyl **177** generated in situ from treatment of the trimethylsilyl enol ether of pyruvic aldehyde dimethyl acetal with TMSOTf (Scheme 20).

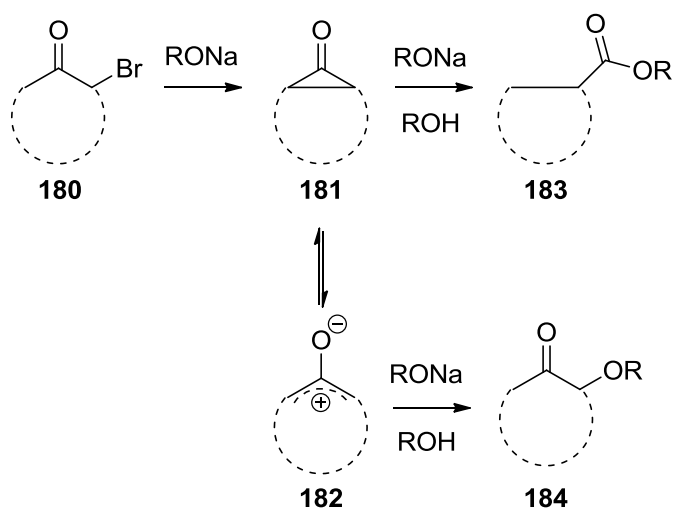


Scheme 20

Nitrogen-stabilised oxyallyl systems have also been reported and these have also been used in similar (4+3) reactions generating bicyclic synthons.<sup>84-86</sup>

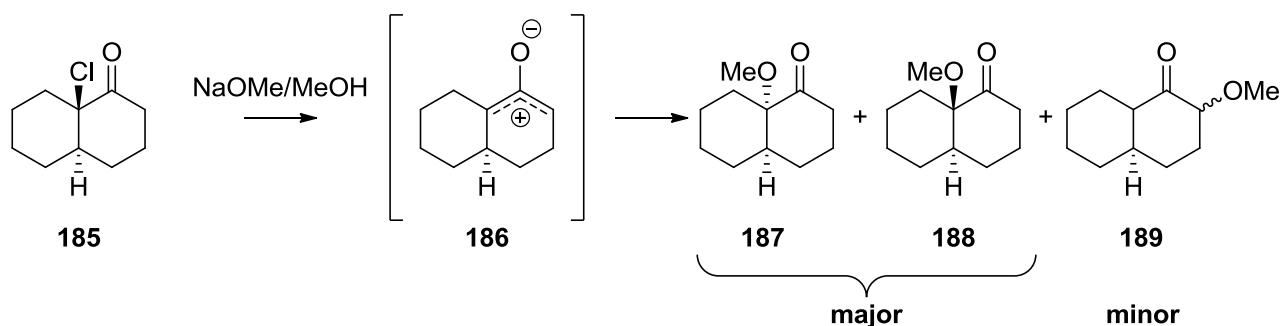
### Oxyallyls and their implication in the Favorskii rearrangement

Oxyallyls have most notably been implicated as intermediates in the Favorskii rearrangement which transforms cyclic  $\alpha$ -haloketones into ring-contracted cycloalkanecarboxylic acids and acyclic alkanones into chain extended carboxylic acids or derivatives (Scheme 21).<sup>87,88</sup>



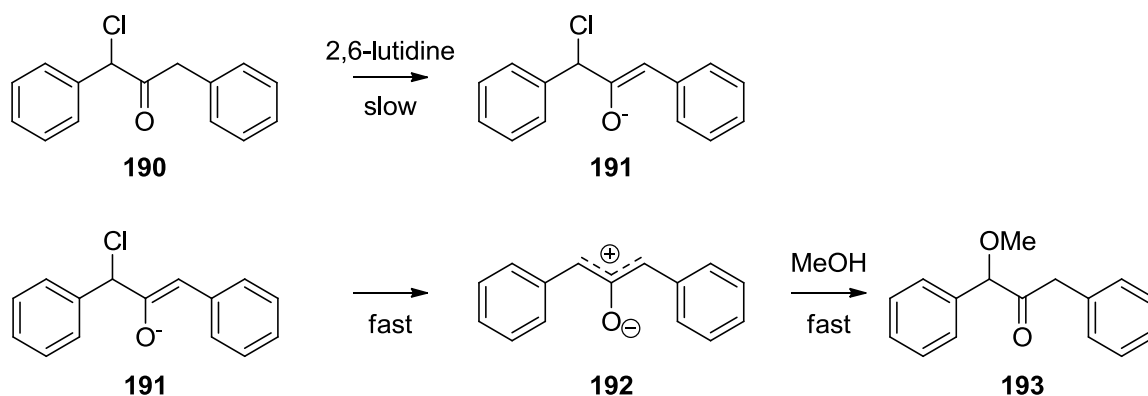
Scheme 21

Evidence suggests that the Favorskii rearrangement proceeds by the intramolecular cyclisation of an enolate generated from an  $\alpha$ -haloketone **180** to give a cyclopropanone **181**, in equilibrium with the oxyallyl intermediate **182**.<sup>88-90</sup> The cyclopropanone intermediate is attacked by alcohol or water giving a hemiacetal which then undergoes cyclopropane ring opening affording the final product **183**. The rearrangement is usually conducted using alkoxide or hydroxide as both base and nucleophile, affording esters or acids respectively. When conformationally constrained  $\alpha$ -haloketones are used, both ring contracted products **183** and alkoxide  $\alpha$ - and  $\alpha'$ -addition products **184** can be observed.<sup>87</sup> House showed that Favorskii reaction of decalone **185** where the halide, conformationally locked into an axial position to encourage oxyallyl zwitterion formation and no cyclopropane formation, gave exclusively  $\alpha$ - and  $\alpha'$ -addition products (Scheme 22).<sup>91</sup> The retention of stereochemistry in **188** was taken as evidence of an intermediate oxyallyl **186**, however major products **187** and **188** could conceivably also occur via an  $\text{S}_{\text{N}}1$  reaction. The minor product **189** arising from  $\alpha'$ -addition is supporting evidence for an oxyallyl intermediate.

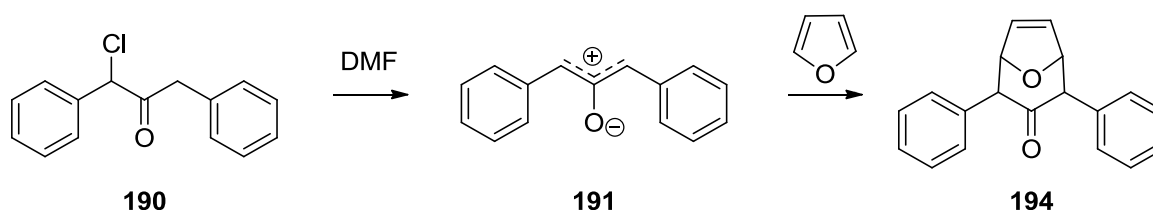


**Scheme 22**

Fort investigated the kinetic parameters of the methanolysis of  $\alpha$ -chlorodibenzyl ketone in the presence of 2,6-lutidine, finding them to be consistent with a rapid concerted or synchronous enolate formation and loss of chloride ion (Scheme 23).<sup>92</sup> The methanolysis of chloroacetone under analogous conditions was found to be far slower, consistent with the importance of the formation of an oxyallylic system stabilised by conjugation with the phenyl substituents. Shortly following this Fort efficiently trapped the oxyallyl intermediate **192** via (4+3)-cycloaddition with furan which unequivocally established the presence of the oxyallyl species (Scheme 24).<sup>93</sup>



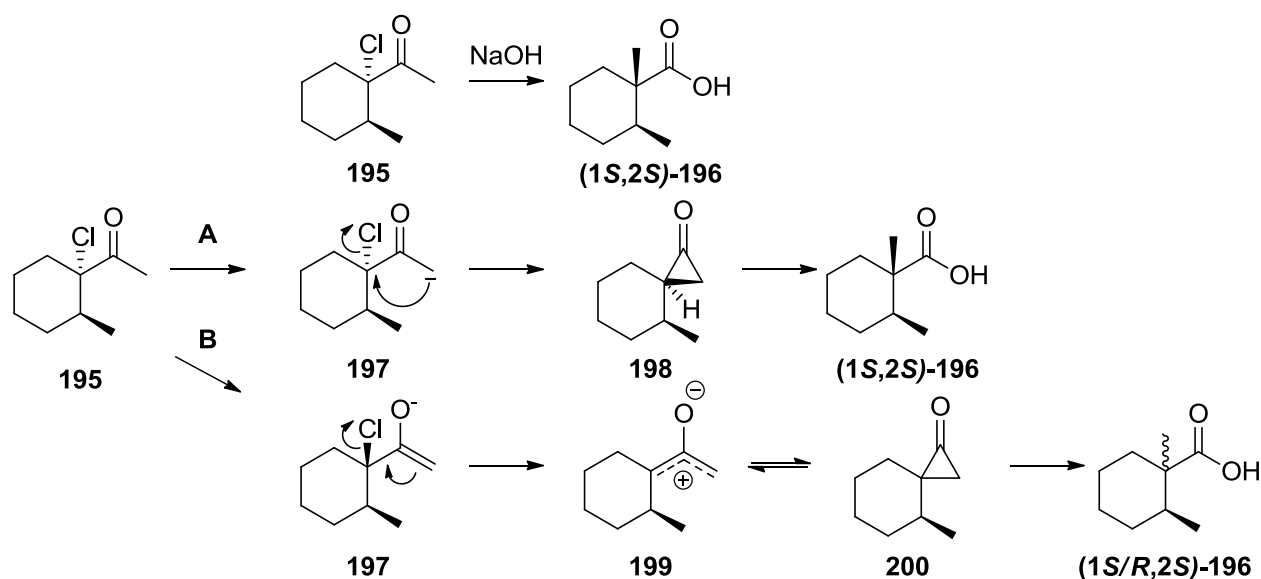
**Scheme 23**



**Scheme 24**

Stork provided good evidence for direct synchronous cyclopropane formation in the Favorskii rearrangement of 1-chloro-1-acetylcyclohexane **198** (Scheme 25).<sup>94</sup> In this instance, Pathway A

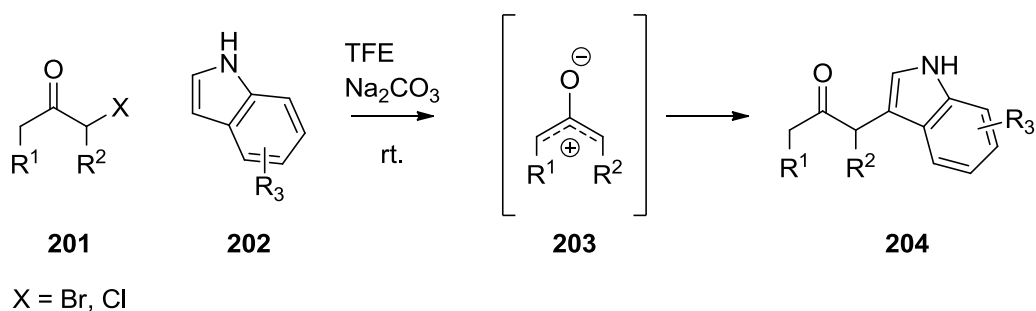
involves direct cyclopropane formation via intramolecular displacement of a chloride ion by an enolate, and as such, inversion of configuration at the centre bearing the halogen would be expected. Conversely, if a zwitterionic intermediate were responsible as in Pathway B, then a mixture of diastereomers would be expected to be obtained. Stork demonstrated that the reaction proceeds with complete stereoselectivity, ruling out the possibility of any zwitterionic intermediate in this instance.



**Scheme 25**

### Direct $\alpha$ -functionalisation of ketones via oxyallyls

While (4+3)-cycloadditions and Favorskii rearrangements involving oxyallyls such as those described above are relatively mature fields of study, considerably less attention has been given to oxyallyls as a direct means of  $\alpha$ -functionalisation of ketones via nucleophilic trapping. Inspired by Baran's protection group-free direct oxidative coupling of carbonyls and indoles allowing facile construction of  $\alpha$ -ketoindole scaffolds and efficient access to indole-containing natural products,<sup>95</sup> Chi et al. investigated an alternative by which the  $\alpha$ -ketoindoles may be accessed via an oxyallylic intermediate.<sup>96</sup> Chi et al. achieved the coupling under relatively mild conditions of a variety of  $\alpha$ -haloketones with both substituted and unsubstituted indoles in 2,2,2-trifluoroethanol (TFE) with  $\text{Na}_2\text{CO}_3$  (Scheme 26).

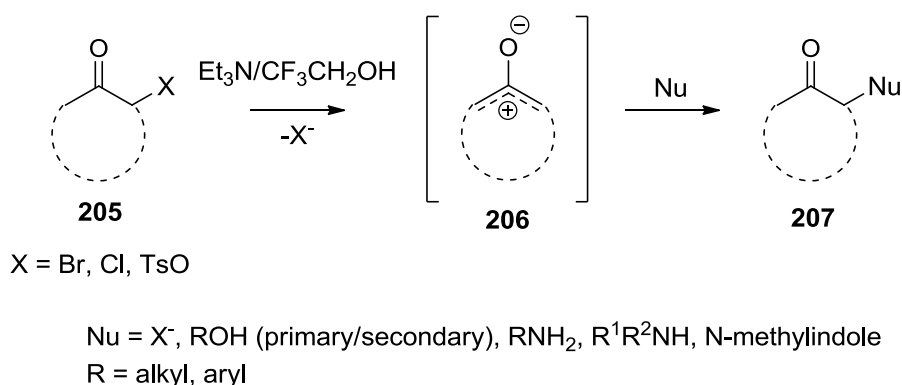


**Scheme 26**

Chi demonstrated that the use of TFE as a solvent was key to the reaction outcomes. This was reasoned on the basis of its high polarity that stabilises the zwitterionic intermediate while having attenuated nucleophilicity compared to other polar protic solvents.

This coupling had previously been achieved under harsher conditions from  $\alpha$ -hydroxycyclohexanone, with refluxing in aqueous phosphoric acid generating an oxyallyl intermediate that was trapped by indole.<sup>97</sup>

Macmillan et al. have recently expanded the use of oxyallyls as tools for  $\alpha$ -functionalisation by generating these intermediates from  $\alpha$ -halo and -pseudohalo cycloalkanones **205** and trapping with a wide variety of halide, heteroatom and soft- $\pi$  nucleophiles, under mildly basic conditions with TFE as solvent (Scheme 27).<sup>98</sup>

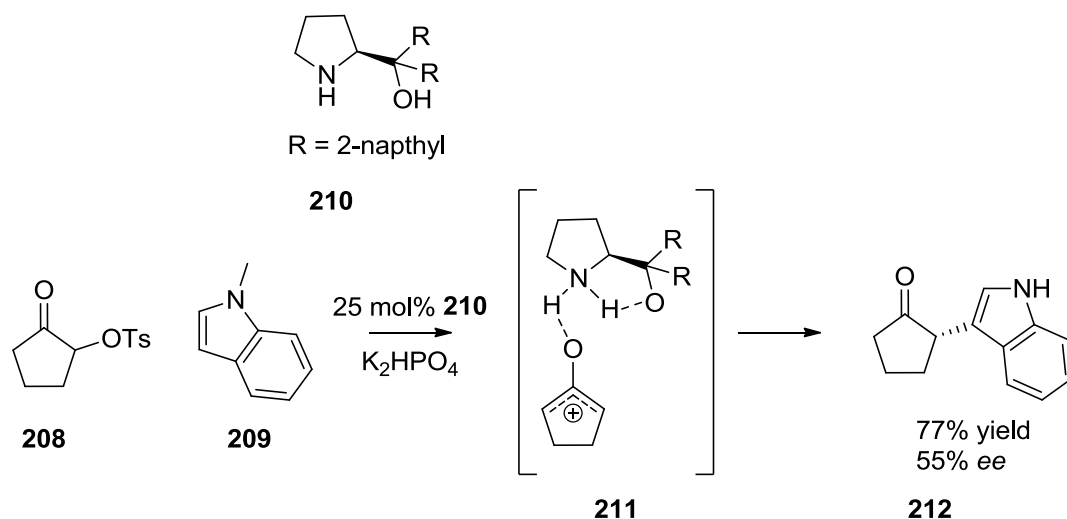


**Scheme 27**

Contrary to Chi, Macmillan argues that TFE acts as a weak Lewis acid that activates the carbonyl such that the mild amine base can generate an enolate that subsequently forms the oxyallylic intermediate **206**.

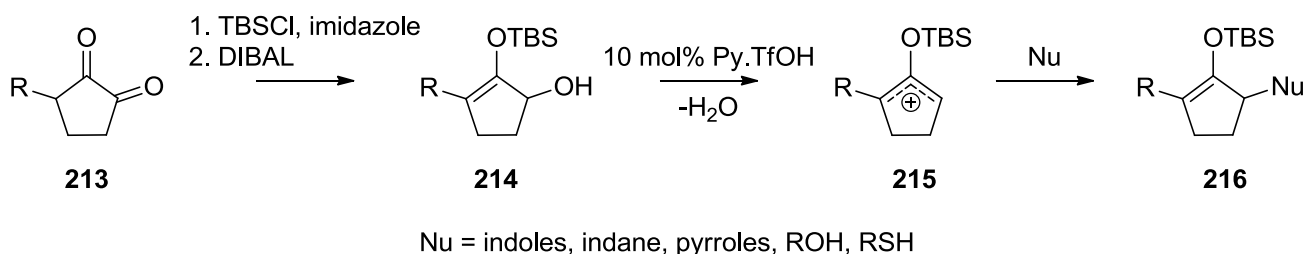
Obvious issues of stereo- and regioselectivity arise in these types of functionalisations, as the reaction generates a new chiral centre from a planar S<sub>N</sub>1-type intermediate at either the  $\alpha$ - or  $\alpha'$

position of the ketone. In the report described above, Macmillan showed that modest asymmetric induction during  $\alpha$ -functionalisation of  $\alpha$ -tosyloxycyclopentanone **208** with *N*-methylindole **209** could be achieved by using a prolinol-derived H-bond catalyst **210** to activate the carbonyl of **208**, with subsequent formation of a chiral oxyallylic intermediate **211** providing the source of enantioselectivity (Scheme 28).



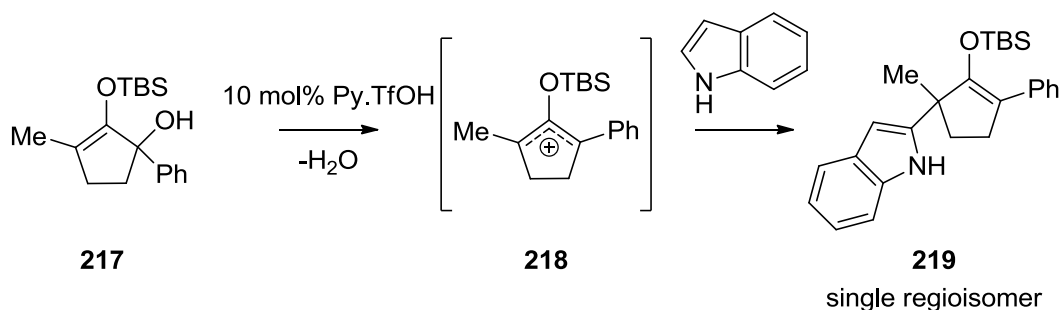
**Scheme 28**

A recent novel approach to the problem of regioselectivity in  $\alpha$ -functionalisations via a putative *tert*-butyldimethylsilyloxyallylic cation has been described by Kartika et al.<sup>99,100</sup> In their approach, an  $\alpha$ -hydroxysilylenol ether is synthesised from an  $\alpha$ -substituted 1,2-cyclopentanedione and a catalytic amount of a mild Bronsted acid employed to eliminate water and generate the oxyallylic cation that may then be trapped by a variety of nucleophiles (Scheme 29). The regioselectivity is controlled simply by steric factors, with the only product observed being that of addition to the less sterically hindered  $\alpha$ - or  $\alpha'$ -position.



**Scheme 29**

Kartika also reports the extension of this protocol to analogous six-membered ring systems with a methoxyallyl cation in place of the silyloxyallyl cation. The protocol also allows for generation of quaternary centres  $\alpha$  to a carbonyl in a regioselective manner from unsymmetrical  $\alpha,\alpha'$ -disubstituted enol ethers such as **217** and is therefore of great synthetic utility (Scheme 30).



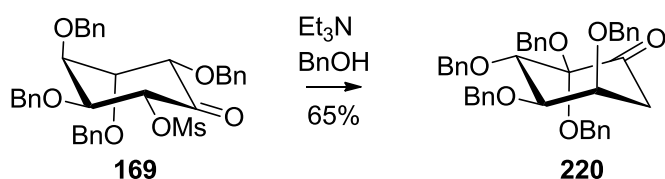
**Scheme 30**

Thus, with the observation that **169** undergoes exclusively  $\alpha'$ -addition of azide with loss of the mesylate group to give a quaternary stereocentre, consistent with a proposed oxyallyl intermediate, investigation into the substrate scope and validity of such a mechanism was undertaken. The current report details the findings in this regard.

## RESULTS AND DISCUSSION

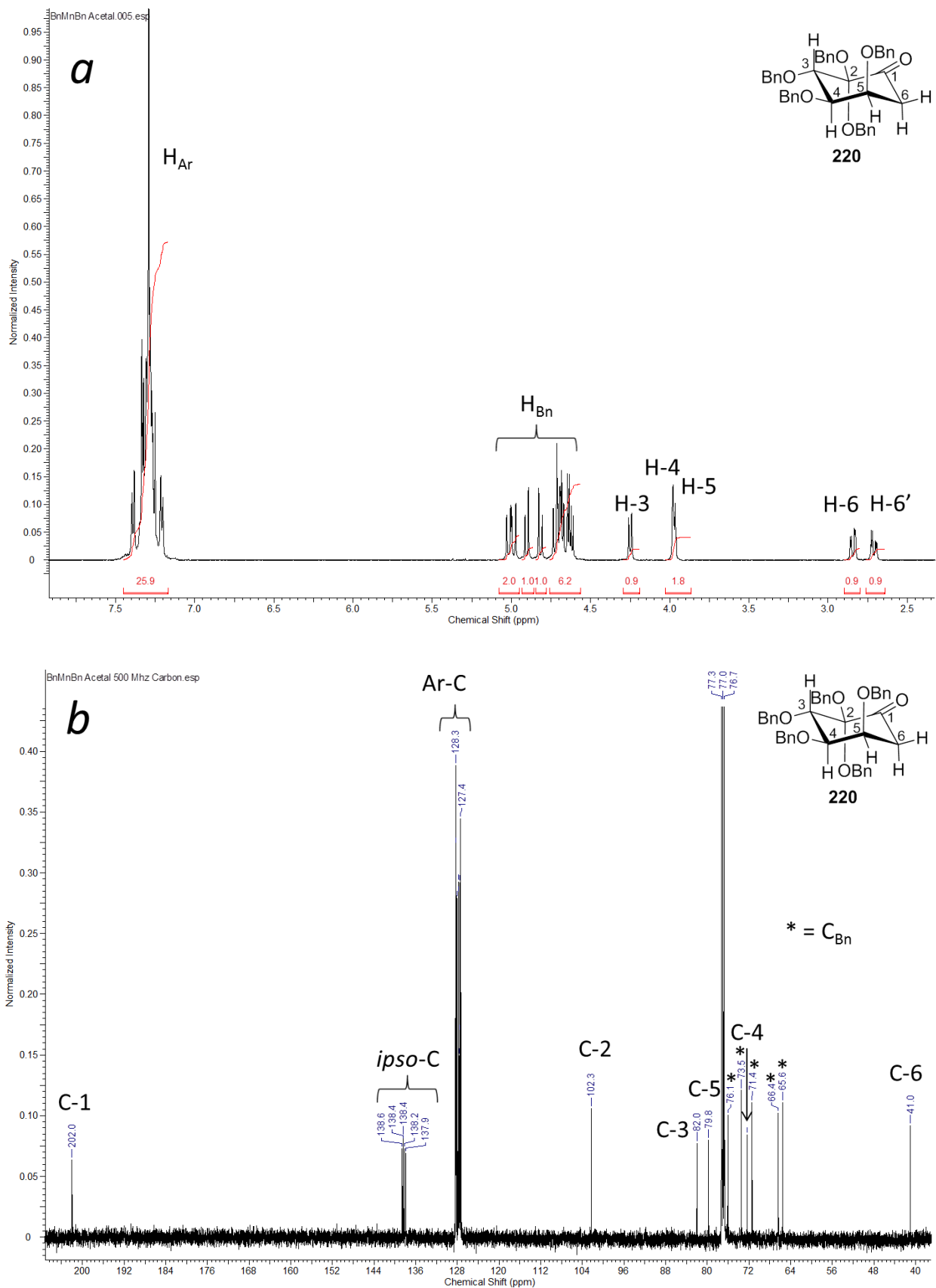
### Alcoholysis reactions of inosose-2-*O*-mesylates

After the reaction outcome detailed in Scheme 18, it was reasoned that other nucleophiles may be used to trap the proposed oxyallyl intermediate. Thus, mesylate **169** was stirred with benzyl alcohol, which fulfilled the role of solvent and nucleophile and afforded a good yield of ketal **220** (Scheme 31).



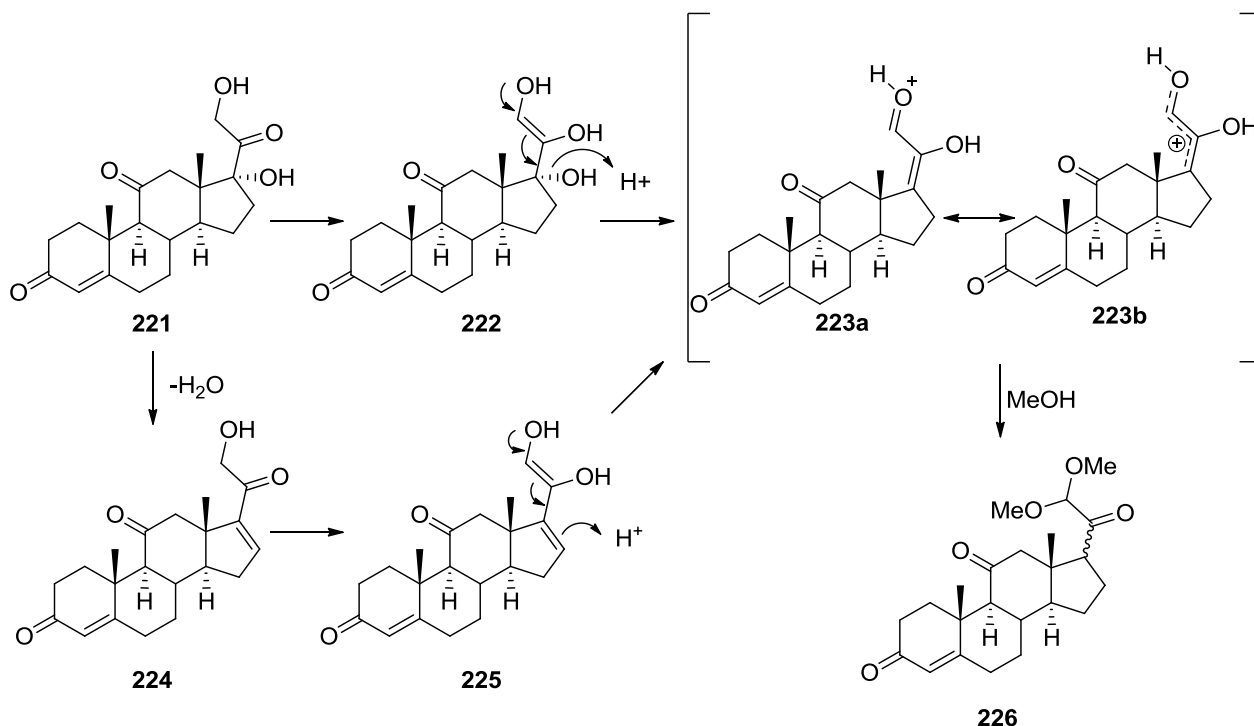
**Scheme 31**

The characterisation of ketal **220** was performed using 1D and 2D <sup>1</sup>H and <sup>13</sup>C NMR spectroscopy. A methylene group, not present in the starting material, was assigned on the basis of two upfield resonances at 2.87 and 2.73 ppm in the <sup>1</sup>H NMR spectrum (Figure 24a). Identification of these protons allowed straightforward assignment of other resonances in the ring. Aside from the large 13 Hz geminal coupling for the methylene protons, both had small couplings to H5 (3.4 and 4.5 Hz) indicating that this neighbour was equatorial. H3 appeared as a doublet at 4.25 Hz with an 8.8 Hz *trans*-diaxial coupling with H4. The stereochemistry of the product was consistent with the starting material although the conformation is ring-flipped in comparison. The assigned <sup>13</sup>C NMR spectrum is presented in Figure 24b.



The  $^{13}\text{C}$  NMR spectrum of **220** exhibits 5 *ipso*-aromatic resonances (on the basis of chemical shift and a 2D HSQC experiment) and a characteristic ketal resonance at 102 ppm consistent with the proposed structure.

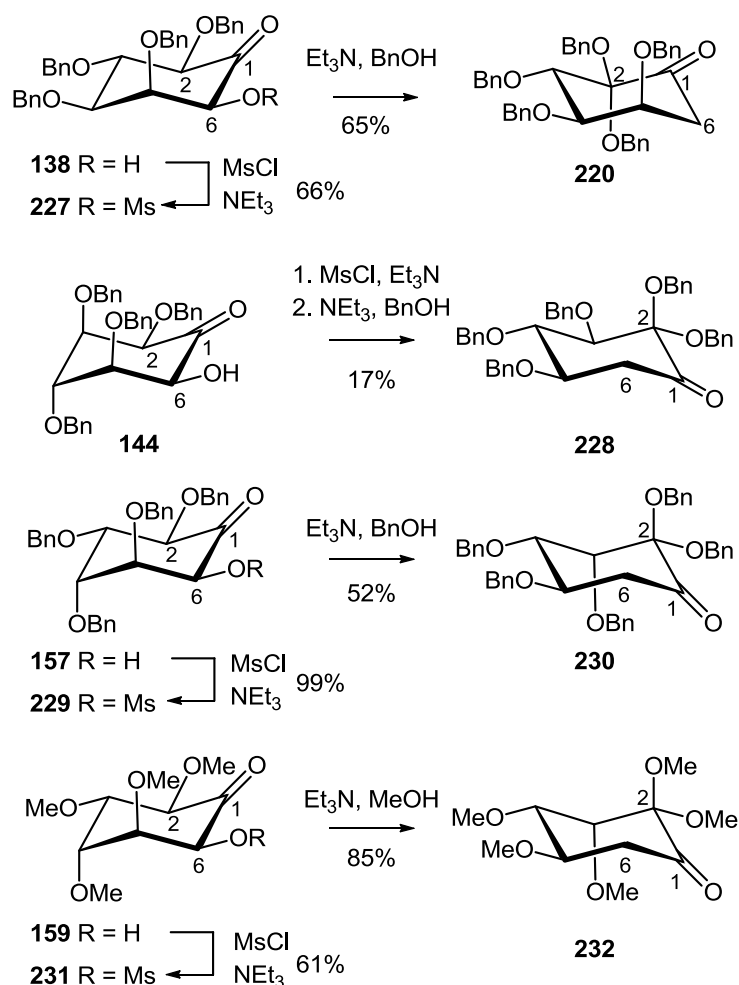
The observed reaction outcome is similar to the Mattox rearrangement which converts a steroidal dihydroxyacetone motif to a ketoacetal under acidic conditions (Scheme 32).<sup>101</sup>



**Scheme 32**

Two pathways are proposed in the Mattox rearrangement. In the first pathway, the enol tautomer of dihydroxyacetone derivative **221** undergoes elimination of  $\text{H}_2\text{O}$  to give hydroxycarbenium cation **223a**. Although Mattox does not explicitly implicate an oxyallylic intermediate, it is conceivable that **223a** is in equilibrium with the delocalised oxyallylic cation **223b** which is stabilised by the neighbouring hydroxyl group. Alternatively,  $\text{H}_2\text{O}$  may be eliminated first to give **224**, with subsequent rearrangement of its enol tautomer **225** giving the same reactive intermediate represented by **223a** and **223b**. Methanolysis of this intermediate yields the dimethyl ketoketal **226**. A base-promoted variant of this rearrangement on betamethasone dipropionate has been reported by Li et al. who proposed hydrolysis and rearrangement of an intermediate enol.<sup>102</sup>

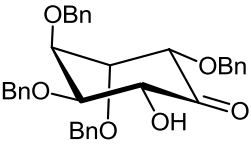
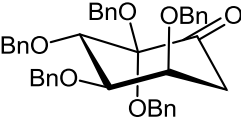
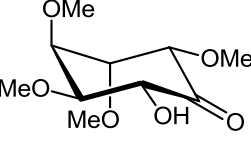
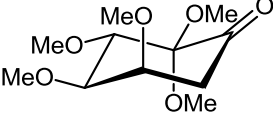
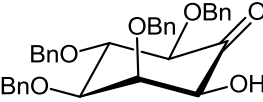
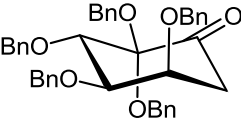
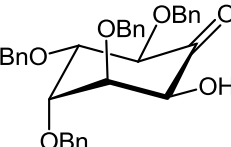
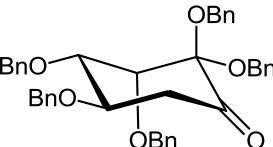
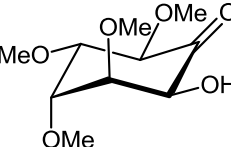
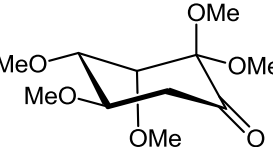
Many, indeed most reactions on carbohydrates and inositols show dependence on the stereochemistry of the substrate. The reaction was tentatively assigned to be proceeding through an oxyallyl as in the Favorskii rearrangement, and in cyclohexyl substrates these rearrangements are influenced by the relative geometry of both the acidic proton and the leaving group.<sup>88</sup> To examine the scope of the reaction and the effect of stereochemistry, the partially-protected inososes prepared in Chapter 1<sup>103</sup> were subjected to the reaction conditions (Scheme 33).



**Scheme 33**

Mesylation of the alcohols **138**, **157** and **159** under standard conditions afforded **227**, **229** and **231** which were then treated with triethylamine in benzyl alcohol or in the case of **231** with triethylamine in methanol. The reaction was generally tolerant to stereochemistry and good yields of ketal **220**, **230** and **232** were obtained from **227**, **229** and **231** respectively. The product isolated from the reaction of **227** was spectroscopically identical to the product obtained from the reaction of **169** as both of the epimeric  $\alpha$ -centres are eliminated in the rearrangement. Attempted isolation

of the mesylate derived from **138** was unsuccessful and so the crude mesylate obtained after precipitating ammonium salts using ethyl acetate was treated with benzyl alcohol and triethylamine which afforded minor amounts of ketal **228**. Inosose **138** was a difficult substrate, prone to decomposition, especially on silica which may have contributed to the low yield of **228**. All mesylates underwent varying degrees of decomposition on silica so the chromatography-free procedure for **138** was applied to the other hydroxyketones (Table 4).

Entry <sup>a</sup>	Starting material	Product	Yield
1	 <b>129</b>	 <b>220</b>	58
2	 <b>130</b>	 <b>233</b>	27
3	 <b>138</b>	 <b>220</b>	64
4	 <b>157</b>	 <b>230</b>	45
5	 <b>159</b>	 <b>232</b>	30

<sup>a</sup> Reactions were performed on 40-60 mg of hydroxyketone using 2 equiv MsCl and 2.2 equiv. Et<sub>3</sub>N and once complete ammonium salts were precipitated with EtOAc, the mixture filtered, concentrated and benzyl alcohol or methanol (2 mL) and triethylamine (4 equiv.) added.

**Table 4 Chromatography-free rearrangements starting from hydroxyketones**

The yields obtained from **129** and **157** were superior using this chromatography-free methodology, however both **138** and **159** afforded inferior isolated yields of ketals. Application of the conditions to the methyl ether **130** afforded a poor yield of ketal **233**.

Conformations of the products were able to be unambiguously assigned on the basis of coupling constants, and a summary of the key coupling constants used in structural assignment is provided in Figure 25. As with **220**, the conformation in CDCl<sub>3</sub> solution of ketals **228**, **230**, **232** and **233** were found to be ring-flipped relative to the starting materials.

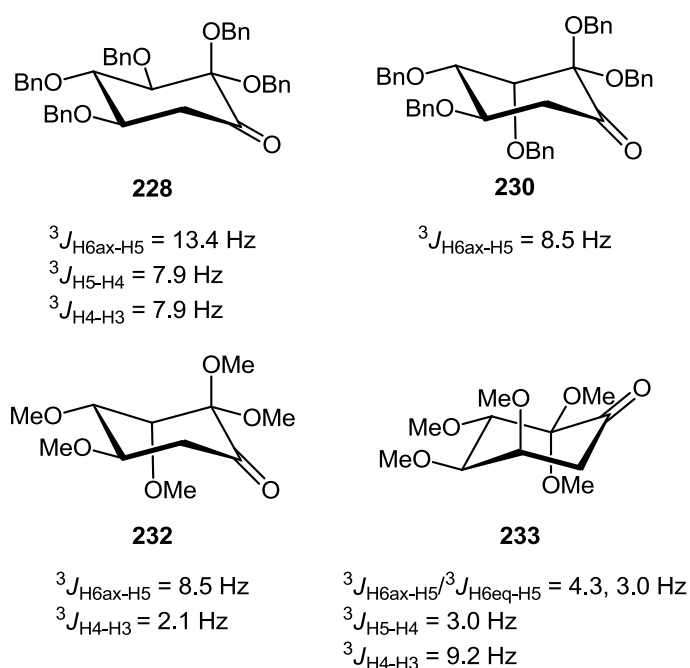
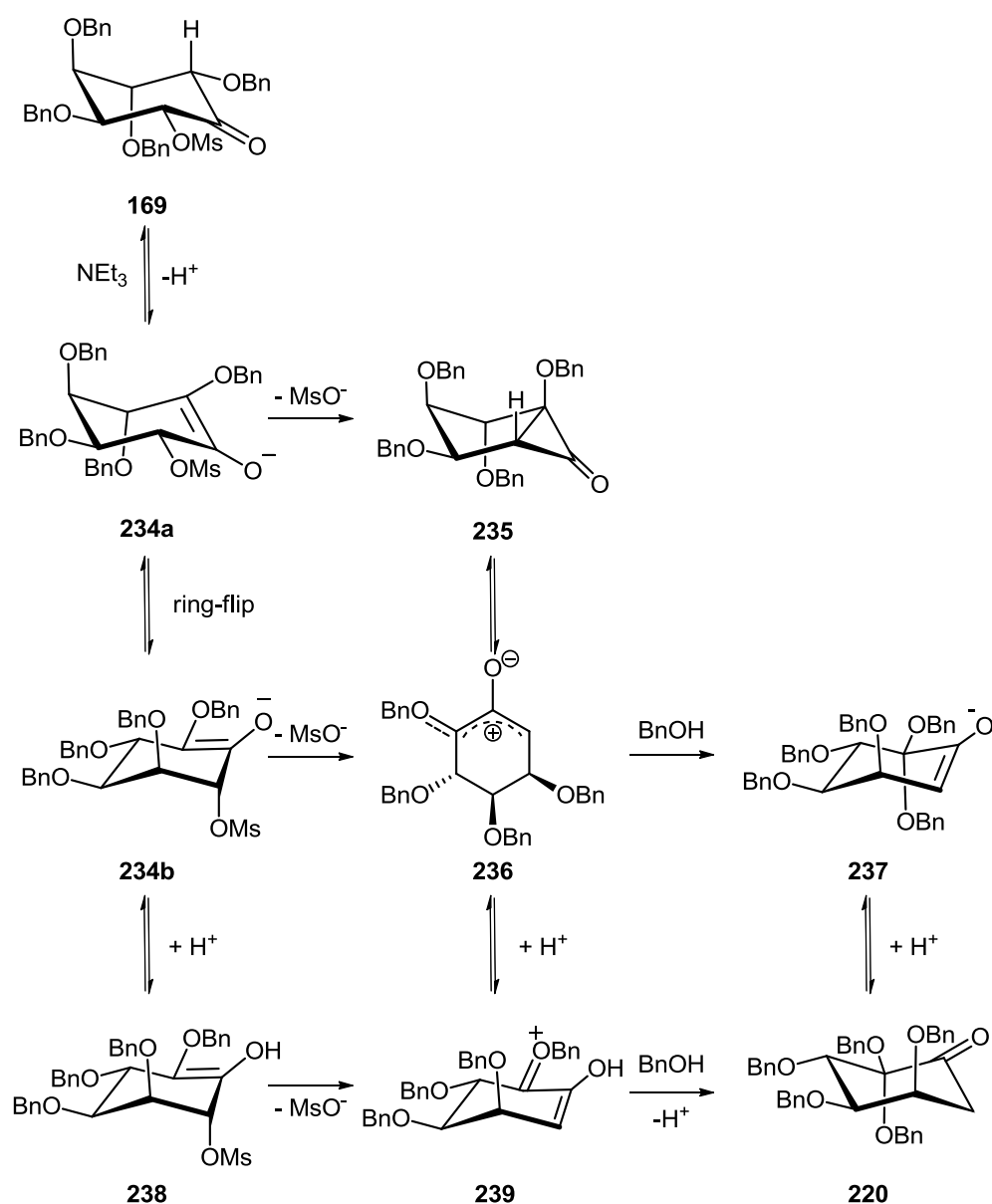


**Figure 25** Key coupling constants used in determination of structure and conformation in CDCl<sub>3</sub> solution of acetals **228**, **230**, **232** and **233**

### Mechanistic investigations in the rearrangement of inosose-2-*O*-mesylates

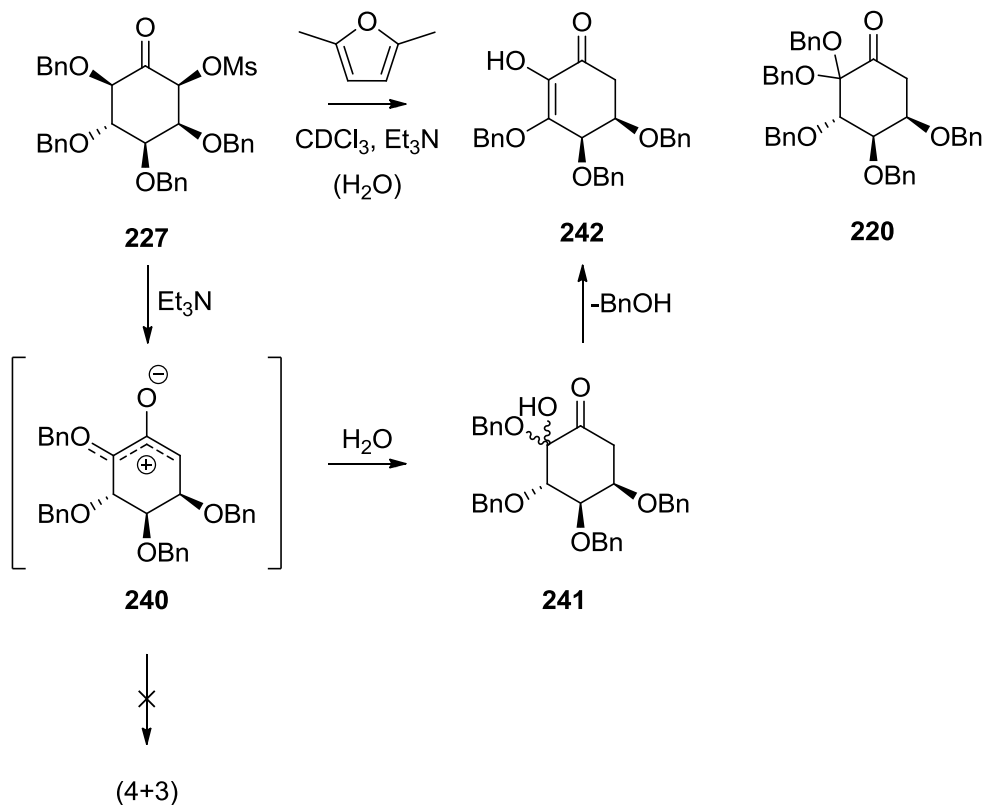
A mechanism for the reaction of **169** which explains the observed product **220** is shown in Scheme 34. Axial  $\alpha$ -hydrogens are more acidic than equatorial hydrogens as the orbitals are aligned such that the developing carbanion can be stabilised by the carbonyl group. Equatorial leaving groups are required for the formation of the cyclopropanone as this makes the C-X  $\sigma^*$  orbital accessible to the enolate carbanion.<sup>10</sup> The conformation in solution for **169** shown in Scheme 34 is based upon the 10 Hz *trans*-diaxial coupling seen for H6 and H5. Thus, starting with **169**, the triethylamine in the reaction mixture promotes the formation of enolate **234a** from which the cyclopropanone **235** can form by direct ring-closure due to the equatorial mesylate. Ring-opening of the cyclopropanone **235** promoted by the benzyloxy group gives the alkoxyoxyallyl intermediate **236**. Alternatively, a ring flip of enolate **234a** to give **234b** makes the

mesylate axial and elimination can afford **236** without the involvement of the cyclopropanone **235**. Formation of the final product could proceed by protonation of **236** to give **239** and then nucleophilic addition of the alcohol, or by addition of alcohol to give **237** and then protonation. Formation of intermediate tautomer **238** from mesylate **169** could avoid oxyallyl **236**, proceeding through the oxocarbenium ion **239**, and such a mechanism would be similar to that proposed for the Mattox rearrangement.



Scheme 34

Attempted small scale trapping of the proposed benzyloxyoxyallyl species **240** generated from **227**, with 2 equivalents of 2,6-dimethylfuran in  $\text{CDCl}_3$  gave only dibenzyl ketoacetal **220** and unstable  $\alpha,\beta$ -unsaturated enol **242** (Scheme 35).



### Scheme 35

The formation of enol **242** can be explained if adventitious water is present in the reaction mixture. The formation of the oxyallyl **240** from **227** proceeds as usual in the presence of  $\text{Et}_3\text{N}$ . As the furan is not nucleophilic enough, and no (4+3) trapping occurs, water adds to give hemiacetal **241** which eliminates benzyl alcohol to give **242**. The eliminated benzyl alcohol then goes on to react with the oxyallylic intermediate **240** and give the acetal **220**. Furan and cyclopentadiene were also employed in attempts to trap the oxyallylic intermediate **240** but gave complex mixtures with no clear evidence for any (4+3) reactions.

Computations performed by Professor Stephen Glover and Dr Ben Greatrex (UNE) further examined aspects of the reaction mechanism. A model methoxyoxyallyl system (**243**) was analysed using DFT B3LYP/631++G\*\* to examine energy-minimised conformers (Figure 26 and Table 5). Previous computational studies have examined the semibenzylic and cyclopropanone pathways for the Favorskii rearrangement but have not examined the effect of alkoxy substitution

adjacent to the ketone.<sup>104</sup> The oxyallyl species has previously been studied computationally which has shown the ground state to be a singlet diradical.<sup>105</sup>

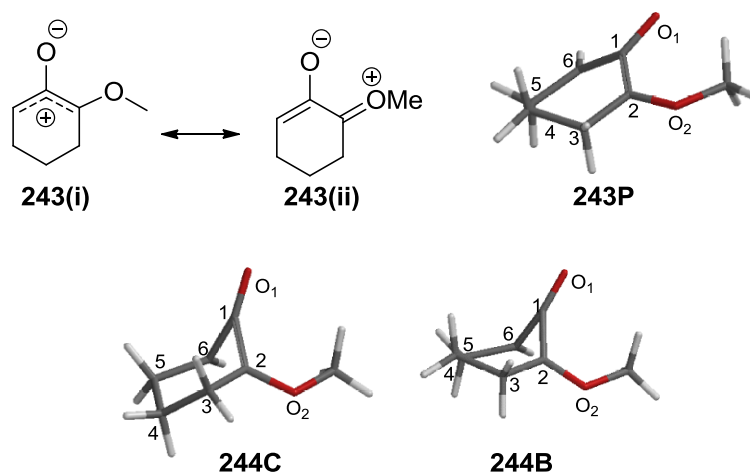


**Figure 26** Energy minimised structures for the model system **243**

	Interatomic distance (Å)					Rel. Energy (kcal/mol)	Solv. Energy (kcal/mol)	Natural Charges	
	C1-C6	C1-C2	C2-C6	C1-O1	C2-O2			C2	C6
<b>244C</b>	1.48	1.47	1.61	1.20	1.39	+4.9	+6.30	+0.21	-0.33
<b>243P</b>	1.41	1.46	2.33	1.26	1.31	0	0	+0.52	-0.16
<b>244B</b>	1.47	1.47	1.65	1.21	1.38	+0.9	+6.16	+0.23	-0.30

**Table 5** Selected properties of energy minimized structures using DFT B3LYP/631++G\*\*

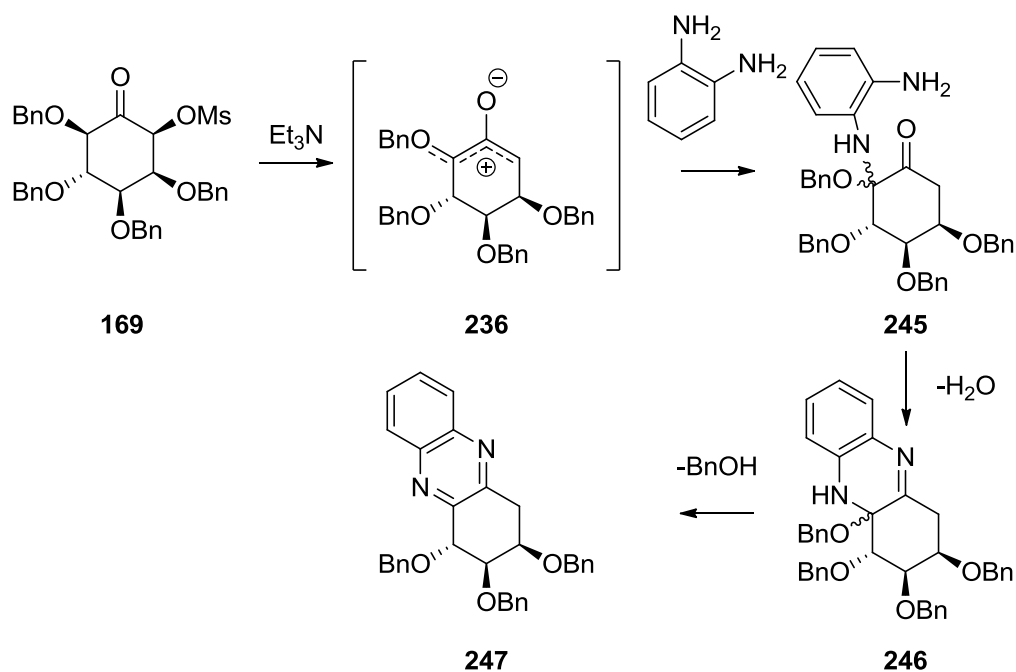
There were three energy minimised structures found for 2-methoxyoxyallyl **243**, corresponding to the planar singlet structure **243P**, the chair cyclopropanone **244C** and the boat cyclopropanone **244B** (Figure 26). In vacuum, the planar conformation **243P** was 0.9 kcal/mol more stable than the lowest energy boat cyclopropanone **244B**, while the alternative chair **244C** was destabilised by 4.9 kcal/mol as the methoxy group eclipsed the neighbouring C-H bond. In vacuum, the triplet diradical was calculated to be 10.8 kcal/mol higher in energy than **243P**.

The p-type lone pair found on the alkoxy oxygen stabilises the planar conformation **243P** as rotation around the C-O bond taking these electrons out of conjugation causes the structure to collapse to the cyclopropanone **244B**. The empirical solvation model<sup>22</sup> implemented in Spartan '14 shows significant stabilisation of the planar **243P** relative to the cyclopropanones. The polar solvents used would stabilise **243P** as an intermediate and this may explain why ring-contraction products are not observed.

The long C1-O1 bond favours resonance hybrid **243** and the short C1-C6 bond relative to the C1-C2 bond as well as the short C2-O2 bond relative to the same bond in **244C** or **244B** favour canonical form **243(ii)**. Calculation of the natural charges<sup>24</sup> showed cationic character at C2 (+0.52) and anionic character at C6 (-0.16). The charges and bond-lengths explain why addition is observed adjacent to the alkoxy group at C2 and not at the allylic C6 position. In this sense, the alkoxy group provides a means of predicting regiochemical outcomes of the nucleophilic addition. In addition, the enolate formed by reaction of methanol at C2 of **243P** is computed to be 11.4 kcal/mol more stable than the enolate formed from addition at C6.

### Alternative nucleophiles for trapping of the oxyallyl intermediate

With the successful trapping of various putative oxyallylic intermediates generated from inosose-2-*O*-mesylates with azide and alcohols, attention was turned to the use of other nucleophiles. It was reasoned that the use of *o*-phenylenediamine to trap the reactive intermediate would give a hemiaminal that would then undergo addition to the ketone with concomitant elimination of benzyl alcohol and aromatisation yielding a fused quinoxaline. Gratifyingly, when **169** was stirred with Et<sub>3</sub>N and *o*-phenylenediamine at room temperature, a compound that was tentatively assigned as fused quinoxaline **247** was isolated from the reaction mixture in 54% yield (Scheme 36).



**Scheme 36**

The characterisation of quinoxaline **247** relied on 1D and 2D NMR spectroscopy. The assigned  $^1\text{H}$  and  $^{13}\text{C}$  NMR spectra are provided in Figure 27.

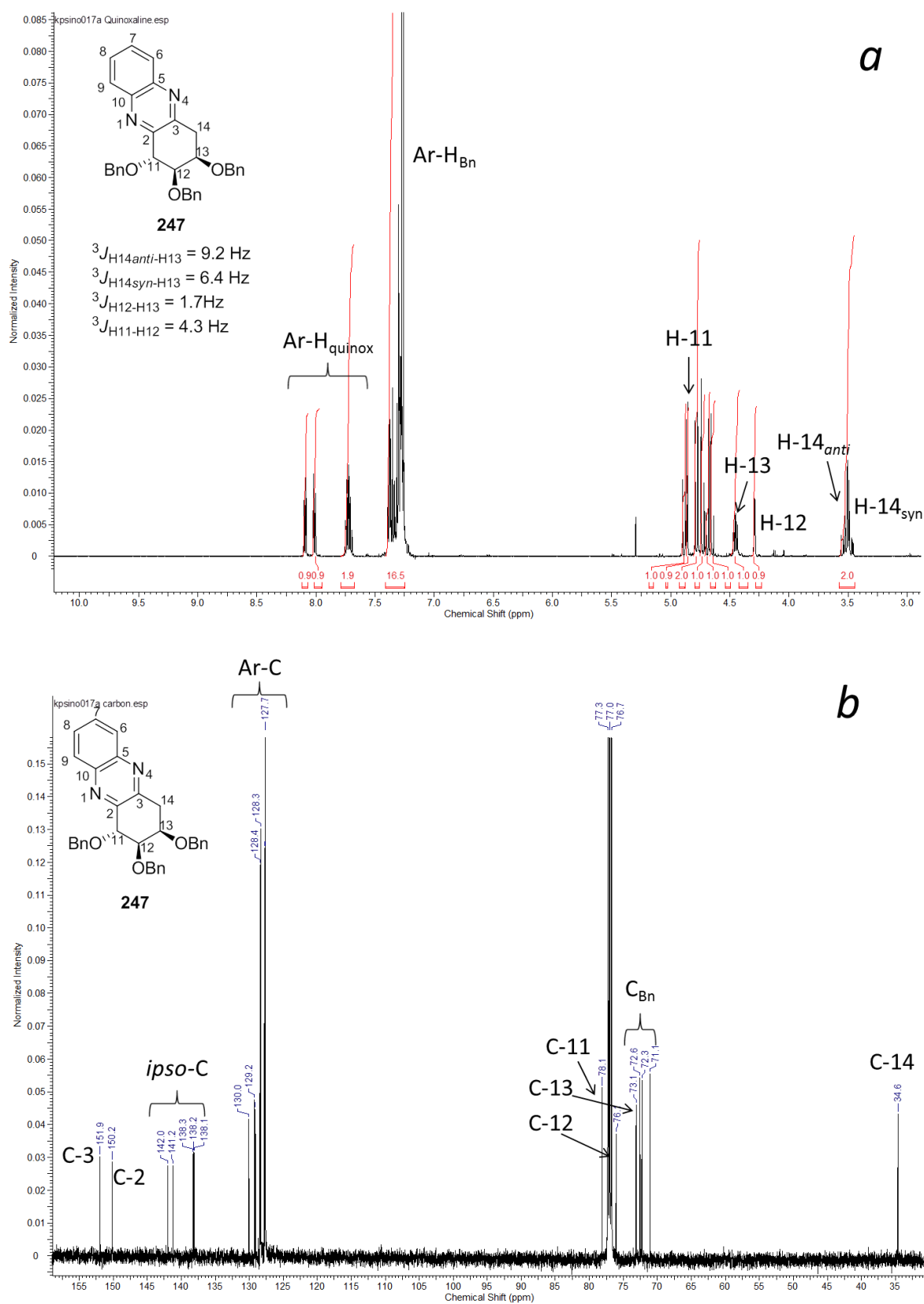


Figure 27a) 500 MHz  $^1\text{H}$  and b) 125 MHz  $^{13}\text{C}$  NMR spectrum of **247** in  $\text{CDCl}_3$

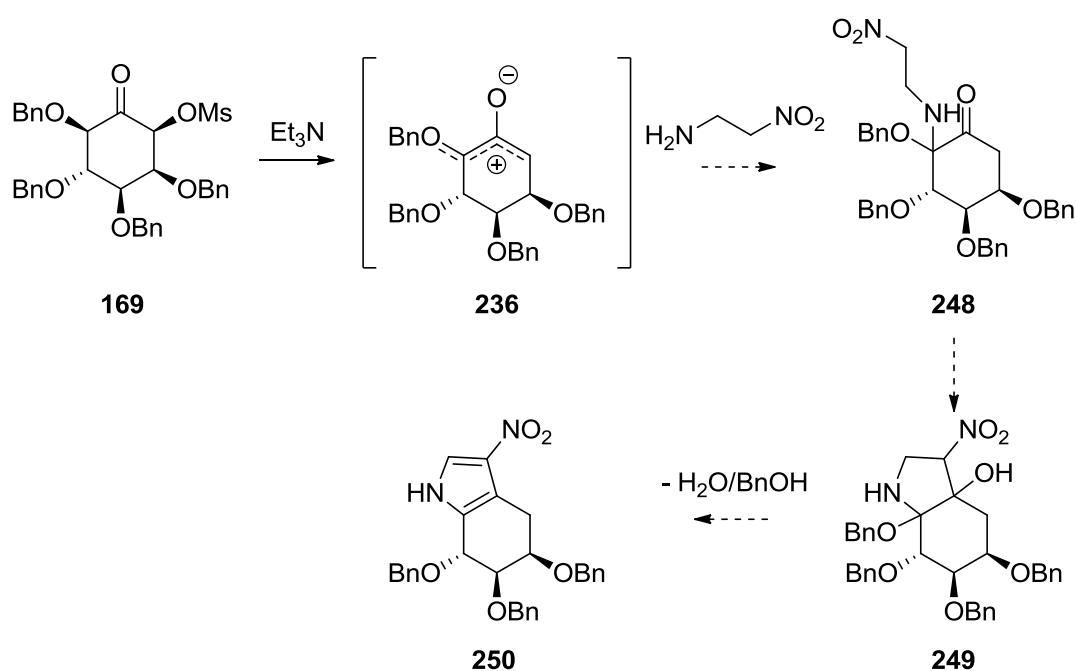
The fused quinoxaline ring distorts the geometry of the alkyl ring and this is evident in the extracted coupling constants for the five ring protons. The observed coupling constants deviate from those typically observed in a classic six-membered chair conformation where all dihedral angles for the various protons are approximately 180° or 60°. The observation of a large pseudo *trans*-diaxial coupling for one of the methylene protons at C14 formed the basis of an assumption that the conformation could be described as a half-chair. The two resolved methylene resonances at 3.53 and 3.48 ppm were assigned as H14<sub>anti</sub> and H14<sub>syn</sub> respectively, with *anti* and *syn* referring to their relation to the neighbouring proton. H14<sub>anti</sub> was assigned on the basis of a 9.2 Hz coupling to the neighbouring proton, indicating a pseudo *trans*-diaxial relation to this proton, thus assignment of the benzyloxy substituent at C13 as pseudo-equatorial is appropriate. The configurations at the other two stereocentres (C11 and C12) are less easily assigned, and an assumption was made that no epimerisation occurred at either position during the reaction and the stereochemistry could therefore be assigned from that of the starting material. For C12 this assumption is valid in that this centre is remote to the proposed reactive oxyallylic centre in the intermediate. For C11 however, this assumption is more contentious as it is adjacent to the reactive centre in the proposed oxyallylic intermediate. It is noted that in reactions with azides and alcoholic nucleophiles in the presence of base, no epimerisation at the equivalent position was observed in any of the products.

Although specific conformational detail couldn't be extracted, the weak 1.7 Hz coupling of H13-H12 indicates the dihedral angle between these protons approaches 90°. H11 appeared as a 4.3 Hz doublet due to a sole coupling with H12, and again this is ambiguous in terms of indication of stereochemistry at this centre. The assignment of the downfield proton resonances as quinoxalinic is consistent with literature data for simple 1,2-disubstituted quinoxalines.<sup>106</sup> The 7 *ipso*-aromatic carbons were identified by a 2D HSQC experiment and are consistent with the structural assignment. C2 and C3 were able to be assigned on the basis of crosspeaks in the HMBC NMR spectrum between these carbons and H11 and the H14 methylene protons respectively.

Quinoxalines are a privileged structural scaffold in many compounds with diverse biological activities including anti-inflammatory,<sup>107-109</sup> antitubercular<sup>110</sup> and anticancer.<sup>111,112</sup> The protocol described in this chapter allowing for the generation of a chiral quinoxaline derivative from a putative oxyallylic intermediate might complement existing strategies in quinoxaline synthesis and allow access to unique structural motifs.

## CONCLUSION

In this chapter it has been demonstrated that 2-*O*-alkyl-6-*O*-mesylinososes undergo an oxyallyl- or oxyallyl cation-mediated rearrangement in the presence of alcohols and amine base yielding solely  $\alpha'$ -addition products to generate a quaternary centre. The intermediates may be trapped using both azide and alcohols forming  $\alpha$ -ketoazidoacetals and  $\alpha$ -ketoketals respectively. Using *o*-phenylenediamine as the nucleophilic trapping species, a domino nucleophilic attack-imine formation-aromatisation process was described which generates an unusual sugar-fused quinoxaline. The quinoxalines in particular may find use in the preparation of novel bioactive compounds that incorporate this privileged scaffold. Importantly, the conditions used in the nucleophilic trappings are extremely mild and the examples demonstrate that the reaction is general and tolerant to stereochemistry around the inosose ring. Future work will seek to expand the series of quinoxaline adducts and establish a library of derivatives that will be suitable for evaluation of potential bioactivity. Finally, the work described in this chapter may form a platform for the generation of other novel sugar-fused aromatic systems, such as the use of other bifunctional nucleophiles like 2-amino-1-nitroethane to generate the fused pyrrole derivative **250** (Scheme 37). Many other bifunctional trapping agents can also be envisaged.



Scheme 37